ATRP Grafting from Gel Coated Microspheres

ATRP Grafting from Gel Coated Microspheres

By

Erica I Robinson, B.Sc.

A Thesis

Submitted to the School of Graduate Studies

in Partial Fulfillment of the Requirement

for the Degree

Masters in Chemistry

McMaster University

MASTERS OF SCIENCE (2004)
(Chemistry)

McMaster University
Hamilton, Ontario

TITLE: ATRP Grafting from Gel Coated Microspheres

AUTHOR: Erica I Robinson, B.Sc. (McMaster University)

SUPERVISOR: H. D. H. Stöver

NUMBER OF PAGES: xxii, 121

Abstract

Swellable microspheres prepared by the precipitation polymerisation of divinylbenzene-80 (DVB-80) and 2-hydroxyethyl methacrylate (HEMA), in a solvent mixture of methyl ethyl ketone (MEK) and heptane, were functionalised with 2-bromopropionyl bromide, and 2-bromoisobutyryl bromide to prepare Atom Transfer Radical Polymerisation (ATRP) initiators.

Methyl acrylate (MA) and methyl methacrylate (MMA) were grafted from the microspheres using CuBr and either 4,4'-dinonyl-2,2'-dipyridyl (dNbipy), or *N,N,N',N'',N''*-pentamethyldiethylenetriamine (PMDETA) ligands. The morphology of the grafted microspheres was studied using electron microscopy (ESEM and TEM) and x-ray microspectroscopy. Adding equimolar sacrificial initiator resulted in improved control over the grafting and gave grafted and soluble polymer, with narrow polydispersity (PDI) and number average molecular weight (M_n) close to expected values.

Base catalysed transesterification was used to cleave the grafted polymer. It was found that adding free initiator permits grafting from within lightly cross-linked gels to be carried out with good control over M_n and PDI.

Dedicated to my mentor in life,

President Daisaku Ikeda of Soka Gakkai International

Acknowledgements

First, I would like to thank my supervisor, Professor Harald D. H. Stöver for his support and encouragement over the last two years. I would also like to express gratitude to my two committee members: Dr. Alex Adronov and Dr. Kalai Saravanamuttu for taking the time out of their busy schedules to sit on my committee.

Much of this work would not have been possible without the invaluable skills of Dr. Don Hughes and Mr. Brian Sayer in the NMR facilities in the Chemistry Department, Mrs. Marcia West in the Health Sciences Electron Microscopy Unit, and Mr. Klaus Schultes in the Life Sciences Electron Microscopy Unit. I am appreciative of the hard work of Adam P. Hitchcock and Sherry Zheng for their expertise in explaining and running STXM at the ALS Light Source in Berkley, California. A warm thank you is paid to Dr. Gillian Goward for her help with solid state NMR. I would like to acknowledge George Timmins, and Mike Mallott, for his IT support.

In the Stöver group, I would like to recognize the following past members: Esther, Guodong, Lisa, Swapna and Wen-Hui, who were all invaluable in helping me adjust to McMaster University and Hamilton, Ontario. Current group members: Mukkaram, Xiangchun (Yin), Yan, and Jafar are warmly acknowledged for their kind friendship and insightful discussions. This thesis would not have been possible without the kind, patient, hard work of Dr. Nick Burke, whose presence and expertise in the group are invaluable and greatly appreciated.

Thanks to the ladies in the Chemistry Department office, Carol Dada, Barbara DeJean, Tammy Feher, and Josie Petrie, who have been wonderful and caring over the

past two years. Carol, you have been extremely helpful, encouraging, and funny, and your grace is an inspiration.

My family has been a constant source of unconditional love, support and encouragement. Yoshiko and Keith, you have been incredible, and are wonderful examples of parenting, and companionship. Andrea, you are the best sister in the world, you are incredible. I would like to acknowledge all Robinsons, Yamamotos, Mannings, and Jonas' for being the most wonderful, eccentric, giving and caring group of people. My friends at Mac, in Calgary, and around the world have made it unbearable to leave Calgary, and now to leave Hamilton, you have all truly made an impression on me.

Finally, I would like to thank Dennis John Hoffart for his love and understanding, and for undertaking this journey with me.

Table of Contents

Chapter 1: Introduction to Grafting from Polymeric Materials

Table of Contents (cont'd)

Chapter 2: Grafting Methyl Acrylate from Polymeric Microspheres

Table of Contents (cont'd)

Table of Contents (cont'd)

Chapter 3: Grafting Methyl Methacrylate from Polymeric Microspheres

Table of Contents (cont'd)

Chapter 4: Conclusions

List of Figures

List of Figures (cont'd)

List of Figures (cont'd)

List of Figures (cont'd)

List of Figures (cont'd)

List of Tables

List of Tables (cont'd)

List of Tables (cont'd)

List of Schemes

List of Schemes (cont'd)

List of Abbreviations

AIBN	2,2'-Azobisisobutyronitrile
ATRP	Atom Transfer Radical Polymerisation
BA	*n*-Butyl Acrylate
Bipy	2,2' – Bipyridine
BriB	Bromoisobutyrate
BzA	Benzyl Acrylate
CPMAS	Cross Polarisation Magic Angle Spinning
CTS	2-(4-Chlorosulfonylphenyl) ethyl trichlorosilane
DMA	*N*,*N*-Dimethylacrylamide
DMAEMA	2-(Dimethylamino)ethyl methacrylate
dHbipy	4,4'-Di-*n*-2,2'-bipyridine
dNbipy	4,4'-Dinonyl-2,2'-dipyridyl
DP	Degree of Polymerisation
DVB80	Mixture of Divinylbenzene Isomers and Ethylvinylbenzene Isomer with 80 mol% of Divinyl Components
EA	Ethyl Acrylate
E1	Swellable P(DVB80-*co*-HEMA) microspheres
E1BBr	Isobutyrate functionalised ATRP initiator microspheres
E1PBr	Propionate functionalised ATRP initiator microspheres
E1-PMA-Br	Methyl acrylate grafted microspheres
E1-PMA-Br$_{cleaved}$	Cleaved methyl acrylate grafted microspheres

List of Abbreviations (cont'd)

E1-PMMA-Br	Methyl methacrylate grafted microspheres
E1-PMMA-Br$_{cleaved}$	Cleaved methyl methacrylate grafted microspheres
ESEM	Environmental Scanning Electron Microscope
Et-2-BrP	Ethyl 2-bromopropionate
Et-2-BriB	Ethyl 2-bromoisobutyrate
FRP	Free Radical Polymerisation
FT-IR	Fourier Transform Infrared
GPC	Gel Permeation Chromatography
HEMA	2-Hydroxyethyl Methacrylate
HMTETA	1,1,4,7,10,10-Hexamethyltriethylenetetramine
MA	Methyl Acrylate
MBrP	Methyl 2-Bromopropionate
MeCN	Acetonitrile
Me$_4$Cyclam	1,4,8,11-Tetramethyl-1,4,8,11-Tetraazacyclotetradecane
Me$_6$TREN	Tris[2-(dimethylamino)ethyl]amine
MEK	Methyl Ethyl Ketone
MeOH	Methanol
MMA	Methyl methacrylate
M_n	Number Average Molecular Weight
M_w	Weight Average Molecular Weight
M_w/M_n	Molecular Weight Distribution

List of Abbreviations (cont'd)

MWD	Molecular Weight Distribution
NaOMe	Sodium methoxide
NCSA	N-Chlorosulfonamide
NEXAFS	Near edge X-ray absorption fine structure
NIPAM	*N*-Isopropylacrylamide
NMR	Nuclear Magnetic Resonance
***p*-TsCl**	*para*-Toluenesulfonyl chloride
PD	Polydispersity
PDI	Polydispersity Index
PEGMA	Poly(ethylene glycol)monomethacrylate
PMDETA	*N,N,N',N'',N''*-Pentamethyldiethylenetriamine
RAFT	Reversible Addition Fragmentation Chain Transfer
r.t.	Room Temperature
SEC	Size Exclusion Chromatography
SFRP	Stable Free Radical Polymerisation
STXM	Scanning Transmission X-ray Microscopy
Sty	Styrene
TEM	Transmission Electron Microscopy
TEMPO	2,2,6,6-Tetramethyl piperidinyl
THF	Tetrahydrofuran

Chapter 1 Introduction to Grafting-from Polymeric Microspheres

1.0 Background

Surface functionalisation is commonly used with polymeric materials in order to improve chemical resistance,[1] compatibility,[1] dispersion in solvents,[1] functional group loading,[2] or wear. Potential uses for surface functionalisation are in chemical separation and analysis, biological screening, drug and agrochemical delivery, paper coatings, adhesives and latexes, and in precision engineering and the engineering of new opto-electronic devices.[3] Typically, such surface modification involves either adsorbing or covalently attaching suitable polymers. Such tailoring can impart chemical and biological functionalisation, or ensure the compatibility of organic and inorganic materials, and can be performed through a method known as "grafting", of which there are three subclasses: grafting-to, grafting-through and grafting-from, which will be discussed in further detail below.

Solid supports are used in synthetic chemistry both to support catalysts, and as resins for combinatorial and parallel synthesis.[4,5] These supports are typically cross-linked polymeric microspheres with large internal surface area, traditionally prepared by suspension polymerisation. Such resins traditionally have been hydrophobic, therefore only swell in nonpolar organic solvents, and cannot be used in polar organic solvents or in aqueous conditions. Recently, hydrophilicity has been introduced by grafting hydrophilic polymers.[5]

When grafting polymers from substrates, it is important to consider how they will be anchored, and whether this site is cleavable (**Scheme 1.1**).[6]

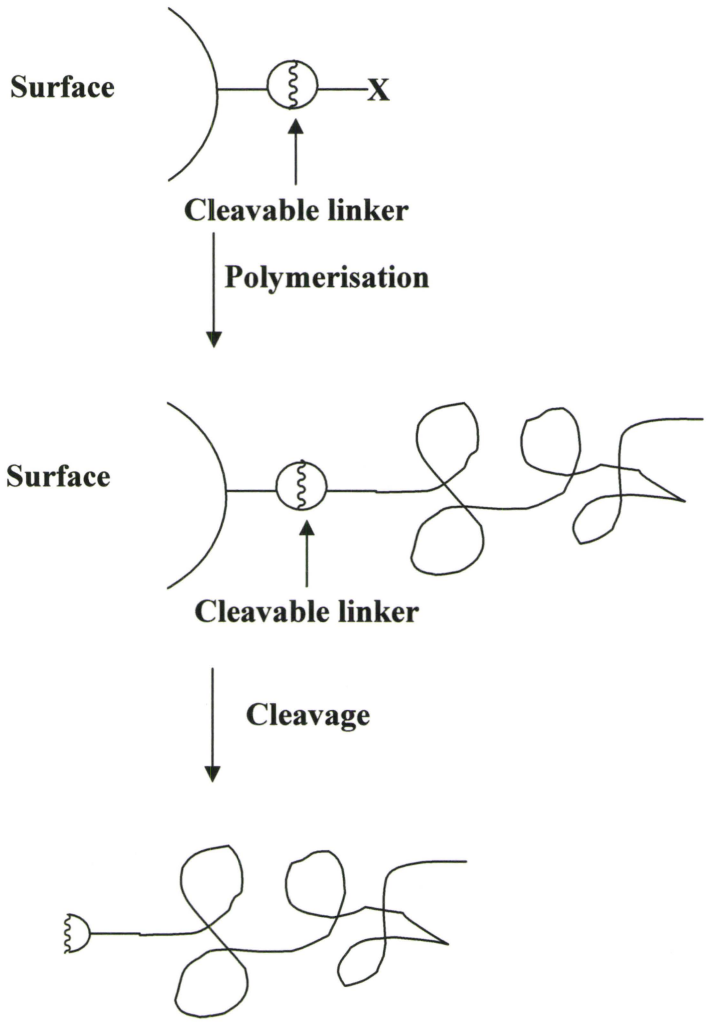

Scheme 1.1:

Schematic of grafting and cleavage incorporating a cleavable linker.

New materials can be prepared by grafting functional polymers from linear or branched backbones, flat surfaces, nanotubes, inorganic and polymeric microspheres, and

three–dimensional monoliths.[3] Permanent binding can be achieved using covalent grafting, rather than adsorption to the substrate.[3]

1.1 Grafting

Grafted polymers are a type of branched copolymer (**Scheme 1.2**), in which the backbone may be a homopolymer, to which is attached one or more blocks of another homopolymer.[7]

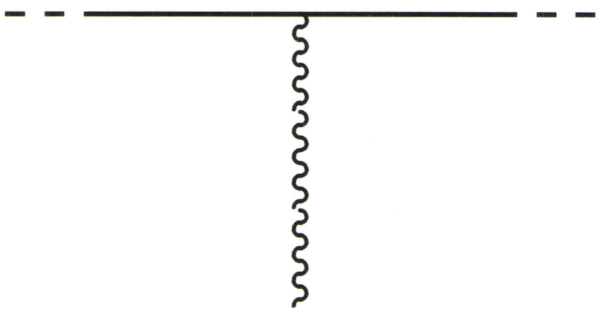

Scheme 1.2:

Schematic of a simple graft copolymer, where the side chains (∿∿∿) are attached to the backbone (——).[7]

Grafting involves the formation of covalent bonds between the substrate and the polymeric material. There are three modes by which grafting can occur.

1.1.1 Grafting-On

In the "grafting-on" approach, pre-formed polymers with a reactive end group are first prepared, and then attached or coupled to a surface bearing matching reactive groups

(**Scheme 1.3 a**). Grafting-on offers the advantage that the preformed polymer can have a well–defined composition and polydispersity (PD), characterised independently of the surface. Also referred to as "grafting-to", the only potential shortcoming of this approach is that diffusion of chain ends to the surface is hindered by crowding of initially grafted chains at the surface.[6]

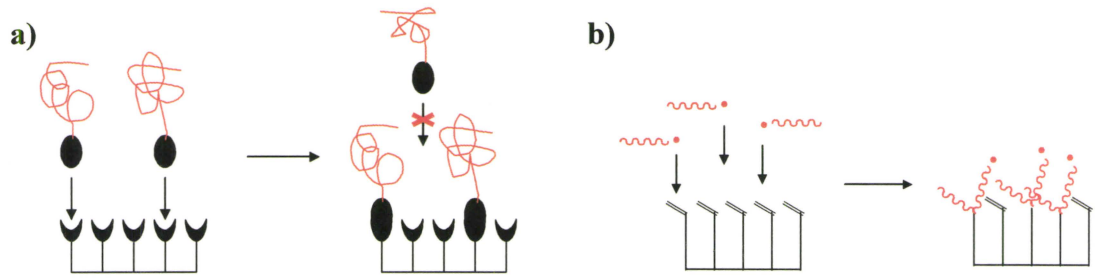

Scheme 1.3:

Schematic for **a)** grafting-on, and; **b)** grafting–through.

1.1.2 Grafting-Through

"Grafting-through" is a copolymerisation method, which requires a polymerisable group attached to the substrate. These reactive groups become incorporated into polymer chains that are initiated in solution (**Scheme 1.3 b**). This process also suffers from steric hindrance, and so high grafting densities can be difficult to obtain.

1.1.3 Grafting-From

"Grafting-from" is a process whereby polymeric layers can be added by *in situ* polymerisation from initiator sites on a surface (**Scheme 1.4**). The grafting-from

approach has a number of advantages over the grafting-on and grafting-through methods, such as: fewer experimental steps are required, and steric hindrance is reduced since it is monomer, not polymer chains that must diffuse to the reactive group at the surface. The improved accessibility to the initiating sites can result in well-defined surfaces with high graft densities,[6] however it is pertinent to ensure that propagation of the side chains is uniform and that chain coupling reactions are reduced.[1]

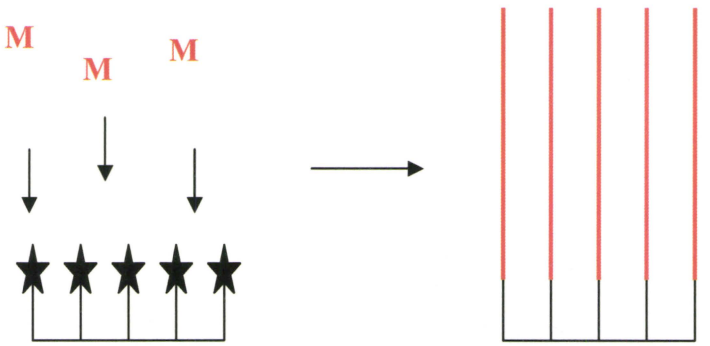

Scheme 1.4:

Schematic for grafting-from.

One potential benefit of the high grafting densities possible by grafting–from methods is that "brush" polymers can be formed. In brush polymers, the grafted chains are forced into elongated conformations due to the high grafting densities (**Scheme 1.5**).

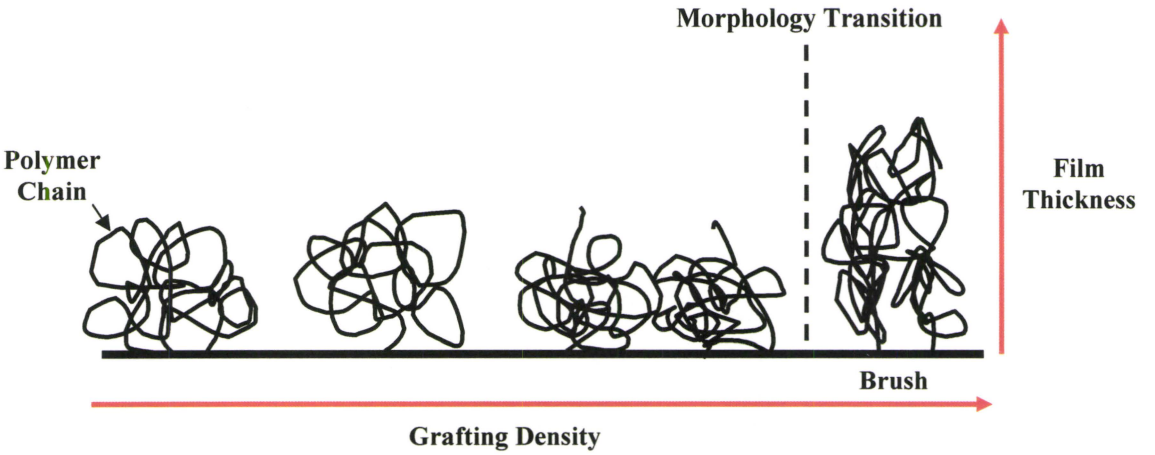

Scheme 1.5:

Scheme of transition from grafted polymer to brush polymer.[8]

These brush materials are interesting because their surface properties can be tuned by changing the composition or structure of the grafted material, such that "smart surfaces", which might have biological compatibility, and potential applications in drug delivery can be prepared.[9]

1.2 Polymerisation Methods

There are a variety of polymerisation modes that have been employed for successful grafting from substrates, including anionic,[10] cationic,[11-13] ring opening,[14-16] ring opening metathesis,[17-19] radical,[20-22] atom transfer radical polymerisation (ATRP),[23-33] and reverse ATRP.[34] The focus of this thesis will be on ATRP, a living/controlled radical polymerisation method.

1.2.1 Free Radical Polymerisation

In solution free radical polymerisation (FRP) there is a high radical concentration, which leads to increased termination resulting in a broad molecular weight distribution (MWD), defined as the ratio of the weight average molecular weight (M_w) over the number average molecular weight (M_n), or M_w/M_n. A high local concentration of radicals during a grafting experiment should similarly lead to termination and broad MWD. Consequently, there is often an upper limit to the thickness of the grafted layer formed by FRP. Prucker and Rühe[20] self-assembled a monolayer of azo initiators on silica gel in order to carry out FRP grafting of styrene (Sty). They obtained high molecular weight brushes with high grafting density, and concluded from their studies that the greatest difference between solution and surface polymerisations is that termination is increased in surface grafting. The environment around the growing radical chain is essentially a gel environment, in which termination by coupling of a free polymer chain and a surface bound polymer chain is unlikely since the free polymer chain must diffuse against the concentration gradient into the grafted film, thus termination of grafted polymer is most likely intraparticle.[20] Therefore, the M_n of the grafted polymer depends on the number of attached chains.[20] Additionally, transfer to solvent or monomer results in termination of surface bound grafted chains.[20]

1.2.2 Living Radical Polymerisation

In living/controlled polymerisation, chains are in equilibrium between active and dormant states with very few chains being active at any instant. The resulting low radical concentration, often on the order of 10^{-8} M, minimises termination, which allows all chains to grow at about the same rate and to about the same M_n (**Scheme 1.6**).

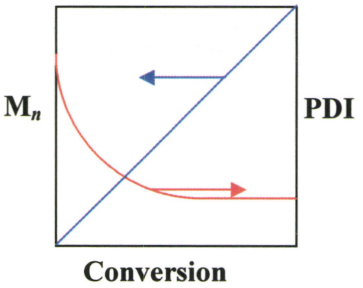

Scheme 1.6:

Schematic of M_n increase and PDI decrease as a function of conversion for living polymerisation.

In addition to the narrow PDI, the M_n may be controlled via the ratio of the initial monomer concentration to initiator concentration ($[M]_o/[I]$), where the theoretical M_n is defined by **equation 1.1:**

$$M_n(\text{expected}) = \left(\text{conversion} \times \frac{[M]_o}{[I]} \times \text{MW of Monomer} \right) + \text{MW of Initiator} \qquad \textbf{Eqn 1.1}$$

where MW is the molecular weight. Finally, when living polymerisation methods are employed the active end–group may be further utilised for end–functionalisation or block copolymer synthesis.

Grafting-from using living polymerisation techniques should result in functional structures with controlled M_n and narrow MWD. The main advantage of living polymerisation techniques is that there is a decrease in the radical concentration, which

leads to better control over the polymerisation process by suppressing bimolecular termination processes.

1.2.2.1 Stable Free Radical Polymerisation (SFRP)

Stable Free Radical Polymerisation (SFRP) or Nitroxide Mediated Polymerisation is a living polymerisation technique that employs a stable free radical to achieve the equilibrium between the active and dormant species (**Scheme 1.7**).

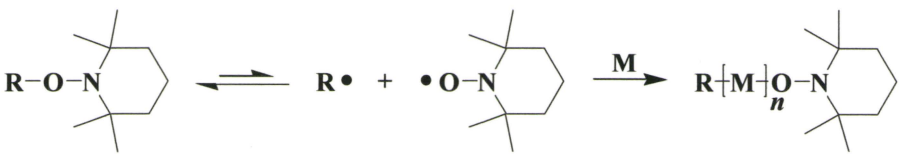

Scheme 1.7:

Schematic for SFRP, with 2,2,6,6-tetramethyl-1-piperidinyloxy, (TEMPO) as the stable free radical.

SFRP has been successfully used for grafting-from polypropylene surfaces,[35] isotactic porous monoliths[36], silica nanoparticles,[37] and silica;[38,39] however the choice of monomers is largely limited to styrenes and copolymers containing styrenes. Hodges has prepared "Rasta resins" by functionalisation of Merrifeld resins with a TEMPO based initiator, which can be targeted for specific applications by adjusting solvent affinity, loading capacity, and the distance between the functionality and the core, for use as synthetic supports and scavenging resins.[40]

1.2.2.2 Reversible Addition Fragmentation Chain Transfer (RAFT)

Reversible Addition Fragmentation Chain Transfer (RAFT) involves a dithioester that establishes the equilibrium between the active and dormant species (**Scheme 1.8**).

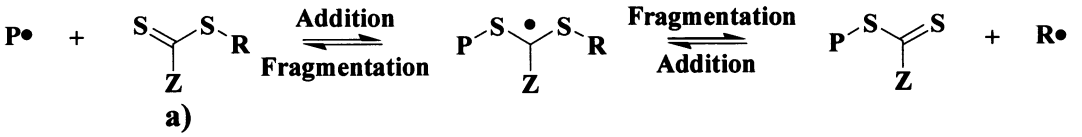

Scheme 1.8:

Schematic for RAFT, where P· is the growing polymer chain, and **a)** is the dithioester RAFT agent.

RAFT has been used to graft from hydrogen–terminated Si(100) (Si–H) surfaces,[41] silicon wafers and silica gels,[42] silica nanoparticles,[43] gold nanoparticles,[44] and propylene solid phase.[45] RAFT is an attractive polymerisation method since a large number of monomers with functional groups can be polymerised under a variety of reaction conditions, and there is no need for subsequent catalyst removal. The major drawbacks of the RAFT process are the odour of the dithioester end groups, and the cost of the RAFT reagents, however, significant progress is being made in this area.

1.2.2.3 Atom Transfer Radical Polymerisation (ATRP)

ATRP also can be used to polymerise a wide variety of monomers to high conversion. **Scheme 1.9** describes the general mechanism for ATRP. Like other living radical polymerisation techniques, it involves an equilibrium between dormant and active species.

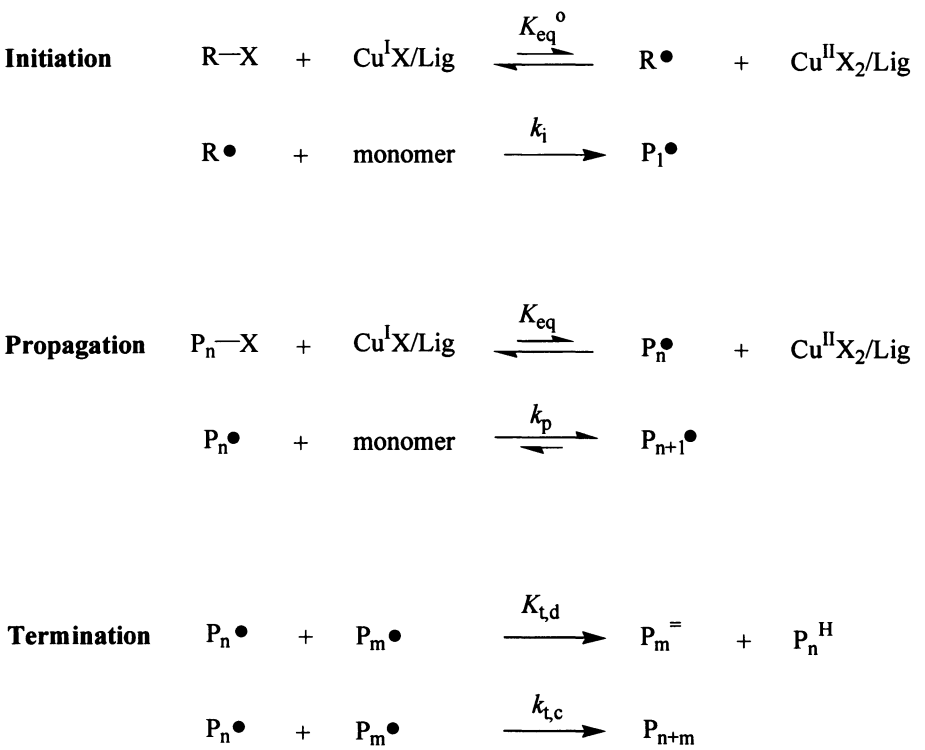

Scheme 1.9:

Schematic of the three stages of polymerisation for ATRP.

In initiation, a transition metal redox catalyst (such as Cu^{I}) abstracts a halogen from the initiator species in a reversible inner-sphere one electron process, increasing its oxidation state (to Cu^{II}), and producing a radical species.[46] This process leads to an equilibrium between dormant halide and active radical, described by the equilibrium constant K_{eq}^{o}, which is defined by **equation 1.2**:

$$K_{eq} = \frac{k_{act}}{k_{deact}} \qquad \textbf{Eqn 1.2}$$

In the above equation k_{act} is the rate constant of activation, and k_{deact} is the rate constant of deactivation. Thus, the resulting free radical is referred to as the active species as it can

undergo propagation (with the rate constant of propagation k_p), or abstract the halogen back from the oxidised metal centre, reverting to the dormant state.[46] The equilibrium between the activated and deactivated species favours the deactivated species. Initiation of all of the chains should occur rapidly on the time scale of the polymerisation, however the concentration of free radicals is low at any one time, such that radical termination is greatly reduced.[46] Termination, which occurs with the rate constant of termination k_t through bimolecular radical coupling or disproportionation, is hence suppressed. Thus, this process fulfills the requirements of a controlled/living polymerisation method (**Scheme 1.6**).[46]

There are a number of components to an ATRP system. The amount of initiator determines the number of growing polymer chains, which should be constant throughout the polymerisation. From the initiator and initial monomer concentration, the degree of polymerisation (DP) can be calculated according to **equation 1.3**:[47]

$$\mathrm{DP} = \frac{[\mathrm{M}]_o}{[\mathrm{I}]_o} \times \text{conversion} \qquad \textbf{Eqn. 1.3}$$

The choice of catalyst is crucial for determining K_{eq}. Copper is easily the most commonly used catalyst metal. Other transition metals such as iron,[48] nickel,[48] and ruthenium[49] have been used for ATRP grafting, but use of these metals is limited because of the cost effectiveness and versatility of copper.[47] Solvent can be used in ATRP, but bulk polymerisations are also common. A good ATRP system is characterised by a constant, low concentration of active species, and first order kinetics with respect to the monomer, shown in the following equation which refers to **Scheme 1.9** (**Eqn. 1.4**):[47]

$$R_p = k_p[M][P_n \bullet] = k_p K_{eq}[M][I]_o \times \frac{[Cu^{I}X/Lig]}{[Cu^{II}X_2/Lig]} \qquad \textbf{Eqn 1.4}$$

In the above equation, R_p is the rate of polymerisation, P• is the growing polymer chain, and X is the halogen, and assuming a constant concentration of radical species, the following conversion, and radical concentration–time plot should be seen (**Scheme 1.10**).

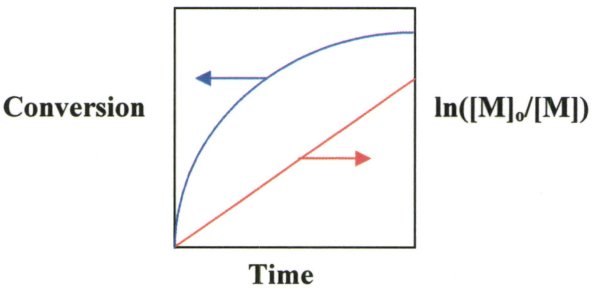

Scheme 1.10:

Schematic plot of conversion versus time assuming constant radical concentration.

The equilibrium between the active and dormant species results in the M_n control of ATRP, though at the cost of decreased polymerisation rates.[25] Termination of surface initiated radical chain ends may be greater than expected due to the proximity of the growing radical chains; however, the low steady state concentration of active radicals should counterbalance this effect when using ATRP, rather than FRP.[50]

1.2.2.3.1 Role of the Ligand in ATRP

The ligand used to complex the metal catalyst plays a key role in ATRP. These ligands, typically multidentate amines, can be used to modulate the solubility and activity of the catalyst. The ligand adjusts the oxidation potential of the catalyst through

electronic and steric effects,[51] which affects the equilibrium constant K_{eq} (**Scheme 1.9** and **Eqn. 1.9**).[52] It is important to match the catalyst activity with the inherent activity of the initiator and monomer.

The first reports of the ATRP of Sty and (meth)acrylic monomers involved using CuBr complexed with 2,2'-bipyridine (bipy).[53,54] Polydispersities were improved by the use of functionalised 4,4'-dialkyl bipy ligands, such as 4,4'-dinonyl-2,2'-dipyridyl (dNbipy), which has been shown to increase catalyst solubility (**Scheme 1.11**).[55-57]

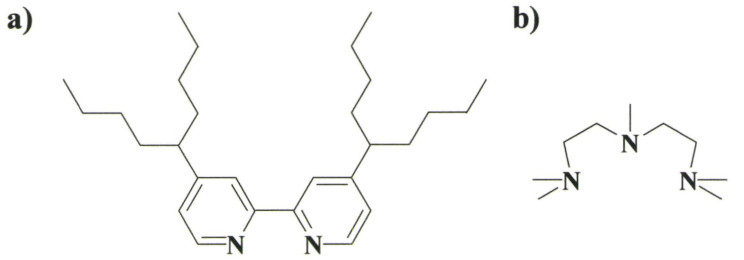

Scheme 1.11:

Schematic of **a)** 4,4'-dinonyl-2,2'-dipyridyl (dNbipy), and; **b)** *N,N,N',N'',N''*-pentamethyldiethylenetriamine (PMDETA) ligands.

Multidentate aliphatic amines, such as *N,N,N',N'',N''*-pentamethyldiethylenetriamine (PMDETA) (**Scheme 1.11 b**) are less expensive, more tunable and more accessible than the bipy ligands, yet still maintain control of the polymerisation.[51,57,58] Their copper complexes are less coloured due to the absence of π-bonding compared to the bipy ligands.[51] The coordination complexes of copper and simple amines often have lower redox potentials than those of Cu/bipy complexes, resulting in a shift in the equilibrium from the deactivated species to the activated species, increasing the radical concentration and the polymerisation rate.[51]

1.2.2.3.2 Role of Initiator in ATRP

The structure of the propagating initiator should match that of the monomer to be polymerised. For example, ATRP of Sty often employs (1-bromoethyl)benzene as an initiator, methyl acrylate (MA) uses methyl 2-bromopropionate (MBrP), and methyl methacrylate (MMA) is structurally similar to methyl 2-bromoisobutyrate (**Scheme 1.12**).

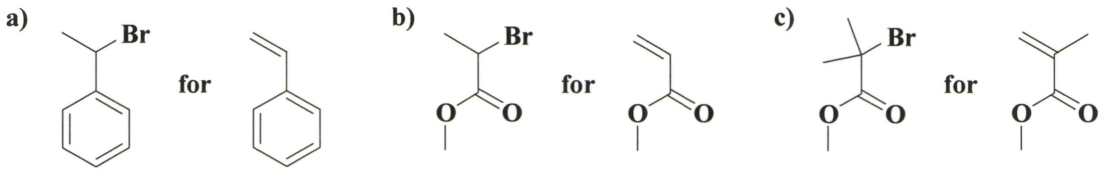

Scheme 1.12:

Select initiators for ATRP including **a)** (1-bromoethyl)benzene for Sty; **b)** MBrP for MA, and; **c)** methyl 2-bromoisobutyrate for MMA.

In this work MA and MMA have been polymerised using ethyl 2-bromopropionate (Et-2-BrP) and ethyl 2-bromoisobutyrate (Et-2-BriB) respectively, as initiating groups.

1.3 Substrates used for Grafting

Numerous surfaces have been explored for the ATRP grafting-from process including gold,[26,59] silicon,[11,23,29,30,60] silica surfaces,[61] and porous substrates.[25,62]

Controlled ATRP grafting from flat surfaces has proven difficult, showing a spike in film thickness growth at short polymerisation times, possibly owing to the low concentration of deactivating species (Cu^{II}), leading to uncontrolled polymerisation.[29,30] Addition of Cu^{II} to the polymerisation system has been used to reduce the radical

concentration and reduce the polymerisation rate and the degree of termination.[29] In another approach, "sacrificial" free initiator is added at the beginning of the polymerisation to lower the $[M]_0/[I]$ ratio, and increase the deactivator concentration.[30]

Several studies have reported that the rate of film thickness growth decreases with time, which suggests that termination is significant in surface initiated ATRP.[63-65]

Despite the plethora of work carried out on grafting from substrate surfaces bearing initiator groups, little work has been done involving polymeric microspheres. ATRP from such surfaces is not fully understood, and cleavage of the grafted polymer has proven challenging.

1.4 Polymeric Microspheres

Polymeric microspheres have seen widespread application in academia and in industry, as HPLC packing resins, scavenger resins, as well as solid supports for catalysis, and combinatorial synthesis. Microspheres can vary widely in their chemical properties as well as in size, porosity, swellability, and mechanical strength. There are a number of methods by which microspheres can be prepared, and characterised.

It has been proposed that surface modification of polymer microspheres with a dense layer of polymer chains may lead to improved separation in chromatography over porous or swellable substrates.[3] Grafting may also lead to resins with increased efficacy in solid phase synthesis.[3]

1.4.1 Preparation of Microspheres

Microspheres can be prepared by emulsion polymerisation, suspension polymerisation, dispersion polymerisation, multistep and dynamic seeded swelling polymerisations, and precipitation polymerisation. The method chosen here was precipitation polymerisation, and it will be discussed below.

1.4.1.1 Precipitation Polymerisation

Precipitation polymerisation does not require added surfactant or stabilizer, and thus the resultant microspheres have clean, uncharged surfaces. Lightly cross-linked, swellable monodisperse microspheres were desired for this study, and can be prepared by precipitation polymerisation. Our group has defined a number of variables that lead to monodisperse microspheres including: low monomer loading ($\leq$ 4 wt. %), a high cross-linking percentage ($\geq$ 5 wt. % relative to monomer), gentle agitation instead of stirring, and sub-*theta* solvency.[66,67] The theta condition is defined as the point where the chain is fully relaxed in the solvent, i.e. polymer-polymer and polymer-solvent interactions are equal. We need to be at sub-theta conditions, where the polymer, once it reaches a certain MW (approximately 2000) prefers polymer-polymer interactions and hence phase separates from the medium. This can be achieved by using a solvent that is more "polar" (with a high solubility parameter) than the polymer, or by using a solvent (or mixture of solvents) that is less polar (lower solubility parameter) than the polymer.

Precipitation polymerisation starts as a homogeneous solution of the radical initiator, such as 2,2'-azo-bis-(2-methylpropionitrile) (AIBN), and the monomer, or comonomers in a suitable solvent or solvent mixture. The first step of precipitation polymerisation is particle nucleation, in which soluble oligomers aggregate to form swollen microgels, and cross–linking induced desolvation of these aggregates results in the formation of particle nuclei. Microsphere growth occurs via the continuous capture of oligomeric radicals, which form a transient gel surface layer that provides colloidal stability (**Scheme 1.13**).[67-69] This surface gel layer subsequently desolvates through further cross–linking to become part of the dense microsphere core, and the cycle continues.[67] In the below example, divinylbenzene 80 (DVB80), a cross–linker, is polymerised.

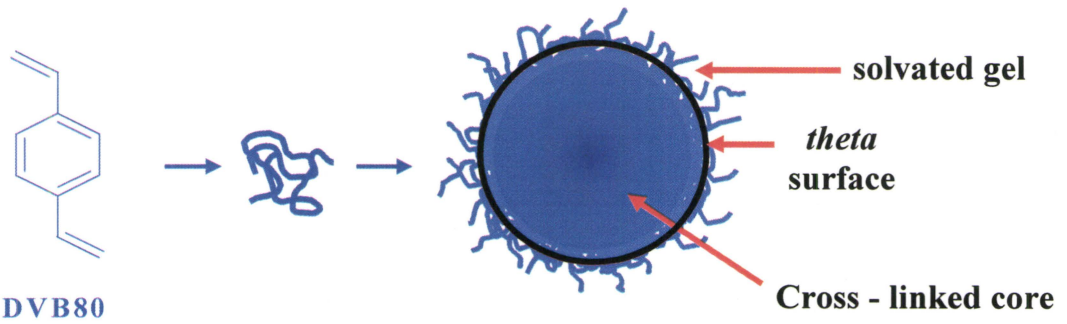

Scheme 1.13:

Formation of DVB80 particles by precipitation polymerisation.

The new particle surface is formed of newly captured oligomers, thus even the final particles have residual double bonds on their surfaces that can be further functionalised if desired. Such functionalisation can lead to high functional group

loading at or near the surface of the polymeric microspheres, where possible functional groups are alcohols, carboxylic acids, amines, and anhydrides.

A variety of functional precipitation polymerisation microspheres have been prepared by copolymerising DVB with 2-hydroxyethyl methacrylate (HEMA),[70] MMA,[70] MA,[70] glycidyl methacrylate ,[70] maleic anhydride,[71] or chloromethylstyrene.[72]

These polymeric microspheres do not have a hard surface, but a rather thin layer of swollen gel on their surface, as indicated in **Scheme 1.13**. Grafting–from has not been extensively explored from such surfaces, and this thesis will probe the effect of a gel layer on the ATRP grafting from polymeric microspheres, as well as the effect of this gel environment on ATRP polymerisation.

1.4.2 Microsphere Characterisation

Due to the solid nature of polymeric microspheres, techniques such as solution Nuclear Magnetic Resonance (NMR), or Gel Permeation Chromatography (GPC) can not be employed; however a number of microscopy techniques can be used for characterisation.

Size and surface morphology of microspheres was observed using an Environmental Scanning Electron Microscope (ESEM), which gives images from secondary electrons released from the samples. Samples are gold coated in order to ensure that they are sufficiently conductive to dissipate any charges developed during the analysis with the electron beam. Particle size and particle size distribution were determined using a Coulter Multisizer interfaced with a computer and fitted with a 50 μm

aperture tube. As the particles pass through the orifice in the aperture, there is a current drop, and this current drop is related to the diameter of the particles. Many particles may be measured in a short amount of time, which allows for good statistical data on the sample. Particle diameters were additionally determined from ESEM images using UTHSCA ImageTool software by measuring at least 100 microspheres. The internal structure of the polymer microspheres was studied using Transmission Electron Microscopy (TEM).

Cross–Polarisation Magic Angle Spinning (CPMAS) ^{13}C NMR is a technique used to determine the chemical structure of materials in the solid state. It has been used here to follow changes in the polymeric microspheres. In addition, Fourier-Transform Infrared spectroscopy (FT-IR) was used to track chemical changes in the polymeric microspheres.

Composition gradients can be determined using Scanning Transmission X-ray Microscopy (STXM), and this has been used to study the core shell composition of microspheres, [73] differentiate polyurethane films from polyurea,[74] and illustrate the effects of thermal imprinting on the phase separation of PSty and PMMA. The spatial resolution which can be achieved is near 50 nm, and the photon energy resolution is approximately 100 meV. The Near Edge X-ray Absorption Fine Structure (NEXAFS) spectral signal is the basis for chemical speciation in STXM, and used to quantitatively map the chemical composition of the material. In this work, the carbon 1s core edge has been used, where C 1s core electrons have been excited to the π^* and σ^* LUMO orbitals. [73] The energy absorbed is mapped out, to yield spatially resolved spectra of the material.

1.5 Cleavage of Grafted Polymers

Typical analytical techniques used to monitor the success of ATRP (control of M_n and polymer architectures) can not be directly applied to surface grafted polymers. A number of researchers have attempted to cleave the grafted chains from the solid surface so that they might be characterised. The polymerisation and cleavage sequence bears some similarities to solid–supported synthesis, and in fact, this approach could be envisioned as a solid–supported synthesis of narrow disperse polymers and block copolymers.

As with solid state organic synthesis, the use of mild reagents to remove the desired product from the resin would be advantageous. When the desired product has been attached to the resin via an activated ester, base catalysed transesterification has been used. Sodium methoxide (NaOMe) in a mixture of 4:1 tetrahydrofuran (THF) to methanol (MeOH) has proven efficacious when refluxed for 3–20 hours.[75-77]

Cleavage of grafted polymer from silica wafers has been attempted with I_2 or potential cycling,[78] or boiling NaOH.[79] Grafted polymer has been removed from silica nanoparticles by employing HF to degrade the silica.[80] When derivatised Wang and Merrifeld resins are used for grafting, they can be cleaved from the resulting polymer by treatment with trifluoroacetic acid (TFA).[5,81] NaOH was used to release grafts from functionalised PSty latex beads by hydrolysis.[33]

1.6 Thesis Objectives

The main purpose of this thesis is to examine the effect of the gel environment on ATRP grafting from polymeric microspheres. This gel environment is well understood in terms of the preparation of polymer microspheres by precipitation polymerisation. Previous studies involving the ATRP grafting of MA, MMA, 2-(dimethylamino)ethyl methacrylate (DMAEMA), saw dramatic weight and size increases.[82] Block copolymers were also grafted from the polymeric microspheres by re–initiation of a second monomer. However, the grafted polymer chains were not cleaved, and this is another objective of this thesis. The following Scheme illustrates the microsphere functionalisation and grafting to be carried out in this thesis.

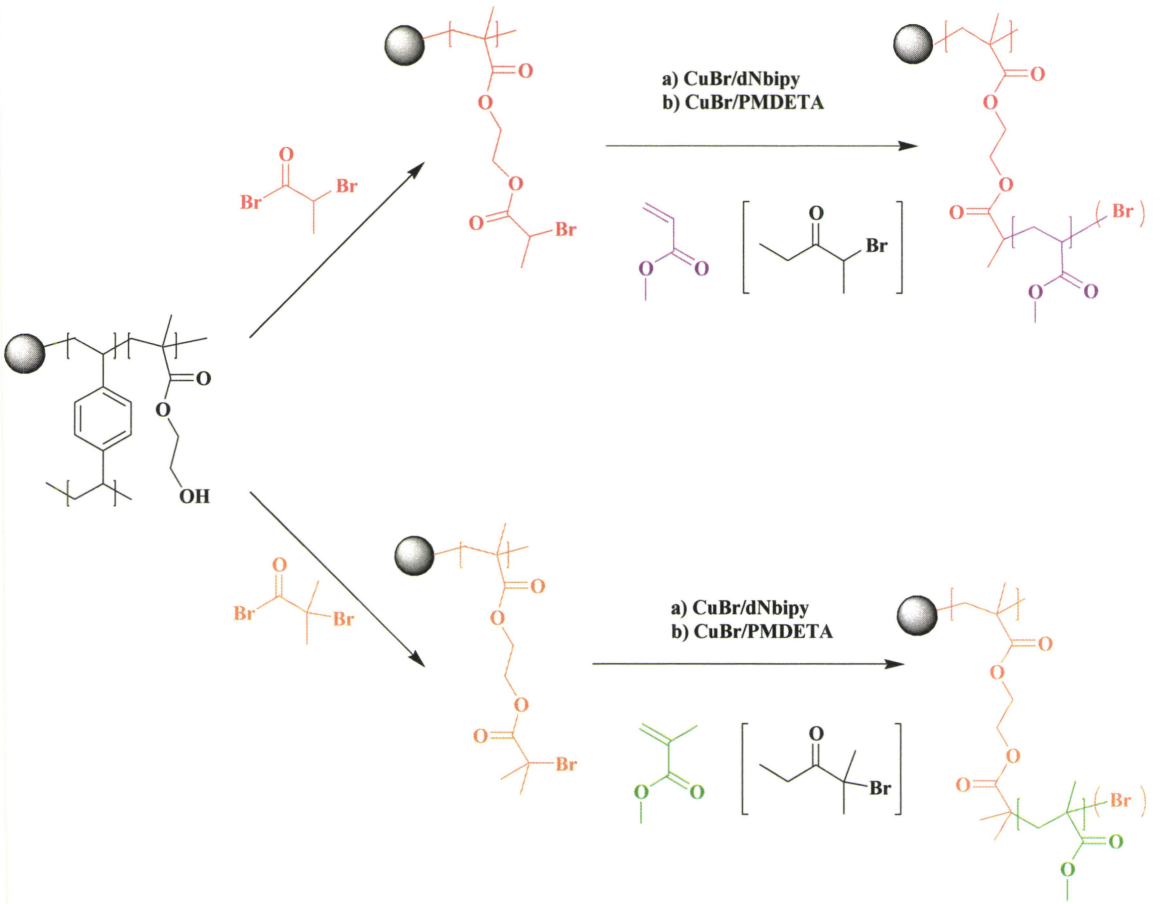

Scheme 1.14:

Chemical compositions of precursor particles (black), propionate initiator particles (red), isobutyrate initiator particles (orange), PMA grafted microspheres (purple), and PMMA grafted microspheres (green).

1.7 References

(1) Börner, H. G.; Matyjaszewski, K. *Macromol. Symp.* **2002**, *177*, 1.

(2) Yu, W. H.; Kang, E. T.; Neoh, K. G.; Zhu, S. *J. Phys. Chem. B* **2003**, *107*, 10198.

(3) Zheng, G.; Stöver, H. D. H. *Chinese Journal of Polymer Science* **2003**, *21*, 21.

(4) Sherrington, D. C. *J. Polym. Sci. Part A: Polym. Chem.* **2001**, *39*, 2364.

(5) Ayres, N.; Haddleton, D. M.; Shooter, A. J.; Pears, D. A. *Macromolecules* **2002**, *35*, 3849.

(6) Parvole, J.; Larulle, G.; Guimon, C.; Francois, J.; Billon, L. *Macromol. Rapid Commun.* **2003**, *24*, 1074.

(7) Odian, G. *Principles of Polymerization*; 3rd ed.; John Wiley & Sons, INC.: New York, 1991.

(8) Freemantle, M. *Chem. Eng. News* **2003**, *81*, 41.

(9) Brack, H.-P.; Padeste, C.; Slaski, M.; Alkan, S.; Solak, H. H. *J. Am. Chem. Soc.* **2004**, *126*, 1004.

(10) Jordan, R.; Ulman, A.; Kang, J. F.; Rafailovich, M. H.; Sokolov, J. *J. Am. Chem. Soc.* **1999**, *121*, 1016.

(11) Zhao, B.; Brittain, W. J. *J. Am. Chem. Soc.* **1999**, *121*, 3557.

(12) Ingall, M. D. K.; Honeyman, C. H.; Mercure, J. V.; Bianconi, P. A.; Kunz, R. R. *J. Am. Chem. Soc.* **1999**, *121*, 3607.

(13) Jones, D. M.; Brown, A. A.; Huck, W. T. S. *Langmuir* **2002**, *18*, 1265.

(14) Möller, M.; Nederberg, F.; Lim, L. S.; Kånge, R.; Hawker, C. J.; Hedrick, J. L.; Gu, Y.; Shah, R.; Abbott, N. L. *Journal of Polymer Science: Part A: Polymer Chemistry* **2001**, *39*, 3529.

(15) Zheng, G.; Stöver, H. D. H. *Macromolecules* **2003**, *36*, 7439.

(16) Husseman, M.; Mecerreyes, D.; Hawker, C. J.; Hedrick, J. L.; Shah, R.; Abbott, N. L. *Angew. Chem. Int. Ed.* **1999**, *38*, 647.

(17) Buchmeiser, M. R.; Sinner, F.; Mupa, M.; Wurst, K. *Macromolecules* **2000**, *33*, 32.

(18) Juang, A.; Scherman, O. A.; Grubbs, R. H.; Lewis, N. S. *Langmuir* **2001**, *17*, 1321.

(19) Liu, Y.; Adronov, A. *Macromolecules* **2004**, *37*, 4755.

(20) Pruker, O.; Rühe, J. *Macromolecules* **1998**, *31*, 602.

(21) de Boer, B.; Simon, H. K.; Werts, M. P. L.; van der Vegte, E. W.; Hadziioannou, G. *Macromolecules* **2000**, *33*, 349.

(22) Pruker, O.; Rühe, J. *Macromolecules* **1998**, *31*, 592.

(23) Ejaz, M.; Yamamoto, S.; Ohno, K.; Tsujii, Y.; Fukuda, T. *Macromolecules* **1998**, *31*, 5934.

(24) Yao, Z.; Braidy, N.; Botton, G. A.; Adronov, A. *J. Am. Chem. Soc.* **2003**, *125*, 16015.

(25) Huang, W.; Kim, J.-B.; Bruening, M. L.; Baker, G. L. *Macromolecules* **2002**, *35*, 1175.

(26) Kim, J.-B.; Bruening, M. L.; Baker, G. L. *J. Am. Chem. Soc.* **2000**, *122*, 7616.

(27) Zhao, B.; Brittain, W. J. *Macromolecules* **2000**, *33*, 8813.

(28) Perruchot, C.; Khan, M. A.; Kamitsi, A.; Armes, S. P.; von Werne, T.; Patten, T. E. *Langmuir* **2001**, *17*, 4479.

(29) Matyjaszewski, K.; Miller, P. J.; Shukla, N.; Immaraporn, B.; Gelman, A.; Luokala, B. B.; Siclovan, T. M.; Kickelbick, G.; Vallant, T.; Hoffmann, H.; Pakula, T. *Macromolecules* **1999**, *32*, 8716.

(30) Husseman, M.; Malmström, E. E.; McNamara, M.; Mate, M.; Mecerreyes, D.; Benoit, D. G.; Hedrick, J. L.; Mansky, P.; Huang, E.; Russell, T. P.; Hawker, C. J. *Macromolecules* **1999**, *32*, 1424.

(31) Wu, T.; Efimenko, K.; Genzer, J. *Macromolecules* **2001**, *34*, 684.

(32) von Werne, T.; Patten, T. E. *J. Am. Chem. Soc.* **2001**, *123*, 7497.

(33) Kizhakkedathu, J. N.; Takacs-Cox, A.; Brooks, D. E. *Macromolecules* **2002**, *35*, 4247.

(34) Yamamoto, K.; Tanaka, H.; Sakaguchi, M.; Shimada, S. *Polymer* **2003**, *44*, 7661.

(35) Miwa, Y.; Yamamoto, S.; Sakaguchi, M.; Shimada, S. *Macromolecules* **2001**, *34*, 2089.

(36) Vicklund, N.; Nordström, A.; Irgum, K.; Svec, F.; Fréchet, J. M. J. *Macromolecules* **2001**, *34*, 4361.

(37) Bartholome, C.; Beyou, E.; Bourgeat-Lami, E.; Chaumont, P.; Zydowicz, N. *Macromolecules* **2003**, *36*, 7946.

(38) Husseman, M.; Morrison, M.; Benoit, D.; Frommer, J.; Mate, C. M.; Hinsberg, W. D.; Hedrick, J. L.; Hawker, C. J. *J. Am. Chem. Soc.* **2000**, *122*, 1844.

(39) Kasseh, A.; Ait-Kadi, A.; Riedl, B.; Pierson, J. F. *Polymer* **2003**, *44*, 1367.

(40) Hodges, J. C.; Harikrishnan, L. S.; Ault-Justus, S. *J. Comb. Chem.* **2000**, *2*, 80.

(41) Yu, W.; Kang, E. T.; Neoh, K. G. *Industrial and Engineering Chemical Research* **2004**, *43*, 5194.

(42) Baum, M.; Brittain, W. J. *Macromolecules* **2002**, *35*, 610.

(43) Tsuji, Y.; Ejaz, M.; Sato, K.; Goto, A.; Fukuda, T. *Macromolecules* **2001**, *34*, 8872.

(44) Raula, J.; Shan, J.; Nuopponen, M.; Niskanen, A.; Jiang, H.; Kauppinenen, E. I.; Tenhu, H. *Langmuir* **2003**, *19*, 3499.

(45) Barnier, L.; Quinn, J. F.; Barner-Kowollik, C.; Vana, P.; Davis, T. P. *Eur. Poly. J.* **2003**, *39*, 449.

(46) Shipp, D. A.; Wang, J.-L.; Matyjaszewski, K. *Macromolecules* **1998**, *31*, 8005.

(47) Matyjaszewski, K.; Xia, J. *Chem. Rev.* **2001**, *101*, 2925.

(48) Yamamoto, K.; Miwa, Y.; Tanaka, H.; Sakaguchi, M.; Shimada, S. *Journal of Polymer Science: Part A: Polymer Chemistry* **2002**, *40*, 3350.

(49) Claes, M.; Voccia, S.; Detrembleur, C.; Jérôme, C.; Gilbert, B.; Leclère, P.; Geskin, V. M.; Gouttenbaron, R.; Hecq, M.; Lazzaroni, R.; Jérôme, R. *Macromolecules* **2003**, *36*, 5926.

(50) Kim, J.-B.; Huang, W.; Miller, M. D.; Baker, G. L.; Bruening, M. L. *J. Polym. Sci. Part A: Polym. Chem.* **2003**, *41*, 386.

(51) Xia, J.; Matyjaszewski, K. *Macromolecules* **1997**, *30*, 7697.

(52) Davis, K. A.; Paik, H.-J.; Matyjaszewski, K. *Macromolecules* **1999**, *32*, 1767.

(53) Wang, J. S.; Matyjaszewski, K. *J. Am. Chem. Soc.* **1995**, *117*, 5614.

(54) Wang, J.-S.; Matyjaszewski, K. *Macromolecules* **1995**, *28*, 7901.

(55) Patten, T. E.; Xia, J.; Abernathy, T.; Matyjaszewski, K. *Science* **1996**, *272*, 866.

(56) Matyjaszewski, K.; Patten, T. E.; Xia, J. *J. Am. Chem. Soc.* **1997**, *119*, 674.

(57) Xia, J.; Matyjaszewski, K. *Macromolecules* **1999**, *32*, 2434.

(58) Xia, J.; Gaynor, S. G.; Matyjaszewski, K. *Macromolecules* **1998**, *31*, 5958.

(59) Shah, R. R.; Merreceyes, D.; Husseman, M.; Rees, I.; Abbott, N. L.; Hawker, C. J.; Hedrick, J. L. *Macromolecules* **2000**, *33*, 597.

(60) Kong, X.; Kawai, T.; Abe, J.; Iyoda, T. *Macromolecules* **2001**, *34*, 1837.

(61) von Werne, T.; Patten, T. E. *J. Am. Chem. Soc.* **1999**, *121*, 7409.

(62) Ejaz, M.; Tsujii, Y.; Fukuda, T. *Polymer* **2001**, *42*, 6811.

(63) Ejaz, M.; Ohno, K.; Tsujii, Y.; Fukuda, T. *Macromolecules* **2000**, *33*, 2870.

(64) Jones, D. M.; Huck, W. T. S. *Adv. Mater.* **2001**, *13*, 1256.

(65) Kim, J.-B.; Haung, W.; Bruening, M. L.; Baker, G. L. *Macromolecules* **2002**, *35*, 5410.

(66) Li, K.; Stöver, H. D. H. *J. Polym. Sci. Part A: Polym. Chem.* **1993**, *31*, 3257.

(67) Downey, J. S.; McIsaac, G.; Frank, R. S.; Stöver, H. D. H. *Macromolecules* **2001**, *34*, 4534.

(68) Downey, J. S.; Frank, R. S.; Li, W.-H.; Stöver, H. D. H. *Macromolecules* **1999**, *32*, 2838.

(69) Li, W.-H.; Stöver, H. D. H. *J. Polym. Sci. Part A: Polym. Chem.* **1998**, *36*, 1543.

(70) Li, W.-H.; Stöver, H. D. H. *J. Polym. Sci. Part A: Polym. Chem.* **1999**, *37*, 2899.

(71) Frank, R. S.; Downey, J. S.; Stöver, H. D. H. *J. Polym. Sci. Part A: Polym. Chem.* **1998**, *36*, 2223.

(72) Li, W.-H.; Li, K.; Stöver, H. D. H. *J. Polym. Sci. Part A: Polym. Chem.* **1999**, *37*, 2295.

(73) Koprinarov, I.; Hitchcock, A. P.; Li, W.-H.; Heng, Y. M.; Stöver, H. D. H. *Macromolecules* **2001**, *34*, 4424.

(74) Croll, L. M.; Stöver, H. D. H.; Hitchcock, A. P. *Macromolecules* **2004**, *In print*.

(75) Frennette, R.; Friesen, R. W. *Tetrahedron Lett.* **1994**, *35*, 9177.

(76) Tietze, L. F.; Hippe, T.; Steinmetz, A. *Synlett.* **1996**, 1043.

(77) Kang, S.-K.; Kim, J.-S.; Yoon, S.-K.; Lim, K.-H.; Yoon, S. S. *Tetrahedron Lett.* **1998**, *39*, 3011.

(78) Haung, X.; Wirth, M. J. *Macromolecules* **1999**, *32*, 1694.

(79) von Natzmer, P.; Bontempo, D.; Tirelli, N. *Chem. Commun.* **2003**, 1600.

(80) Pyun, J.; Matyjaszewski, K.; Kowalewski, T.; Savin, D.; Patterson, G.; Kickelbick, G.; Huesing, N. *J. Am. Chem. Soc.* **2001**, *123*, 9445.

(81) Angot, S.; Ayres, N.; Bon, S. A. F.; Haddleton, D. M. *Macromolecules* **2001**, *34*, 768.

(82) Zheng, G.; Stöver, H. D. H. *Macromolecules* **2002**, *35*, 7612.

Chapter 2: Grafting Methyl Acrylate from Polymeric Microspheres

Abstract

Swellable microspheres were prepared by the precipitation co-polymerisation of DVB-80 and HEMA in a solvent mixture of methyl ethyl ketone (MEK) and heptane, and functionalised with 2-bromopropionyl bromide to prepare microspherical ATRP initiators.

The model ATRP of neat MA was carried out at 70°C with CuBr and either dNbipy, or PMDETA ligands using ethyl 2-bromopropionate (Et-2-BrP) as an analogous small molecule initiator. Homopolymers of M_n of 7 000 g/mol and 7 400 g/mol, respectively, were expected, where a M_n of 9 400 g/mol and PDI of 1.06 (dNbipy), and 10 500 g/mol with a PDI of 1.07 (PMDETA) were obtained.

MA grafting from the swellable microspheres using either of these catalyst systems in bulk at 70 °C was compared to the model polymerisation results above, in order to draw conclusions about the effect of the gel environment on ATRP grafting from microspheres. The morphology of the grafted microspheres was studied using electron microscopy (ESEM and TEM) and x-ray microspectroscopy, and very high weight gains were observed, with particle sizes increasing from 1.8 μm to 4.0 μm with dNbipy, and to 3.0 μm with PMDETA. Adding sacrificial initiator ethyl 2-bromopropionate (Et-2-BrP) to the grafting polymerisations increased the particle sizes to 4.3 and 3.2 μm, indicating a more controlled grafting polymerisation. As well, the soluble polymer showed good PDI

control (M_n of 3200 g/mol and a PDI of 1.08 with the dNbipy catalyst, and M_n of 5000 g/mol and PDI of 1.11 with the PMDETA ligand)

Between 90-95 % of the grafted PMA could be cleaved by base catalysed transesterification with NaOMe in a swellable environment for the microspheres. The cleaved polymer had an M_n of 7000 g/mol and a PDI of 1.14 (dNbipy), and when free initiator was added, an M_n of 5 800 g/mol with a PDI of 1.03. Similarly, PMA of M_n 7 500 g/mol and PDI of 1.21 was observed for cleaved PMA grafted using PMDETA, and this became 1 800 g/mol with a PDI of 1.13 with "sacrificial" initiator.

It was found that the M_n of the soluble polymers were generally 2 to 3 times higher than those of the cleaved polymer; therefore the assumption that the M_n of the soluble polymer is similar to that of the grafted polymer did not apply for grafting MA from swellable P(DVB80-*co*-HEMA) microspheres under the present conditions.

2.0 Overview

Polyacrylates are an important family of polymers with many industrial uses such as adhesives and toners, and a wide range of monomers available. They have been the target of many ATRP's. In spite of this, the use of solid supports for the grafting of acrylate monomers by ATRP has been limited.

2.1 Background

Because there are a number of variables to consider in bulk or grafting ATRP, such as the structure of the initiator, chelating ligand, and solvent, the model solution ATRP of MA will be discussed here, followed by a brief review of grafting MA from surfaces.

2.1.1 Solution Polymerisation of Methyl Acrylate

Propionate initiators such as Et-2-BrP are best suited for the polymerisation of acrylates (**Scheme 2.1**), since the structure of the propagating carbon radical is the same.

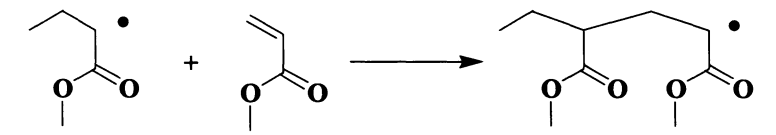

Scheme 2.1:

MBrP initiator radical, and MA propagating radical.

Matyjaszewski and coworkers found that MA can be polymerised in bulk with CuBr/bipy and MBrP with M_n of 29 000 g/mol (where $M_{n,th}$ was 27 500 g/mol) and a narrow PDI of 1.15,[1] they have also determined that the polar solvent ethylene carbonate is a suitable solvent for the polymerisation of MA[2].

In contrast, Semsarzadeh *et al.* used MBrP in a combination with CuCl/bipy or CuCl/PMDETA to polymerise MA in bulk and obtained only low M_n and polydisperse (PDI of 1.42) PMA.[3] Both PDI and molecular weight control were improved by the addition of the polar solvents butanol or acetonitrile (MeCN).[3]

2.1.2 Grafting from Flat Surfaces

In a study by Matyjaszewski *et al.*[4] acrylates and styrene were grafted from silicon wafers, and the effect of monomer diffusion to the growing surface, and its effect on PDI with time was observed. The authors concluded that initiator density on the substrate dictates whether film growth depends linearly on reaction time. They did not consider how the heterogeneous system affected chain termination, and cleavage was not attempted.

Kim *et al.*[5] examined grafting of MA and MMA from thiol functionalised gold surfaces carrying propionate initiators, and using $CuCl/CuBr_2$/Tris[2-(dimethylamino)ethyl]amine (Me_6TREN) in a binary mixture of THF and MeCN at room temperature (r.t.) At low catalyst concentration, growth of the film was slow, whereas at high catalyst concentration, rapid initial growth was followed by a decrease in the polymerisation rate, which was attributed to termination, loss of active catalyst or limited diffusion of the monomer to the growing radical chains.[5] Ejaz *et al.*[6,7] confirmed these findings by grafting MMA from surface attached arenesulfonyl chloride groups using CuBr/4,4'-di-*n*-heptyl-2,2'-bipyridine (dHbipy), and further found that stirring enhanced termination by increasing radical recombination.[5] Neither group attempted cleavage of the grafted chains.

MA was grafted from cellulose fibres, where the hydroxyl groups of the cellulose were functionalised with bromoisobutyrate initiator groups.[8] Grafting was carried out using $CuBr/Me_6TREN$ in the presence of "sacrificial" initiator in ethyl acetate.[8] The MWD of the free polymer was quite low (< 1.1) regardless of the sample, however the

targeted and observed DP varied considerably.[8] The grafted polymer was not cleaved from the cellulose surface for testing, nor was the grafting monitored gravimetrically due to the small amount of grafted polymer.[8]

In summary, ATRP grafting from flat surfaces has proven difficult, and has been observed as a spike in film thickness growth at short polymerisation times, possibly owing to the low concentration of initiator.[4,9] This low initiator concentration results in an initially low concentration of deactivator (Cu^{II}), and thus uncontrolled grafting, which is observed as a spike in film thickness. Therefore, Cu^{II} has been added at the beginning of the polymerisation in order to gain control over the grafting, such that a linear relationship between film thickness and conversion, and M_n of the soluble polymer is observed.[4] Conversely, "sacrificial" free initiator addition serves to lower the $[M]_o/[I]$ ratio, and increase the overall initiator concentration, thereby increasing the deactivator concentration.[9]

2.1.3 MA Grafting from Polymeric Microspheres

MA was previously grafted from swellable P(DVB80-*co*-HEMA) particles functionalised with propionate initiator groups, using the CuBr/1,4,8,11-tetramethyl-1,4,8,11-tetraazacyclotetradecane (Me_4Cyclam) catalyst system in THF.[10] A weight gain of 157 % was observed and the microspheres increased in size from 1.4 μm to 2.2 μm. Since surface grafting alone would lead to size increases on the order of 50 to 100 nm, it was concluded that grafting was carried out from the surface as well as from initiator sites within the particles. Due to a compositional gradient of the initiator species, a

grafting gradient was expected, since the initiator at the surface is more concentrated and easily accessible than the subsurface initiator.[10] The size and weight increases did not correspond, and this was attributed to the different densities of the initiator microspheres and the grafted microspheres, in other words, induced porosity from grafting.

2.1.4 Chapter Objective

The first objective was to prepare monodisperse swellable P(DVB80-*co*-HEMA) particles by adjusting the solvent in the precipitation polymerisation to just below the theta-conditions. Functionalisation was then carried out to prepare microspherical ATRP initiators (**Scheme 1.14**). After grafting from these initiator microspheres, a method for the cleavage of the grafted material was developed, to test the M_n and MWD of grafting from polymeric microspheres in a gel environment.

2.2 Experimental Section

Chemicals

Ethanol (anhydrous) was purchased from Commercial Alcohols Inc. and used as received. Alumina, basic, Brockman activity I (60–325 mesh) was purchased from Fisher Scientific and used as received. Ammonium hydroxide (NH_4OH) (28 %) was purchased from Anachemia and used as received. Acetone (reagent), dichloromethane (CH_2Cl_2) (distilled in glass), diethyl ether (99 %), heptane (99 %,), methanol (MeOH) (99.8 %), and methyl ethyl ketone (MEK) (99 %) were purchased from Caledon, and

used as received. 2-Bromopropionyl bromide (97 %), 4,4'-dinonyl-2,2'-dipyridyl (dNbipy) (97%), divinylbenzene 80 (DVB80) (mixture of isomers), ethyl 2-bromopropionate (99 %), 2-hydroxyethyl methacrylate (HEMA) (97 %), *N,N,N',N'',N''*-pentamethyldiethylenetriamine (PMDETA) (99 %), sodium methoxide (NaOMe) (25 wt. % in MeOH), and triethylamine (Et_3N) (99 %) were purchased from Aldrich, and used as received. 2,2'-Azo-bis-(2-methylpropionitrile) (AIBN) (Eastman Kodak Co.) was recrystallised from MeOH. Tetrahydrofuran (THF) (99+ %, Caledon) was refluxed over potassium and distilled under nitrogen. Methyl acrylate (MA) (99 %, Aldrich) was passed through an inhibitor removal column prior to use. CuBr was prepared by the reaction of $Cu(II)Br_2$ (99 %, Aldrich) with dimethyl malonate (99 %, Aldrich) according to the procedure outlined in the literature.[11]

Preparation of Precursor DVB80-co-HEMA Particles (E1)

The procedures by Li and Stöver,[12] and Zheng and Stöver[10] were followed here, with adjustments. Precursor particles, poly(DVB80-*co*-HEMA) (E1), were prepared by precipitation polymerisation in a mixture of MEK and heptane. DVB80 (2.63 g, 20 mmol), HEMA (12.37 g, 95 mmol), AIBN (0.3 g, 1.8 mmol), MEK (400 mL), and heptane (100 mL) were placed in a 500 mL polyethylene bottle and shaken vigorously. The bottle was placed in a reactor equipped with horizontal rollers and a programmable thermostat; the bottle was allowed to roll at 4 rpm while the temperature was increased from r.t. to 60 °C over an hour, followed by ramping to 70 °C over 100 minutes, and maintained at 70 °C for 24 hours. The resulting particles were washed three times with

THF, and once with diethyl ether. The yield of the clean particles was 7.5 g (50 %) after drying under vacuum at r.t. for 7 days.

Preparation of Propionate Initiator Particles (E1PBr)

Adjustments were made to the procedure outlined by Zheng and Stöver,[10] as noted below. Precursor particles (4.00 g) were suspended in THF (40 mL) and Et_3N (5.12 g, 51 mmoles) in a 100 mL round-bottomed flask for 2 h under nitrogen. The round-bottomed flask was placed in an ice-water bath prior to dropwise addition of 2-bromopropionyl bromide (10.78 g, 50 mmoles). The suspension was allowed to come to r.t. and stirred under nitrogen overnight. The initiator particles were washed with THF (3x), a mixture of THF and MeOH (3x), MeOH (3x), and finally diethyl ether (1x). The yield of the clean particles was 6.05 g after drying under vacuum at r.t. for 7 days, corresponding to esterification of 80 % of the HEMA groups.

Preparation of CuBr

CuBr was prepared by the reduction of $CuBr_2$ according to the procedure by Zheng and Stöver.[11] $Cu^{II}Br_2$ (10.0g, 44.8 mmol) was added to a solution of 25 mL of dimethyl malonate and 25 mL of THF, and the mixture was allowed to reflux for 3 hours. The light yellow precipitate was isolated by filtering over a 0.5 μm membrane filter and washed with methanol and hexane while under a nitrogen atmosphere. The resulting CuBr (6.19 g, 96.3 %) was stored under nitrogen prior to use.

Bulk Homopolymerisation of Methyl Acrylate (MA)

The bulk homopolymerisation of MA with CuBr/dNbipy was based on the literature procedure by Davis *et al.*,[13] with slight adjustments. Under a nitrogen environment, a 10 mL round bottom flask equipped with a stir bar, was charged with CuBr (83.3 mg, 0.58 mmol), and dNbipy (474.8 mg, 1.16 mmol) or PMDETA (100.5 mg, 0.58 mmol)[14]. The flask was then covered with a rubber septum, and previously deoxygenated MA (5.00g, 58 mmol) was added via syringe to the flask. The reaction mixture was allowed to stir at r.t. until it became homogeneous. Et-2-BrP (105.1 mg, 0.58 mmol) was added via a nitrogen filled syringe, and the solution was allowed to stir in order to obtain a homogeneous distribution of initiator prior to placing the round bottom flask in an oil bath equilibrated to 70 °C. The reaction was followed by removing 0.2 mL aliquots every 60 minutes, and was found to be complete after 9 hours. Polymeric solutions were diluted with THF prior to passing through a basic alumina column. The polymeric solution was precipitated into pentane and dried for 24 hours under vacuum (3.22 g, 64 % for dNbipy).

Methyl Acrylate Grafted Particles (E1-PMA-Br)

The procedure of the bulk polymerisation of MA was used with the exception that propionate initiator particles (177.0 mg) were added to a 10 mL round bottom flask equipped with a stir bar first, and the small molecule initiator, Et-2-BrP was not used for every grafting procedure. 0.2 mL aliquots were removed from the reaction flask every 1 hour, until the reaction was terminated after 9 hours. For the studies in which free

initiator was to be used, Et-2-BrP (105.14 mg, 0.58 mmol) was added via a nitrogen filled syringe. The particles were washed with THF (3x), a 9:1 mixture of THF:MeOH containing 1 % NH_4OH (3x), followed by a final wash with THF. The clean white particles were allowed to dry for 7 days under vacuum at r.t. yielding 1.48 g of E1-PMA-Br. The washings were combined and reduced in volume, to remove methanol and excess THF. The polymeric solution was dissolved in THF, passed through a basic alumina column, precipitated into pentane, and the resulting fluffy light yellow polymer was dried for 24 hours (0.15 g, 3 %).

Cleavage of Grafted P(MA) from Methyl Acrylate Grafted Particles (E1-PMA$_{cleaved}$-Br)

MA grafted propionate initiator particles (1.00g), THF (50 mL), and MeOH (12.5 mL), were placed in a 100 mL round bottom flask equipped with a condenser, and allowed to stir under nitrogen for 2 hours. NaOMe (3.0 g, 56 mmol) was added via a nitrogen filled syringe. The reaction mixture was brought to reflux, and allowed to continue refluxing, while under nitrogen for 96 hours. The resultant microspheres were washed with THF (3x), a 9:1 THF: MeOH mixture (3x) and distilled water (3x) to remove any residual sodium salts. Beige coloured particles remained (150 mg). The soluble polymer was isolated from the washings by first reducing the volume of the THF and MeOH mixture, dissolving the residue in CH_2Cl_2 and washing with water to remove any sodium salts. The CH_2Cl_2 was removed and the polymer was dissolved in THF for GPC analysis.

Homopolymerisation of Methyl Acrylate in the presence of precursor DVB80-co-HEMA particles (PMA_{E1})

E1 precursor particles (0.179 g) were allowed to swell in MA (5.00g, 58 mmol) under a nitrogen atmosphere for 0.5 hours. CuBr (83.31 mg, 0.58 mmol), and dNbipy (474.83 mg, 1.16 mmol) were then added under a nitrogen environment, and the solution was allowed to stir for an additional 15 minutes prior to the addition of Et-2-BrP (105.14 mg, 0.58 mmol) via a nitrogen purged syringe. The round bottom flask was then immersed in a 70°C oil bath. After 9 hours, the microspheres were washed with THF (3x), and with diethyl ether (1x), yielding a white solid (0.175 g). The washings were combined and reduced in volume, to remove diethyl ether, and passed through a basic alumina column. This polymeric solution was precipitated into pentane, and the fluffy white polymer was dried for 24 hours (3.81 g, 76 %).

Swelling Measurements

Swelling measurements were carried out in NMR tubes, where the desired microspheres were tightly packed into the bottom of the tube, and the height of microspheres was noted. Solvent or monomer was added via a syringe such that the liquid was administered beneath the microspheres. The initial solvent volume was noted. Changes in the particle and solvent volume was noted every 24 hours for 120 hours in order to allow the particles to settle, and then averaged.

Characterisation

Coulter Multisizer

Particle size and particle size distribution were determined using a 256 channel Coulter Multisizer II interfaced with a computer and fitted with a 50 μm aperture tube. A suspension of particles in a 1:1 mixture of acetone and ethanol was added to 25 mL of Coulter Isoton II electrolyte solution and stirred with the mini-stirrer supplied for 2 min prior to analysis, in order to disperse the sample thoroughly in the Isoton solution.

CPMAS-NMR

CPMAS-NMR was performed on a Bruker AV300 MHz, at a spinning rate of 10 kHz.

ESEM

Particle size and the surface morphology of the microspheres were observed using a Philips ElectroScan 2020 Environmental Scanning Electron Microscope. Samples were prepared by dispersing the sample in THF before casting a drop of the particle suspension on a piece of microscopy glass cover adhered to an ESEM stub. The samples were dried for 24 hours prior to sputter coating with 5 nm of gold.

FT-IR

FT-IR analysis was performed on a Bio–Rad FTS–40 FT–IR spectrometer. Samples were prepared with spectroscopic grade KBr, and pressed into pellets with a

Carver press at 15 000 psi. Spectra were scanned from 4000–400 cm^{-1} in the transmission mode, accumulating 128 scans with a resolution of 2 cm^{-1}.

STXM

STXM was performed on the polymer beamline 5.3.2 at the ALS light source. Sample preparation consisted of first embedding the sample in a resin mixture of trimethylolpropane triglycidyl ether (TTE) and 4,4'-methylenebis (2-methylcyclohexylamine (MMHA) (**Scheme 2.4**) then microtoming the samples to 40–60 nm thickness, in order to obtain cross–sections of the microspheres.

TEM

The internal structure of the polymer microspheres was studied using Transmission Electron Microscopy (TEM) using a JEOL 1200EX transmission electron microscope. Samples were prepared in the same way as for STXM. Staining of the samples was not required since there was sufficient contrast between the sample and the resin.

UTHSCA Image Tool

Particle diameters were determined using UTHSCA ImageTool software by measuring at least 100 microspheres.

2.3 Results and Discussion

The purpose of this work is to study grafting of MA from gels. Although numerous research groups have studied ATRP grafting from flat surfaces, nanotubes, and hard particles, grafting from polymeric surfaces has not been developed fully. There has been difficulty cleaving the resulting grafted polymer to test for M_n and PDI in the literature, additionally extremely large weight gains and size increases have been observed. The approach taken here was to start with monodisperse microsphere substrates coated with a gel layer. Following functionalisation with initiator, grafting was carried out under ideal conditions for both the monomer as determined from the solution polymerisation, and the substrate as determined from swelling measurements. Cleavage of the resulting grafted polymer gave insight into the grafting process from surface bound initiators in a gel environment.

2.3.1 Preparation of Precursor Particles with Hydroxyl Groups

Monodisperse precipitation particles were prepared by copolymerising DVB80 and HEMA, where DVB80 is a commercial mixture of 80 % divinylbenzenes and 20 % ethylstyrenes. Swellable, lightly cross-linked microspheres were obtained when 82.5 % HEMA and 17.5 % DVB80 were copolymerised (E1 particles).[10] This is the minimum amount of cross-linker that can be used in precipitation polymerisation in the formation of discrete polymeric particles.

Such precipitation particles were previously prepared in MeCN,[10,12] however they were not monodisperse. In order to prepare monodisperse particles, different solvents were examined, of which a mixture of MEK and heptane proved the best. Mixtures ranging from 100 % MEK to 100 % heptane were prepared, where narrowly dispersed particles were obtained between 40 and 90 % MEK (see **Figure 2.1**). The solubility parameter δ for heptane is 15.1 $MPa^{1/2}$, and 19.0 $MPa^{1/2}$ for MEK, whereas for MeCN it is 24.3 $MPa^{1/2}$.[15] Between 40 and 90 % MEK, the overall solubility parameter δ_m ranges between 16.7 and 18.6 $MPa^{1/2}$ according to **equation 2.1**.[15]

$$\delta_m = \phi_1\delta_1 + \phi_2\delta_2 \qquad \textbf{Eqn 2.1}$$

In the above equation ϕ is the volume fraction. At 100 % MEK the solubility parameter is 19.0 $MPa^{1/2}$, and the particles are beginning to coagulate, implying that 100 % MEK is too good a solvent.

Subsequently, all E1 particles were prepared with MEK/heptane of 80:20, where the particle diameter showed a lower standard deviation as measured by UTHSCA ImageTool (**Figure 2.1d**), and showed the best hexagonal close packing.

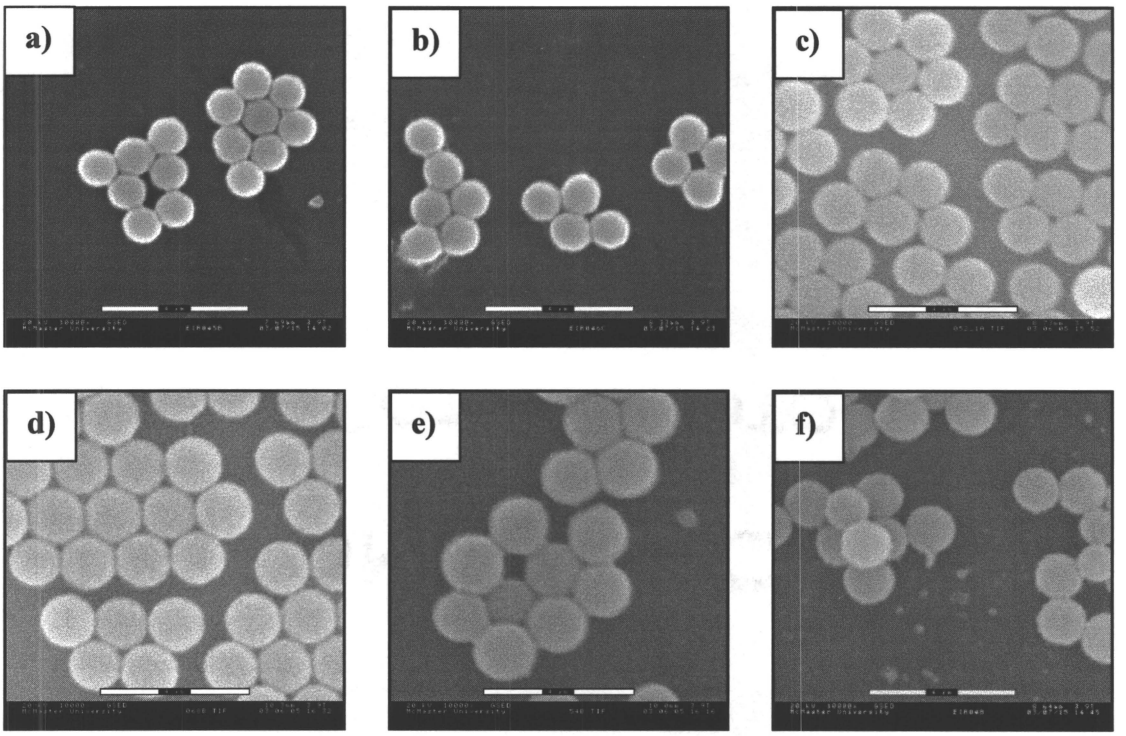

Figure 2.1:

ESEM images of E1 particles prepared in the following ratios of MEK to heptane: **a)** 40:60; **b)** 60:40; **c)** 70:30; **d)** 80:20; **e)** 90:10; **f)**100:0 (scale bars are 4μm).

Monomer loading was also examined in the range of 2 % to 4 % (**Figure 2.2**), where monodisperse particles were prepared; 3 % monomer loading was used again because of the lowest standard deviation ($1.6 \pm 0.2_0$ μm) as measured by UTHSCA ImageTool (**Figure 2.2b**). The effect of doubling the monomer loading from 2 % to 4 % does not have a dramatic effect on the diameter of the particles which increased from 1.5 $\pm 0.2_6$ μm to $1.8 \pm 0.2_5$ μm.

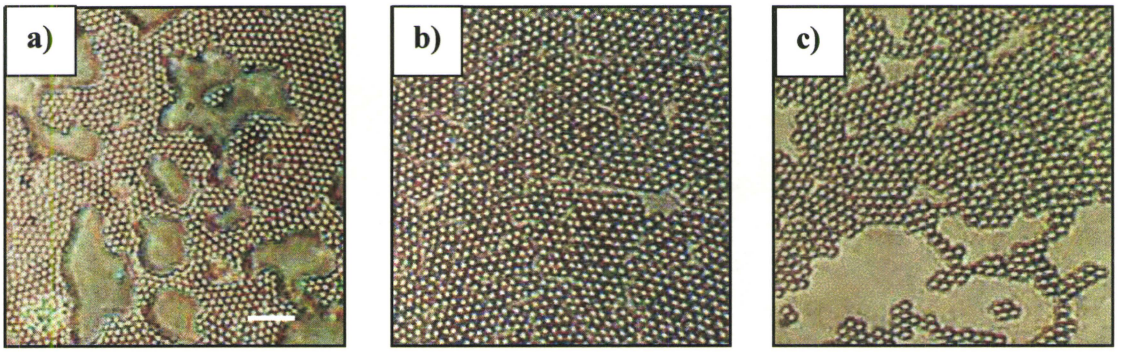

Figure 2.2:

Optical microscopy images of E1 particles prepared using the following monomer loadings: **a)** 2 %; **b)** 3 %; **c)** 4 % (scale bar is 8μm).

Particle size at 3 % monomer loading was found to be 1.6 ± 0.2 μm by Coulter Multisizer. A typical Coulter size distribution is plotted below (**Figure 2.3**).

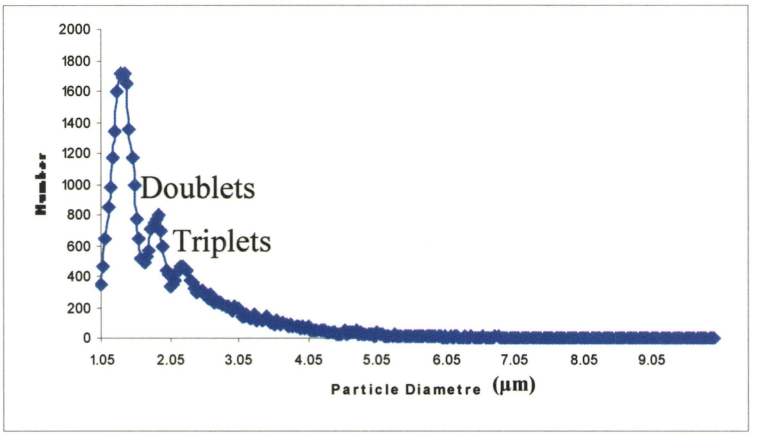

Figure 2.3:

Typical Coulter Multisizer spectrum.

The number average particle diameter, $\overline{Dn}$, and the coefficients of variation, CV, are calculated on a computer attached to the Coulter Multisizer. In the above figure, there are also artifacts due to aggregates of 2 (doublets), and 3 microspheres (triplets)

which result when 2 or more particles pass through the orifice at the same time, hence particle size and size distributions are calculated only according to the main peak.

It was found that these lightly cross-linked particles were swollen in a variety of organic solvents (**Table 2.1**) as was expected. THF was tested for swelling since it was to be used as the solvent for esterification, and MeOH was tested since it was to be used in the work-up of the functionalised microspheres in order to remove any unfunctionalised initiators. Water and ethanol were also tested for comparison.

Table 2.1:

Swelling ratios of E1 particles in a number of common organic solvents:

Solvent	Swelling ratio (%)
Ethanol	190
H_2O	160
MeOH	140
THF	170

The swelling ratio was calculated according to the following equation (**Eqn 2.2**):

$$\text{Swelling ratio} = \frac{\text{Particle volume}_{\text{solvent}}}{\text{Particle volume}_{\text{dry}}} \times 100\% \qquad \textbf{Eqn 2.2}$$

TEM was used to examine the cross-section of these microspheres prepared in 80:20 MEK to heptane. A typical cross-section of E1 particles can be seen in **Figure 2.4**, where there is a dark central core outlined by a lighter shell, which is roughly 200 nm in thickness.

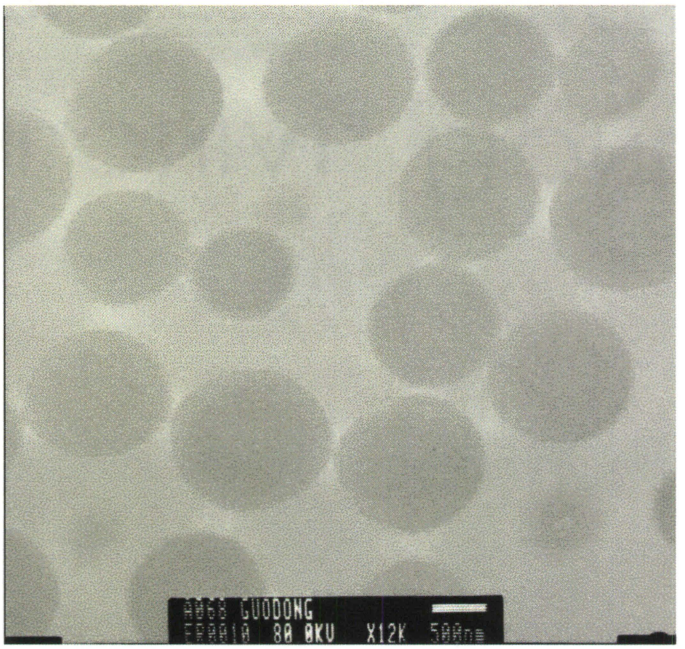

Figure 2.4:

TEM of cross–section of E1 particles (scale bar is 500 nm).

The free radical reactivity ratios for Sty and MMA (two monomers similar to DVB and HEMA) are both about 0.5.[16] This implies that the two monomers, DVB80 and HEMA, when copolymerised, tend towards an alternating copolymer structure. Since the amount of DVB80 is less than that of HEMA, DVB80 is consumed more rapidly and preferentially located in the core. The dark core is hence more highly cross–linked than the outer lighter shell, which consists primarily of HEMA. This outer HEMA rich shell is approximately 200 nm thick, and its OH groups would be expected to be more readily accessible. The average chemical structure of the E1 particles is shown below (**Scheme 2.2**):

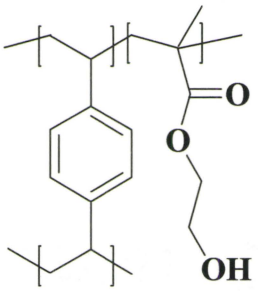

17.5 % **82.5 %**

Scheme 2.2:

Average structure of E1 particles containing both DVB and HEMA.

2.3.1.1 Study of Precursor Particles by FT-IR

The E1 microspheres show the expected stretches for HEMA (3466 cm^{-1}, and 1724 cm^{-1}), however, the expected stretches for DVB at 1603 cm^{-1} and 1511 cm^{-1} are hidden in the background (**Figure 2.5**).

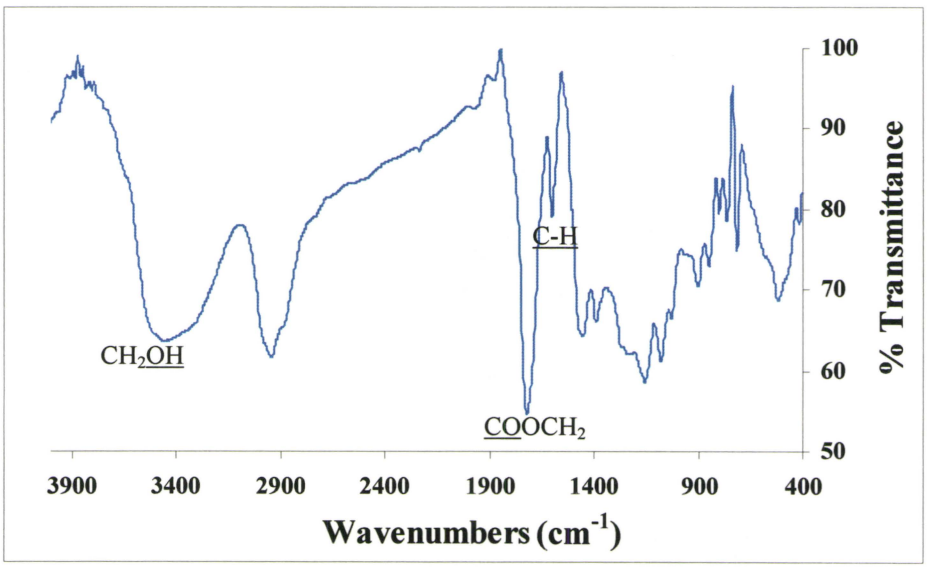

Figure 2.5:

FT-IR Spectrum of E1 particles in the transmission mode.

2.3.1.2 Study of Precursor Particles by CPMAS-NMR

CPMAS-NMR was used to confirm the composition of the E1 particles (**Figure 2.6**) and peaks consistent with both DVB (145.6 ppm, and 127.1 ppm) and HEMA (177.2 ppm, 66.2 ppm, 59.9 ppm, 44.9 ppm, and 18.7 ppm) were observed.

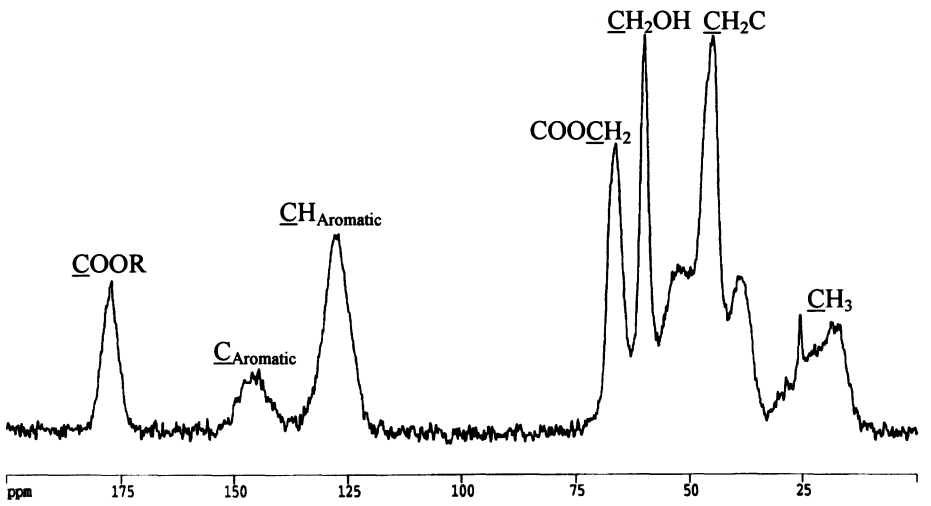

Figure 2.6:

CPMAS-NMR spectrum of E1 particles.

2.3.1.3 Study of Precursor Particles by STXM

STXM was used to examine the spatial distribution of the carbonyl and aromatic groups in the E1 particles as seen in **Figure 2.7**. The relative contributions of the aromatic and carbonyl absorptions (285 and 289 eV, respectively) are similar in the three regions examined (blue, brown, and green); however there is a slight decrease in area under the blue peak on the right shoulder in the aromatic region. Thus, STXM is able to detect a slight gradient in the DVB/HEMA content that was expected.

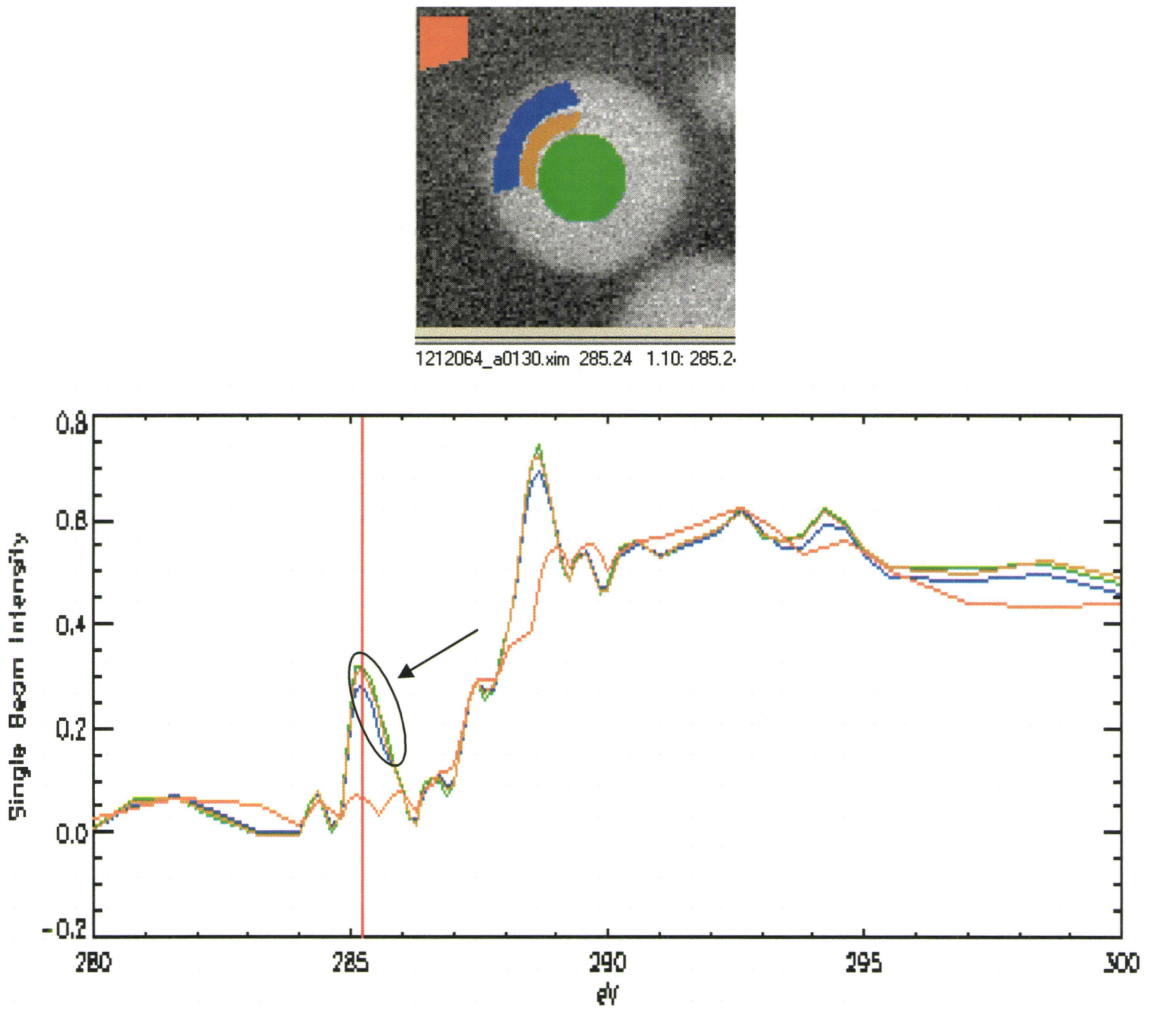

Figure 2.7:

STXM scan of DVB80-*co*-HEMA particles.

2.3.2 Preparation of Propionate Initiator Particles

Hydroxyl groups on the E1 seed particles were treated with a 2:1 excess of 2-bromopropionyl bromide / Et_3N in THF to give 80 % esterification (**Scheme 2.3**) as determined by weight gain, FT-IR and CPMAS-NMR.

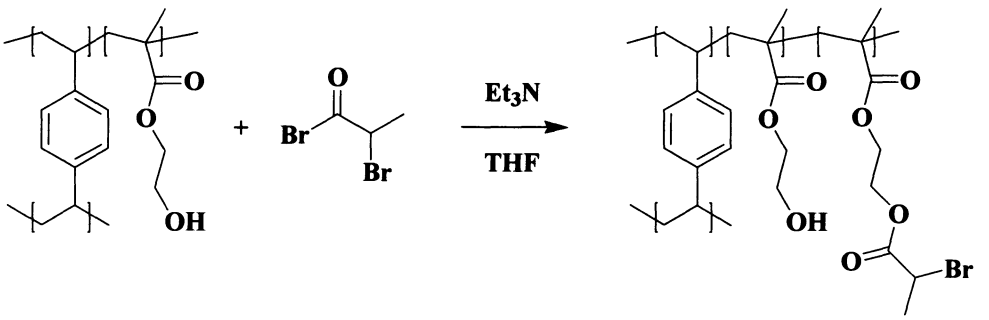

Scheme 2.3:

Preparation of E1PBr microspheres from E1 particles.

Functionalisation can be varied by changing the molar ratio of reagent to precursor particle (**Table 2.2**).

Table 2.2:

Functionalisation of E1 particles in the formation of E1PBr particles:

2-bromopropionyl bromide: HEMA	Esterification (%)
0.8:1	50
1:1	63
2:1	80

The size of the microspheres increased from an average diameter of 1.6 ± 0.2 μm to 1.8 ± 0.2 μm upon functionalisation. The surfaces remained smooth, and the particles pack in a crystalline hexagonal array, and are quite monodisperse (**Figure 2.8a**). The core shell morphology previously discussed appears to be more distinct post functionalisation (**Figure 2.8b**). The core, which was uniform in the E1 particles, is now grainy. Knife cutting artifacts, which occur when the particle is harder than the resin, are apparent in the core. The outer 200 nm shell remains.

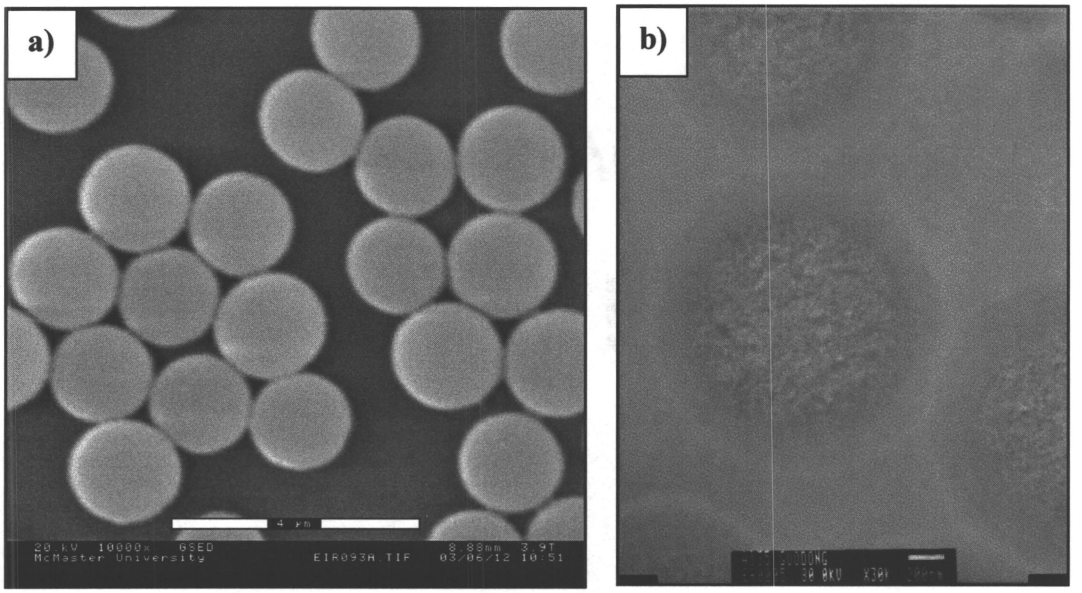

Figure 2.8:

E1PBR particles: **a)** ESEM (scale bar is 4 μm), and; **b)** TEM (scale bar is 200 nm).

Functionalised propionate initiator particles were slightly less swollen by water, but slightly more swellable in THF than their precursor particles (**Table 2.3**) as is expected from their more hydrophobic nature. MA was also tested for its swelling ability of the E1PBr particles in order to ensure that grafting would be carried out under swelling conditions.

Table 2.3:

Swelling ratios of E1 particles and E1PBr particles in common organic solvents and MA:

Solvent	E1 Swelling ratio (%)[a]	E1PBr Swelling ratio (%)[a]
Ethanol	190	150
H_2O	160	110
MeOH	140	160
MA	-	140
THF	170	210

a) Swelling ratios were determined according to **Eqn. 2.2**.

2.3.2.1 Study of Esterification by FT-IR

The functionalisation was followed gravimetrically, where a weight gain corresponding to an esterification of 80 % was determined, as well as by FT-IR where a significant decrease in the hydroxyl signal at 3450 cm^{-1} was observed, compared to the carbonyl (**Figure 2.9**).

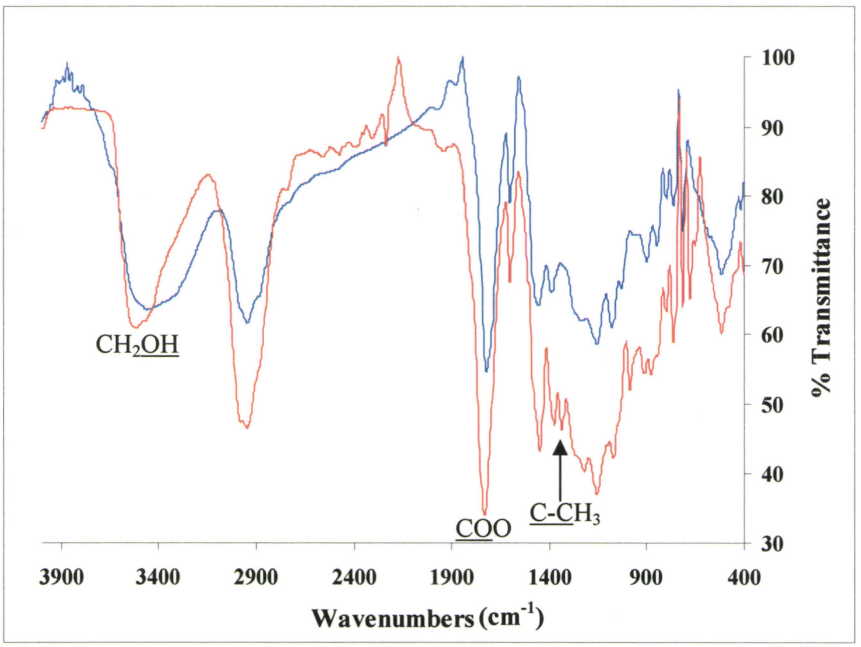

Figure 2.9:

FT-IR of E1PBr (in red), and E1 particles (in blue).

Functionalisation was further confirmed by the shift of the ester carbonyls from 1724 cm^{-1} to 1735 cm^{-1}, due to the nature of the electron withdrawing bromine on the α-bromopropionate. Esterification is additionally confirmed by the appearance of an absorption band at 1335 cm^{-1} assigned to the methyl group of the initiator. This new band should decrease after ATRP grafting.

2.3.2.2 Study of Propionate Initiator Particles by CPMAS-NMR

CPMAS-NMR confirms the functionalisation, where the carbonyl for the propionate is apparent at 170.3 ppm, and the $COO\underline{C}H_2$ and $\underline{C}H_2OH$ peaks of HEMA are replaced by a single peak at 63.0 ppm due to the $COO\underline{C}H_2$ groups (**Figure 2.10**). The propionate group appears at 22.1 ppm. This disappearance of the $\underline{C}H_2OH$ signal supports the near quantitative esterification measured gravimetrically. The peak area for the propionate carbonyl does not match that of the HEMA carbonyl. This discrepancy may be due to less efficient cross–polarisation to the more mobile propionate groups.

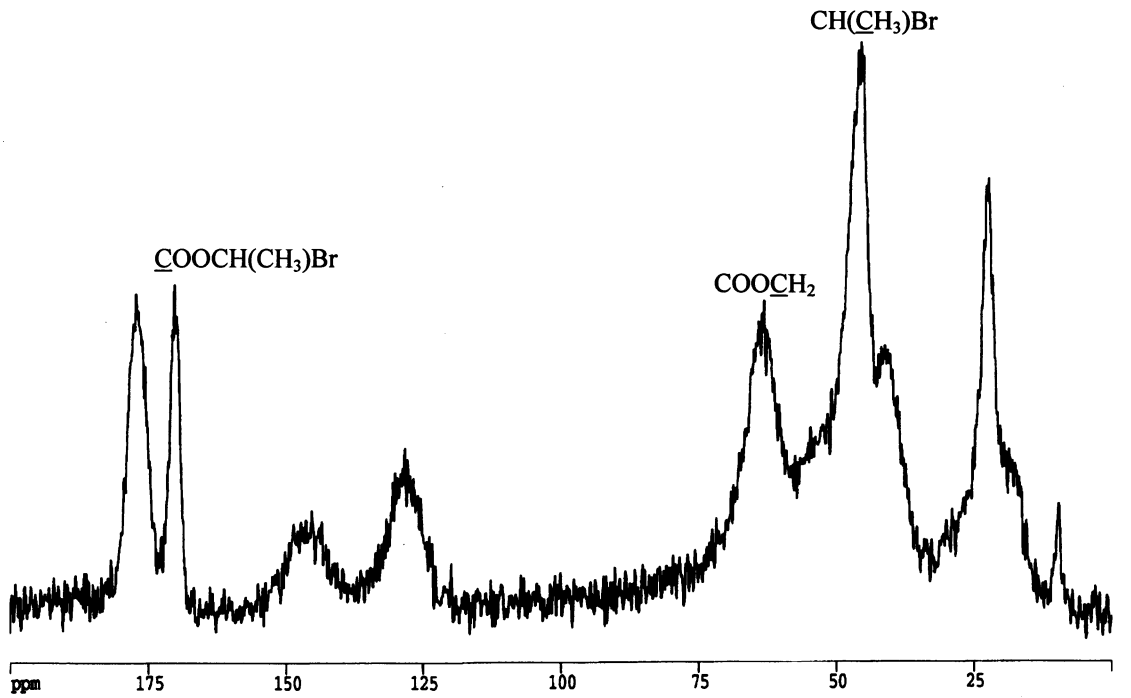

Figure 2.10:

CPMAS-NMR of E1PBr particles.

2.3.2.3 Study of Propionate Initiator Particles by STXM

Four regions were examined, where the three inner sections, corresponding to the blue, brown and green regions, which have the same carbonyl excitation, differ from the orange peak, which corresponds to the propionate carbonyl in the shell (**Figure 2.11**). This propionate is slightly shifted to higher energy, due to the electronegative bromine. This carbonyl is only observed in the shell, and not in the core, which implies that functionalisation occurs primarily in the shell. The core shell nature of the E1 particles is more apparent since the brown and green traces overlap through the aromatic region, but the brown trace has higher intensity at the carbonyl, again indicating that cross-linking is greatest at the centre of the particle, and HEMA and derivatised HEMA become more dominant outwards from the shell. The embedding resin is composed of TTE and MMHA (**Scheme 2.4**).

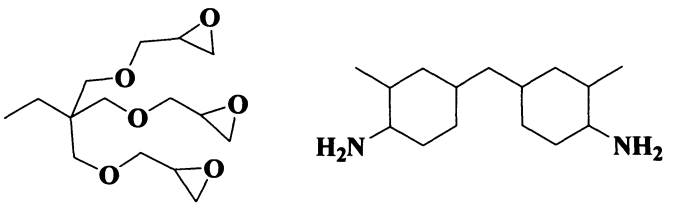

Scheme 2.4:

Chemical Structure of TTE and MMHA.

Some unsaturation appears which may result from elimination of HBr from the α-bromopropionate, followed by addition of the amine (MMHA) to the double bond via Michael addition (**Scheme 2.5**).

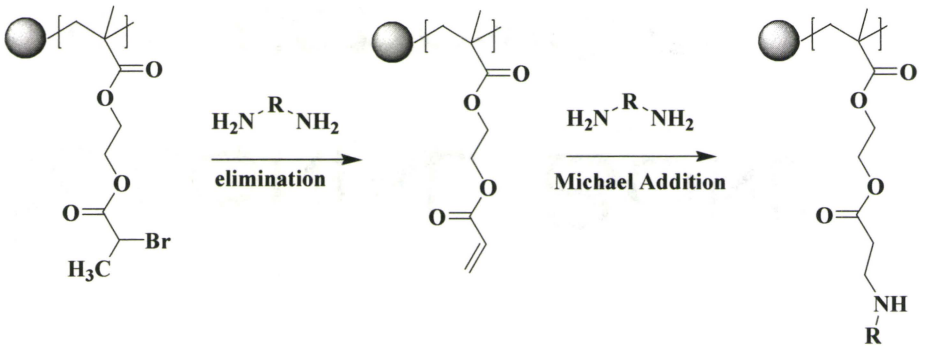

Scheme 2.5:

Results of elimination of α-bromopropionate by MMHA (represented as NH_2-R-NH_2), followed by Michael addition of MMHA.

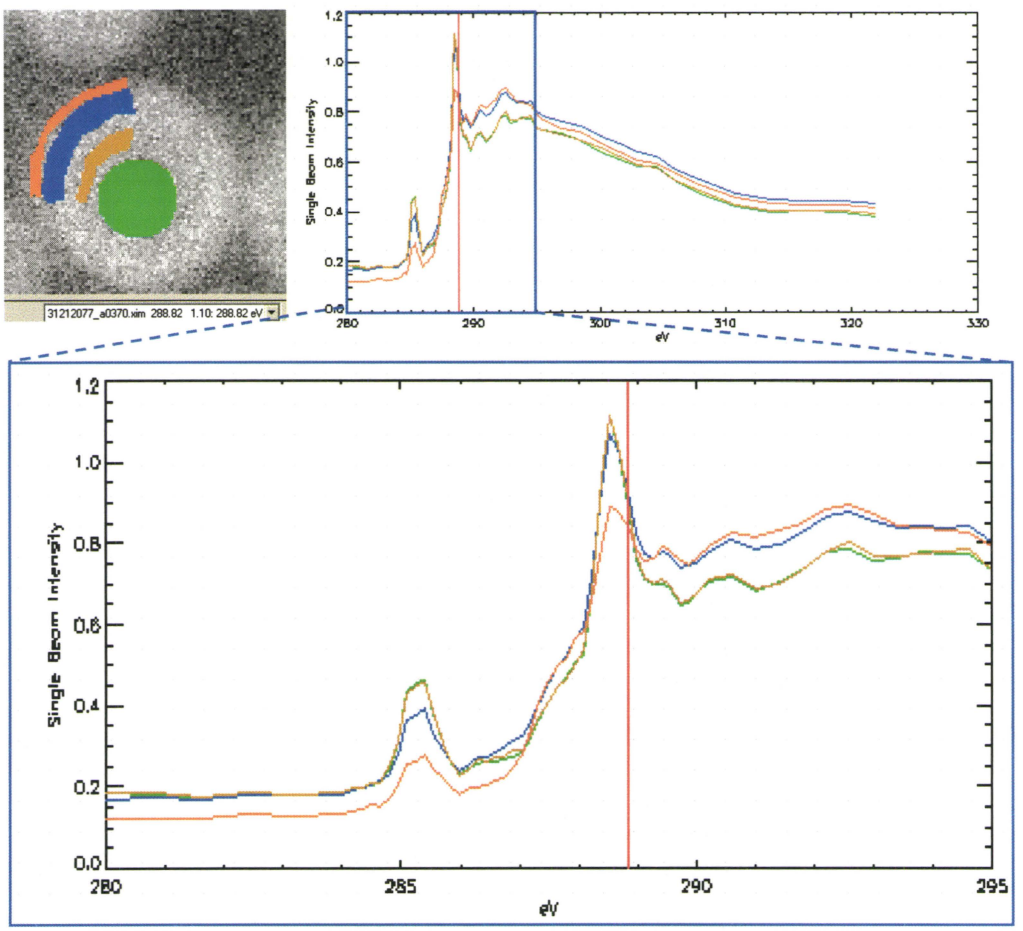

Figure 2.11:

STXM scan of E1PBr particles.

2.3.3 Polymerisation of Methyl Acrylate

Homopolymerisation of MA was carried out according to the procedure by Matyjaszewski's group,[13] with slight adjustments. Homopolymerisation of MA was attempted with ethyl 2-bromopropionate initiator in a 4:1 solvent to monomer ratio using ethyl acetate, DMF, ethylene carbonate, *p*-xylene, THF, and in bulk, with a catalyst system of either CuBr/dNbipy or CuBr/PMDETA. The results are summarised in **Table 2.4**. All reactions were run for 9 hours at 70 °C (with the exception of the polymerisation in ethylene carbonate) with a $[M]_o/[I]$ ratio of 100:1. However, bulk homopolymerisation of MA gave optimal results in terms of conversion, M_n, and MWD, hence grafting was carried out in bulk conditions.

Table 2.4:

Homopolymerisation of MA under a number of solvent and catalyst conditions:

Solvent	CuBr/dNbipy	CuBr/PMDETA	Conversion	Mn (g/mol)	PDI
Bulk	X		79	9 500	1.06
		X	84	10 500	1.07
Ethyl acetate	X		28	4 000	1.04
DMF	X		0	-	-
Ethylene Carbonate	X[a]		6	5 800	1.35
	X[b]		18	18 800	1.25
***p*-xylene**	X		0	-	-
		X	23	5 300	1.05
THF	X		4	800	1.07
		X	14	2 400	1.14

a) Polymerisation at 90°C for 1.5 hours
b) Polymerisation at 90°C for 9 hours

Wang and Matyjaszewski[1] prepared PMA in the bulk using CuBr/bipy initiated with Et-2-BrP and obtained an M_n of 21 500 g/mol, where 19 100 g/mol was expected,

and a PDI of 1.25; this has been improved upon here where the M_n obtained was 9 500 g/mol (expected M_n of 7000 g/mol) and the PDI was 1.06. The procedure of Ma and Wooley[14] was followed for the bulk polymerisation of MA using CuBr/PMDETA initiated by Et-2-BrP where they obtained an M_n of 9 100 g/mol with a PDI of 1.04 and 54 % conversion; comparable results were obtained here with PMA at 84 % conversion with an M_n of 10 500 g/mol and a slightly broader PDI of 1.07.

The homopolymerisation of MA using CuBr/bipy initiated by MBrP in ethylene carbonate, was carried out following the procedure by Shipp *et al.*[2] who obtained PMA with an M_n of 5 910 g/mol after 1.5 hours with a PDI of 1.32, which is quite similar to the M_n of 5 800 g/mol and PDI of 1.35 obtained here. After 9 hours, the M_n of the PMA was 18 800 g/mol and the PDI decreased to 1.25.

The kinetic plots for the bulk polymerisation of MA using CuBr/dNbipy and CuBr/PMDETA are shown below (**Figure 2.12**). Monomer conversion is plotted as a function of time, and a near linear relationship is observed (**Figure 2.12a**), which is not expected according to the kinetic profile shown in **Scheme 1.10**. Precipitation of the Cu^{II} species was observed, which would cause the reaction to become more active and faster. Within the same figure is a plot of $\ln([M]_o/[M])$ as a function of time, and the measured conversion is higher at higher M_n: there is a slight inverse curvature, indicating that the radical concentration is not constant due to the one data point at the higher M_n. The result is an increase in M_n as a function of percent conversion as expected, which is shown in **Figure 2.12 b)** and **d)**. As well, there is a decrease in MWD with increasing conversion, as expected for a controlled ATRP.

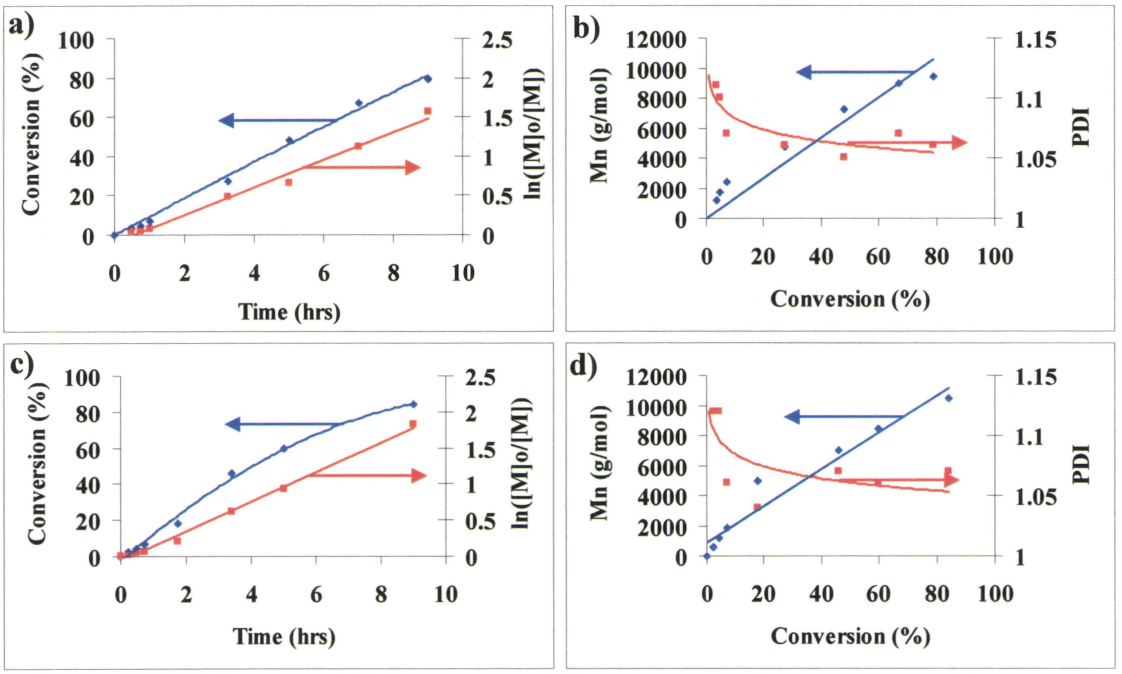

Figure 2.12:

Kinetics of homopolymerisation of MA: **a)** plot of conversion, and $\ln([M]_o/[M])$ with time, and; **b)** plot of M_n, and PDI with conversion using CuBr/dNbipy. **c)** Plot of conversion, and $\ln([M]_o/[M])$ with time, and; **d)** plot of M_n, and PDI with conversion using CuBr/PMDETA.

These plots indicate a controlled ATRP for the bulk homopolymerisation of MA with either catalyst system, and the final results are summarised below, where the total reaction time at 70 °C is 9 hours (**Table 2.5**).

Table 2.5:

Results of bulk polymerisation of MA using either CuBr/dNbipy or CuBr/PMDETA with Et-2-BrP:

Experimental Conditions	Conversion (%)	$M_{n\,th}$ (g/mol)	M_n (g/mol)	PDI
$PMA_{dNbipy+Et\text{-}2\text{-}BrP}$	79	7 000	9 400	1.06
$PMA_{PMDETA+Et\text{-}2\text{-}BrP}$	84	7 400	10 500	1.07

The M_n obtained was higher than expected, but the PDI was narrow. Deviations in the grafting situations can now be attributed to the heterogeneous environment and the surface bound initiator.

2.3.4 Grafting Methyl Acrylate from Propionate Initiator Particles

Acrylates are structurally similar to propionates in terms of the propagating radical (**Scheme 2.1**). Thus, MA was chosen for the grafting procedure from propionate initiator particles. In addition, MA was chosen because the pendant group should remain unchanged upon cleavage with NaOMe in the subsequent cleavage step (**Scheme 2.6**).

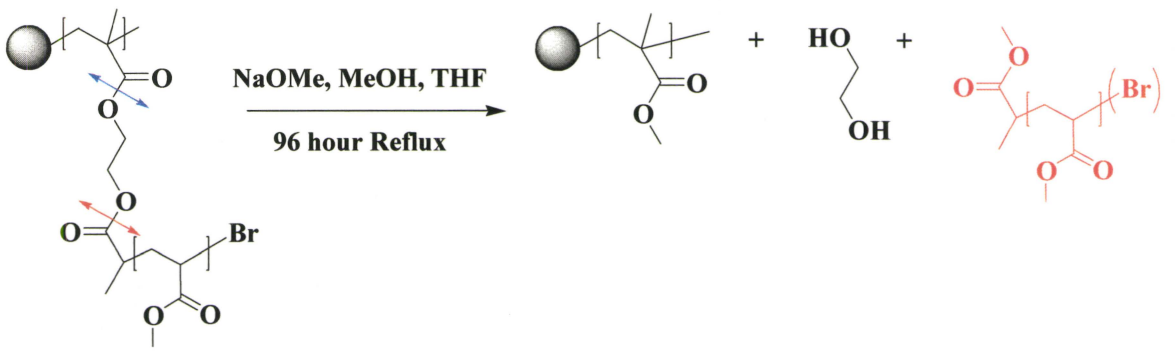

Scheme 2.6:

Schematic of cleavage of PMA grafted microspheres using NaOMe.

Grafting conditions were identical to those used for the homopolymerisation with either CuBr/dNbipy or CuBr/PMDETA, and bulk conditions were used so that a direct comparison between the homopolymerisation and grafting polymerisation could be made. The results of grafting with both catalysts are shown below (**Table 2.6**). Free

"sacrificial" initiator, ethyl 2-bromopropionate, Et-2-BrP, was also added to some reactions, in order to suppress termination of surface–bound radicals.

Table 2.6:

Grafting MA from E1PBr initiator particles using either CuBr/dNbipy or CuBr/PMDETA with and without free Et-2-BrP:

Experimental Conditions	Wt. Gain (%)[a]	Conversion to Grafted Polymer (%)	Particle Size (μm)[a]
E1PBr	-	-	1.8 ± 0.2
E1-PMA_{dNbipy}-Br	740	26	4.0 ± 0.5
E1-$PMA_{dNbipy+Et\text{-}2BrP}$-Br	840	35	4.3 ± 0.5
E1-PMA_{PMDETA}-Br	400	13	3.4 ± 0.4
E1-$PMA_{PMDETA+Et\text{-}2\text{-}BrP}$-Br	440	16	3.2 ± 0.3

b) Particle Size measured using Coulter Multisizer

Weight gain was measured according to **equation. 2.3**:

$$\text{Weight gain} = \frac{\text{Weight of grafted particles} - \text{Weight of initiator particles}}{\text{Weight of initiator particles}} \times 100\% \qquad \textbf{Eqn 2.3}$$

Quantitative conversion of monomer to grafted polymer would result in a weight gain of 2800 %, however grafting was not quantitative. In the case of PMDETA, there is less PMA grafted from the particles, implying that PMDETA is not as efficient at grafting. This could be due to its greater activity, which causes increased termination of the chain ends, resulting in less grafted polymer. Again, in the presence of "sacrificial" initiator, monomer conversion to grafted polymer increases, most likely due to the increased concentration of Cu^{II} species, which reduces termination.

The increase in size measured by the Coulter Multisizer for the particles grafted with CuBr/dNbipy was measured as a function of time, and found to be linear at first (◆), and then to level off near the end of the polymerisation (**Figure 2.13a**); while in the

presence of free initiator, a near linear increase is observed (■). Similar effects are observed when grafting is carried out with CuBr/PMDETA (**Figure 2.13b**). In the absence of free initiator (◆), particle diameter increase is dramatic at first and then levels off, whereas when free initiator is added (■), the increase is less dramatic at first, and shows better control of grafting. Results indicate an average of three experiments run in parallel where a standard deviation of less than 10 % was accepted.

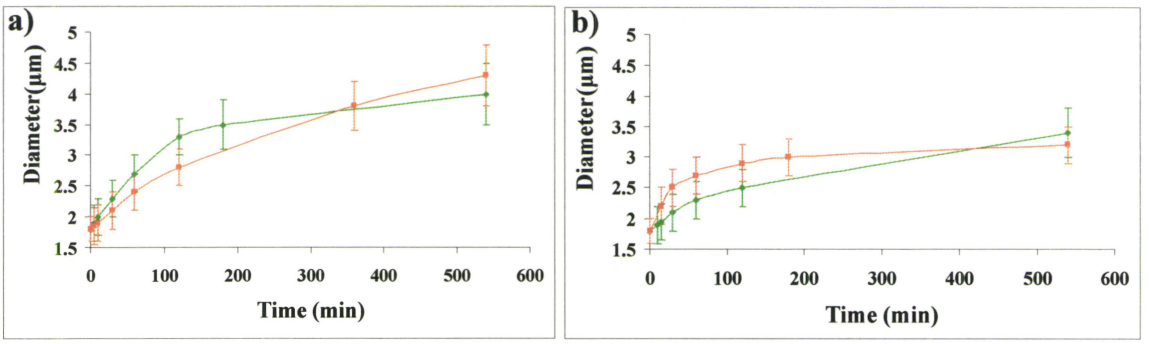

Figure 2.13:

Figure of **a)** diameter increase with time for PMA grafted microspheres using CuBr/dNbipy without free initiator (◆), and with free initiator (■). **b)** E1-PMA_{PMDETA}-Br diameter increase as a function of time without free initiator (◆), and with free initiator (■).

ESEM images of these grafted microspheres at the end of the grafting procedure are shown in **Figure 2.14.**

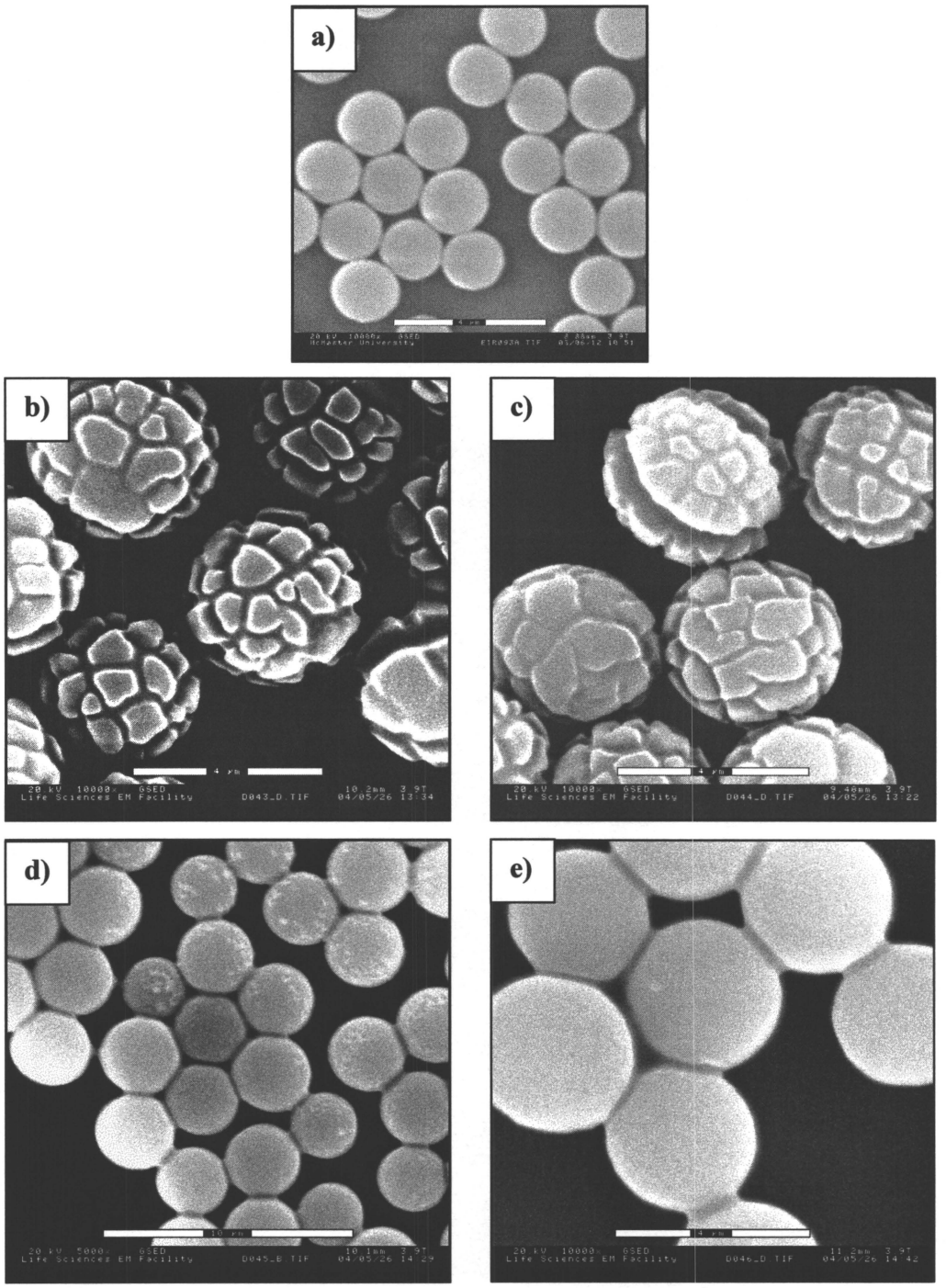

Figure 2.14:

ESEM images of **a)** E1PBr; **b)** E1-PMA$_{dNbipy}$-Br; **c)** E1-PMA$_{dNbipy+Et-2-BrP}$-Br (scale bars are 4 μm); **d)** E1-PMA$_{PMDETA}$-Br (scale bar is 10 μm), and; e) E1-PMA$_{PMDETA+Et-2-BrP}$-Br (scale bar is 4 μm).

Both images in **Figure 2.14b)** and **c)** show monodisperse grafted particles, which implies that the initiator particles were grafted within identical environments and that the initiator particles were homogeneously dispersed in the continuous monomer phase. Additionally, a "cracking" morphology can be observed, which has been attributed to the grafting process by which grafting induces "cracking" of the DVB scaffold as the microspheres grow, and is also seen in the TEM images of these particles (**Figure 2.15 a,** and **b**).

Images in **Figure 2.14d)** and **e)** do not show any "cracking" which is most likely because they have not grown so much as to cause the stress that caused the previously seen cracking. However, the diameter increase still indicates that polymer is grafted both from the surface as well as from initiator sites located within the swellable microspheres.[17] CuBr/PMDETA is more polar than CuBr/dNbipy, thus, it is less likely to penetrate the particles, and would prefer to remain in the continuous monomer phase. When it is able to penetrate the particles, it may activate numerous initiating sites, which then terminate, causing the monomer conversion to grafted polymer to be low. Additionally, the propagating species must be considered, the MA secondary radical is quite reactive, and when formed will terminate readily especially when surface-tethered and where Cu^{II}/PMDETA species are not as likely to "cap" the radical.

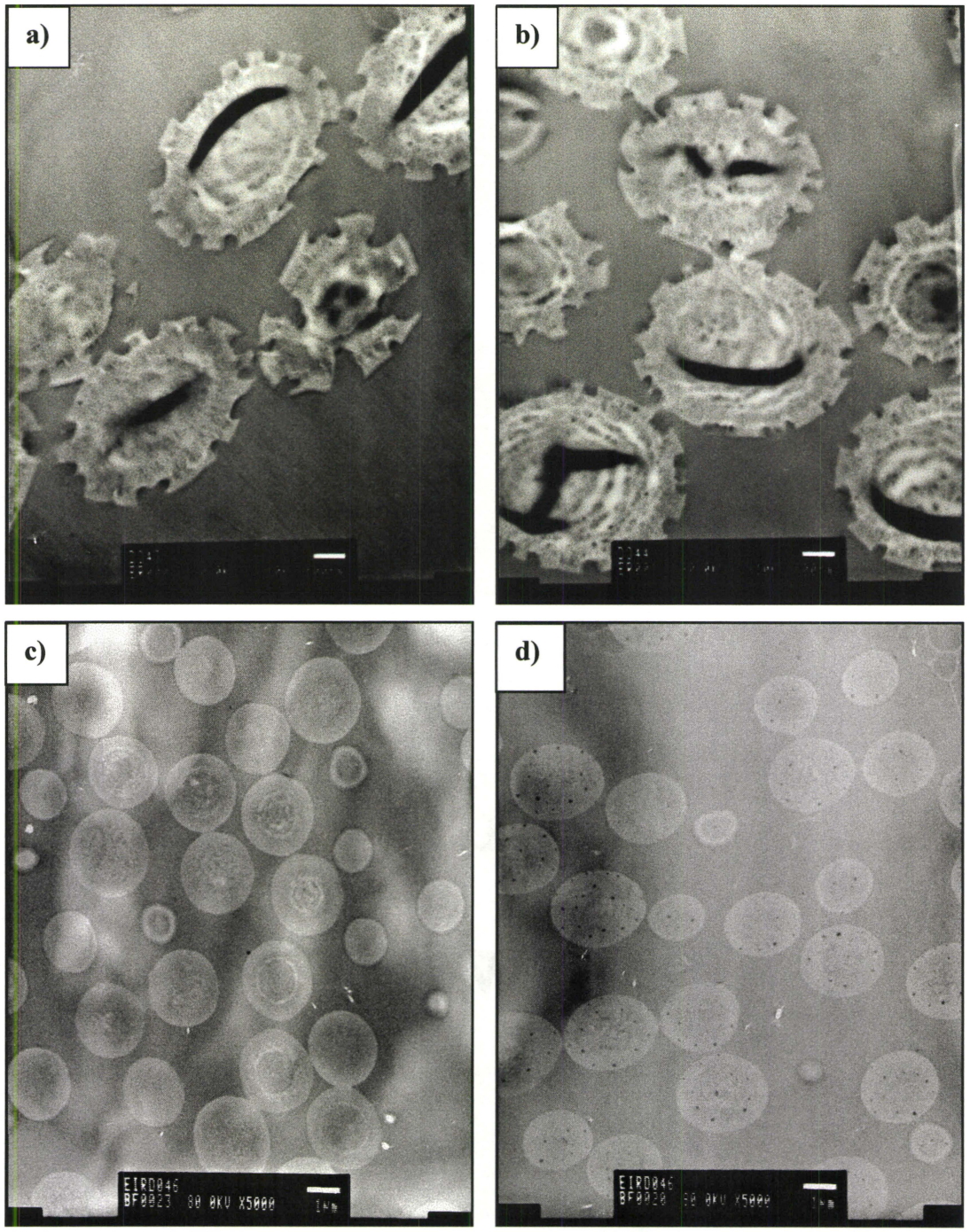

Figure 2.15:

TEM of **a)** E1-PMA$_{dNbipy}$-Br; **b)** E1-PMA$_{dNbipy+Et\text{-}2\text{-}BrP}$-Br; **c)** E1-PMA$_{PMDETA}$-Br (scale bars are 500 nm), and; **d)** E1-PMA$_{PMDETA+Et\text{-}2\text{-}BrP}$-Br (scale bars are 1 μm).

In the TEM images in **Figure 2.15a)** and **b)**, the core of the particles is no longer visible, and so it would appear as though grafting MA from propionate initiator particles with CuBr/dNbipy occurs throughout the E1 particles. The dark ellipsoids are due to folding of the particles. The cracking appears to be limited to the PMA shell, and stops where the cross–linked scaffolding is present.

Concentric rings (**Figure 2.15 a, b**, and **c**), not seen in the TEM of E1 or of the E1PBr microspheres, suggest onion–like morphology, likely originating from the precipitation polymerisation. Other research in our group has shown thermal oscillations during precipitation polymerisation can cause onion type morphology. This effect usually requires a cross–linker percent of approximately 10 % relative to the total monomer. Though the present precipitation polymerisation started with 17.5 % DVB80, or roughly 15 % DVB, the different reactivity ratios of DVB and HEMA would lead to a decreasing cross–linking density with reaction progress, running into the region where the copolymerisation would be sensitive to any temperature oscillation present. Furthermore, these rings are amplified by grafting with PMA to the point where they become noticeable by TEM. We are currently checking the precipitation polymerisation for small, regular temperature oscillations.

The TEM images in **Figure 2.15c)** and **d)** are those taken of E1-PMA_{PMDETA}-Br, and E1-$PMA_{PMDETA+Et\text{-}2\text{-}BrP}$-Br, respectively. Cracking is not observed, corresponding to the ESEM images in **Figure 2.14 d)** and **e)**, and the lower weight gains. The core is again visible in both images, and concentric rings are visible in only a few microsphere sections.

2.3.4.1 Study of Soluble PMA Prepared During MA Grafting

In addition to grafted polymer, monomer was also converted to soluble polymer, which was isolated from the washings of the particles. The molecular weight evolution and PDI were plotted as a function of time (**Figure 2.16**).

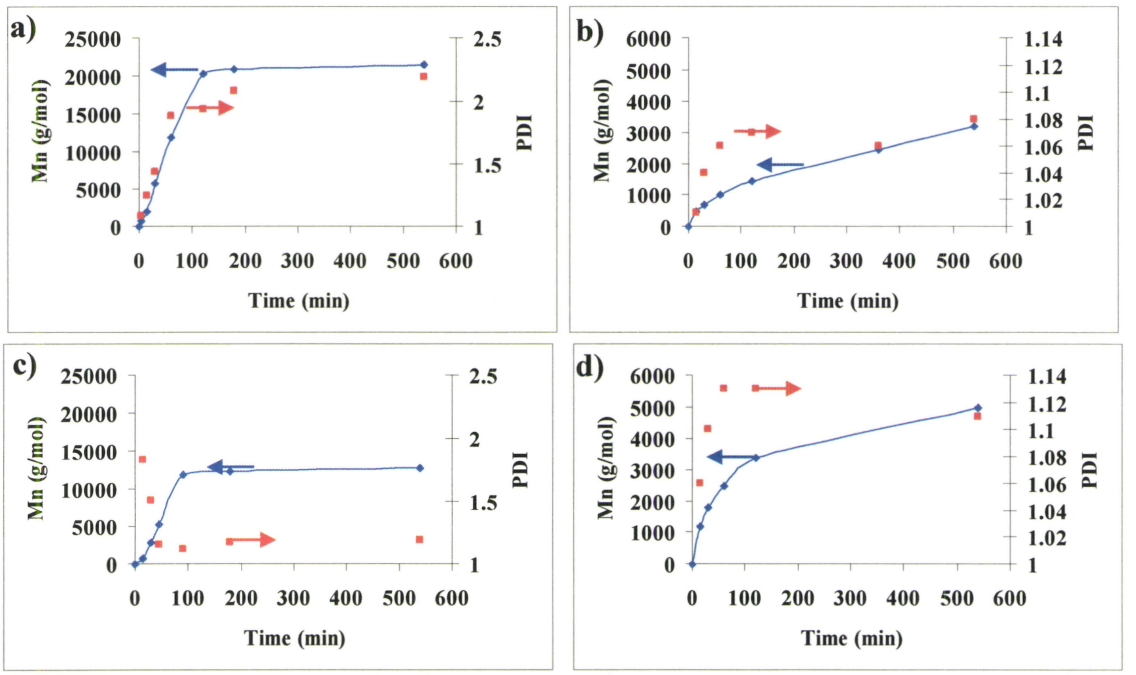

Figure 2.16:

Soluble polymer from E1-PMA-Br grafting: with CuBr/dNbipy **a)** without free initiator where M_n (blue) and PDI (red) are plotted with time, and; **b)** with free initiator where M_n (blue) and PDI (red) are plotted with time; with CuBr/PMDETA: **c)** without free initiator where M_n (blue) and PDI (red) are plotted with time, and; **d)** with free initiator where M_n (blue) and PDI (red) are plotted with time.

These plots show the increased control achieved upon addition of free initiator. The soluble polymers at the end of the grafting procedure (9 hours) were analysed for their monomer conversion, M_n, and PDI (**Table 2.7**).

Table 2.7:

Soluble polymer prepared during grafting MA from E1PBr particles using either CuBr/dNbipy or CuBr/PMDETA without and with free Et-2-BrP:

Experimental Conditions	M_n expected (g/mol)	M_n (g/mol)	PDI	Conversion to Soluble Polymer (%)	Total Conversion to Polymer (%)
PMA_{dNbipy}	7 000	9 400	1.06	79	79
E1-PMA_{dNbipy}-Br	-	21 500	2.19	3	29
E1-$PMA_{dNbipy+Et\text{-}2\text{-}BrP}$-Br	4 300	3 200	1.08	48	83
PMA_{PMDETA}	7 400	10 500	1.07	84	84
E1-PMA_{PMDETA}-Br	-	12 800	1.19	4	17
E1-$PMA_{PMDETA+Et\text{-}2\text{-}BrP}$-Br	5 500	5000	1.11	62	78

In the absence of free initiator, only small amounts of high M_n, polydisperse PMA are formed. The overall conversion of monomer to polymer when Et-2-BrP is added is quite close to the monomer conversion to polymer in the absence of particles. The PDI in the presence of Et-2-BrP is rather narrow, and close to the PDI of the homopolymer. Additionally, the M_n observed is quite close to that expected for both catalyst systems despite the lower monomer conversion in the presence of E1PBr particles. Thus, the bulk phase polymerisation does not appear to be greatly affected by the presence of the particles, while the graft polymerisation benefits greatly from the presence of the free initiator.

When grafting is carried out using PMDETA there is less monomer converted to grafted polymer. The more polar CuBr/PMDETA complex is less likely to penetrate the particles, and so less grafted polymer results. The rate of formation of the soluble polymer is faster than that of the grafted polymer, which results from a partitioning effect. Again, the MWD of the soluble polymer is quite narrow and the M_n of the polymer prepared in the presence of free initiator is exactly what is expected.

2.3.4.2 Study of MA Grafting by FT-IR

FT-IR indicates an additional decrease in the hydroxyl stretch of the residual E1 particles that were not functionalised by esterification (**Figure 2.17**), due to the dilution with grafted polymer and the increased hydrophobicity. Other changes in the E1PBr spectrum are consistent with PMA grafting: the carbonyl has shifted from 1735 cm^{-1} to 1732 cm^{-1}, and the aromatic stretches are no longer visible.

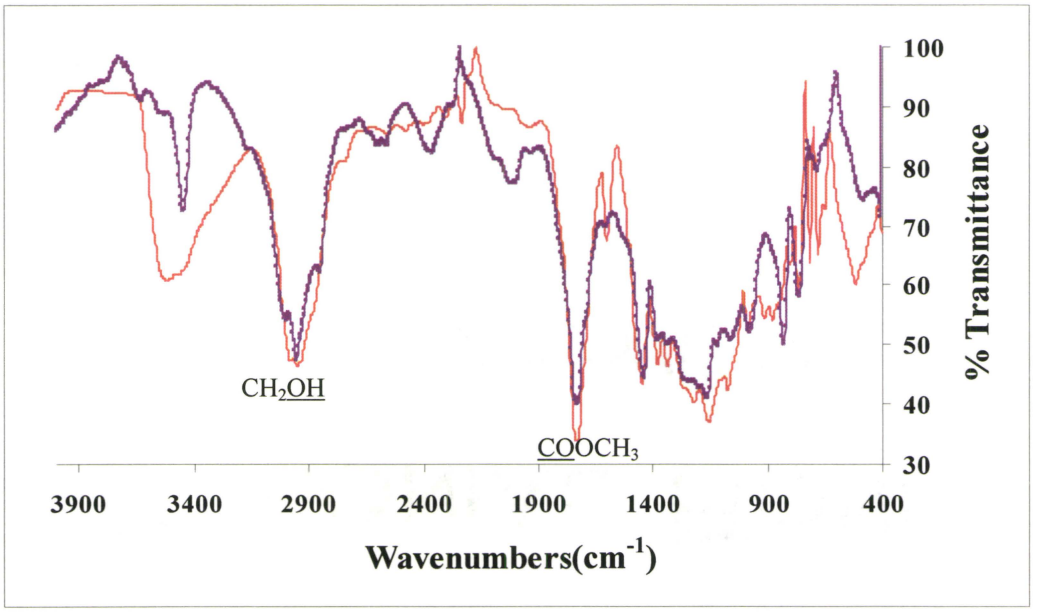

Figure 2.17:

FT-IR of E1-PMA-Br particles (purple), superimposed over E1PBr particles (red).

2.3.4.3 Study of MA Grafted Microspheres by CPMAS-NMR

A sample of E1-PMA-Br particles prepared using dNbipy (weight gain of 841 %) was analysed by CPMAS-NMR (**Figure 2.18**). The result is a clean spectrum of PMA, with no aromatic peaks, and no peaks due to E1 or E1PBr particles. This is consistent

with the large weight gain which results in these particles being 90 weight % PMA, and the STXM results, which show a large increase in the carbonyl region. The low signal to noise ratio is likely due to poor cross-polarisation, given the low glass transition temperature of PMA.

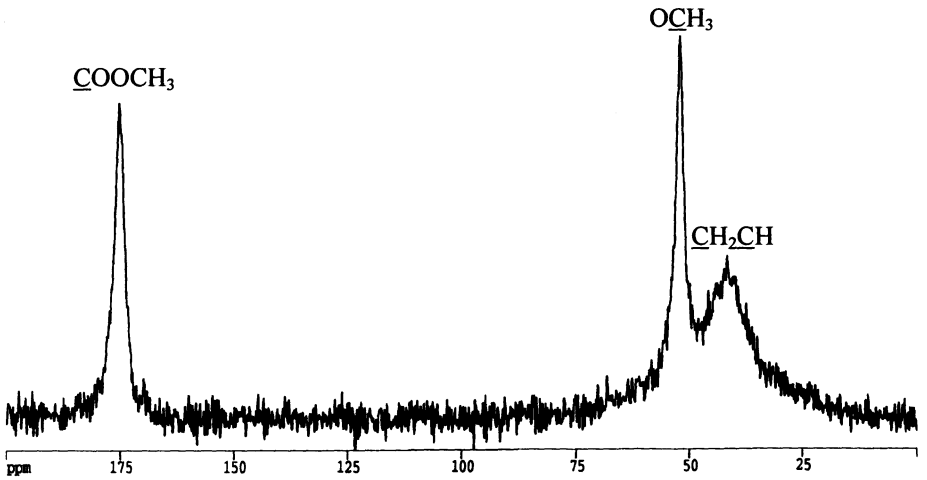

Figure 2.18:

CPMAS-NMR spectrum of E1-PMA_{dNbipy}-Br.

2.3.5 Cleavage of PMA Grafted Microspheres

Cleavage was carried out using base catalysed transesterification with the use of NaOMe. NaOMe was chosen in order to avoid hydrolysis of the grafted PMA (**Scheme 2.6**). Cleavage reactions were carried out for 96 hours, and were nearly quantitative (**Figure 2.19** represents cleavage of dNbipy grafted microspheres). Coulter Multisizer measurements of these particles indicate a size decrease from 4.3 μm to 1.6 μm. **Figure 2.19** represents the microspheres after THF washings and water washings.

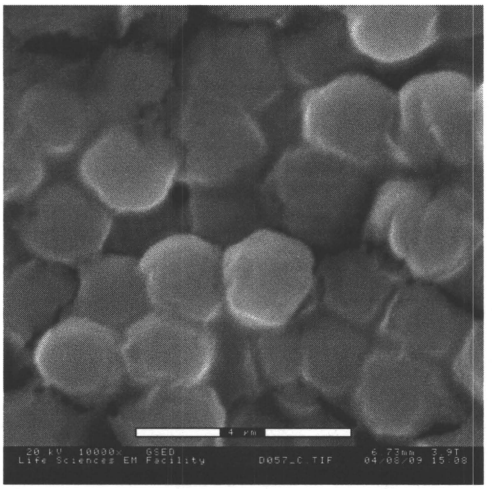

Figure 2.19:

ESEM of PMA cleaved microspheres (previously grafted with dNbipy) (scale bar is 4 μm).

It is apparent that the microspheres do not completely return to their original shape. The particle sizes before and after cleavage, as well as the amounts of particles and polymer recovered are shown below (**Table 2.8**).

Table 2.8:

Size of particles grafted with MA before, and after cleavage:

Grafting Conditions		Cleavage		
	Particle Size (μm)[a]	Particle Size (μm)[a]	Particles Recovered (%)[b]	PMA Recovered (%)[b]
E1-PMA_{dNbipy}-Br	4.0 ± 0.5	1.6 ± 0.2	94	93
E1-$PMA_{dNbipy+Et\text{-}2\text{-}BrP}$-Br	4.3 ± 0.5	1.6 ± 0.2	95	89
E1-PMA_{PMDETA}-Br	3.4 ± 0.4	1.7 ± 0.2	93	90
E1-$PMA_{PMDETA+Et\text{-}2\text{-}BrP}$-Br	3.2 ± 0.3	1.5 ± 0.2	95	93

a) measured by Coulter Multisizer **b)** measured gravimetrically

Cleavage of the grafted particles is nearly quantitative. The recovered polymer was characterised by GPC and the results are shown below (**Table 2.9**). For comparison, the M_n and PDI of the soluble polymer are included.

Table 2.9:

Results of cleavage of PMA grafted particles, both those prepared with and without free initiator:

Grafting Conditions	**Soluble PMA**			**Cleaved PMA**			
	$M_{n\ th}$ (g/mol)	**M_n (g/mol)**	**PDI**	**$M_{n\ th}$ graft (g/mol)**	**M_n (g/mol)**	**PDI**	**PMA recovered (%)**
PMA_{dNbipy}	7000	9 400	1.06	-	-	-	-
E1-PMA_{dNbipy}-Br	-	21 500	2.19	2 400	7 000	1.14	93
E1-$PMA_{dNbipy+Et\text{-}2\text{-}BrP}$-Br	4 300	3 200	1.08	3 200	5 800	1.03	89
PMA_{PMDETA}	7400	10 500	1.07	-	-	-	-
E1-PMA_{PMDETA}-Br	-	12 800	1.19	1 300	7 500	1.21	90
E1-$PMA_{PMDETA+Et\text{-}2\text{-}BrP}$-Br	5 500	5000	1.11	1 600	1 800	1.13	93

The cleaved PMA is higher in M_n than expected according to the conversion to grafted polymer; however it is quite narrow disperse when either catalyst is used to carry out the grafting. As expected, the PDI is broader when PMDETA was employed rather than dNbipy, since it is a more active catalyst. A narrowing of the PDI is also observed when free initiator was added. This can be attributed to an increase in the Cu^{II} species formation, which would lead to better control of the polymerisation process. These PDI's do not differ significantly from the bulk homopolymerisations of MA using either catalyst system over the same time frame; the M_n of the cleaved PMA is lower than the soluble PMA (for dNbipy) or the model PMA. Grafting with dNbipy and free initiator

gives the expected M_n, however grafting with PMDETA gives a very low M_n (**Table 2.9**). Perhaps the activity of the PMDETA ligand was too great, and the chains terminated, despite the increased Cu^{II} concentration afforded by the free initiator. The decrease in the M_n of the cleaved PMA when free initiator is added indicates a decrease in termination in the case of grafting with PMDETA where there is essentially the same amount of grafted polymer.

2.3.5.1 CPMAS-NMR of PMA Cleaved Particles

A sample of E1-PMA-$Br_{cleaved}$ particles were analysed by CPMAS-NMR, and the resulting spectrum is shown below (**Figure 2.21**).

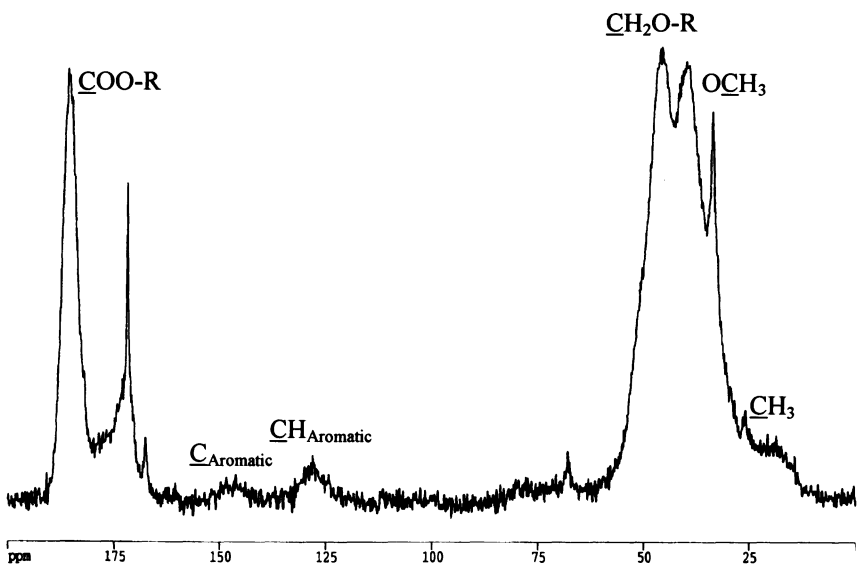

Figure 2.21:

CPMAS of E1-PMA-$Br_{cleaved}$ particles.

There are aromatic peaks, corresponding to the DVB (CCH, and CH). However, PMA, derivatised HEMA, and HEMA still remain. The carbonyl (COO-R) at 185.9 ppm is shifted to higher energy than expected for the carbonyl of MMA (expected at 177.0 ppm). The broad signal between 25 and 60 ppm contains contributions from MA, MMA, HEMA, and the backbone carbons of DVB. Regardless, CPMAS-NMR does confirm that cleavage has occurred, as does the FT-IR (not shown).

2.3.6 Bulk Homopolymerisation of Methyl Acrylate in the presence of DVB80-*co*-HEMA particles

To study the solution polymerisation of MA in a gel environment, MA was polymerised in the presence of DVB80-*co*-HEMA particles (0.03 volume %: 0.17g of particles in 5 g of MA), and the results are tabulated below (**Table 2.10**).

Table 2.10:

Results of homopolymerisation of MA in the absence and in the presence of DVB80-*co*-HEMA particles:

Experimental Conditions	Conversion (%)	M_n	PDI
PMA_{dNbipy}	59	9 400	1.06
$PMA_{dNbipy+E1}$	68	7 000	1.23
PMA_{PMDETA}	64	10 500	1.07
$PMA_{PMDETA+E1}$	88	10 200	1.12

A number of interesting phenomena occur when MA is homopolymerised in the presence of DVB80-*co*-HEMA particles: the monomer conversion to polymer increases, as does the PDI. The broad PDI indicates that the ATRP is no longer controlled, which would suggest why the M_n increases.

It is possible that the hydroxy groups chelate the catalyst, and if this is the case, then Cu^{II} would be preferentially complexed, deactivation efficiency would drop, and a free radical type polymerisation would ensue. Although there are residual hydroxyl groups in the propionate initiator particles, they should not play a role in the polymerisation. These hydroxyl groups were not accessible to the 2-bromopropionyl bromide, so it is not likely that they are accessible to the Cu^{II} complex, especially if grafted polymer incurs further steric hindrance. In essence, hydroxyl functionalised E1 particles may function as analogous water droplets, leading to faster but less controlled polymer.

2.4 Conclusions

The size distribution of precursor swellable DVB80-*co*-HEMA particles was narrowed by tuning the solvent conditions of their precipitation polymerisation. Grafting MA from initiator particles resulted in large weight gains, as well as particle size increases. Particle size was shown to increase with polymerisation time. These microspheres had an interesting morphology resulting from the grafting process, and demonstrated onion-like morphology. Soluble polymer was isolated from the washings of the grafted microspheres, and the M_n and PDI of the soluble polymer narrowed with the introduction of sacrificial initiator. In fact, it was found that the cleaved polymer had a M_n and PDI similar to that found in the "free" polymer, and cleavage was 90 - 95 % effective.

2.5 References

(1) Wang, J.-S.; Matyjaszewski, K. *Macromolecules* **1995**, *28*, 7901.

(2) Shipp, D. A.; Wang, J.-L.; Matyjaszewski, K. *Macromolecules* **1998**, *31*, 8005.

(3) Semsarzadeh, M. A.; Mirzaei, A.; Vasheghani-Farahani, E.; Haghighi, M. N. *Eur. Poly. J.* **2003**, *39*, 2193.

(4) Matyjaszewski, K.; Miller, P. J.; Shukla, N.; Immaraporn, B.; Gelman, A.; Luokala, B. B.; Siclovan, T. M.; Kickelbick, G.; Vallant, T.; Hoffmann, H.; Pakula, T. *Macromolecules* **1999**, *32*, 8716.

(5) Kim, J.-B.; Huang, W.; Miller, M. D.; Baker, G. L.; Bruening, M. L. *J. Polym. Sci. Part A: Polym. Chem.* **2003**, *41*, 386.

(6) Ejaz, M.; Yamamoto, S.; Ohno, K.; Tsujii, Y.; Fukuda, T. *Macromolecules* **1998**, *31*, 5934.

(7) Ejaz, M.; Ohno, K.; Tsujii, Y.; Fukuda, T. *Macromolecules* **2000**, *33*, 2870.

(8) Carlmark, A.; Malmström, E. *J. Am. Chem. Soc.* **2002**, *124*, 900.

(9) Husseman, M.; Malmström, E. E.; McNamara, M.; Mate, M.; Mecerreyes, D.; Benoit, D. G.; Hedrick, J. L.; Mansky, P.; Huang, E.; Russell, T. P.; Hawker, C. J. *Macromolecules* **1999**, *32*, 1424.

(10) Zheng, G.; Stöver, H. D. H. *Macromolecules* **2002**, *35*, 7612.

(11) Zheng, G.; Stöver, H. D. H. *Macromolecules* **2002**, *35*, 6828.

(12) Li, W.-H.; Stöver, H. D. H. *J. Polym. Sci. Part A: Polym. Chem.* **1999**, *37*, 2899.

(13) Davis, K. A.; Paik, H.-J.; Matyjaszewski, K. *Macromolecules* **1999**, *32*, 1767.

(14) Ma, Q.; Wooley, K. L. *J. Polym. Sci. Part A: Polym. Chem.* **2000**, *38*, 4805.

(15) *Polymer Handbook*; 4th ed.; John Wiley & Sons, Inc.: New York, 1999.

(16) In *Polymer Handbook*; 4th ed.; Brandrup, J., Immergut, E. H., Grulke, E. A., Eds.; John Wiley & Sons, INC.: New York, 1999, pp VI / 200, VI 202, II 259.

(17) Zheng, G.; Stöver, H. D. H. *Chinese Journal of Polymer Science* **2003**, *21*, 21.

Chapter 3: Grafting Methyl Methacrylate from Polymeric Microspheres

Abstract

Monodisperse swellable microspheres were prepared by precipitation co-polymerisation of DVB80 and HEMA as described in Chapter 2. They were further reacted with 2-bromoisobutyryl bromide to prepare ATRP initiator particles suitable for MMA grafting.

Model ATRP of neat MMA was carried out at 90°C with CuBr and either dNbipy or PMDETA ligands, and ethyl 2-bromoisobutyrate (Et-2-BriB) initiator, with a 100:1 MMA: Et-2-BriB ratio. Homopolymers of M_n 9 700 g/mol were expected where an M_n of 10 100 g/mol and PDI of 1.13 (dNbipy), and 10 200 g/mol with a PDI of 1.15 (PMDETA) was obtained.

Neat MMA was grafted from the swellable microspheres using either of these above catalytic systems at 90°C, and compared to the model homopolymerisations above in order to draw conclusions about the effect of the gel environment on ATRP grafting-from. Particle size increased from 1.7 μm to 4.4 μm and 4.5 μm upon grafting using the dNbipy and PMDETA ligands, respectively.

The grafted PMMA was found to have an M_n of 60 400 g/mol and a PDI of 1.90 for the dNbipy ligand, and an M_n of 22 300 g/mol and PDI of 1.98 for the PMDETA ligand, indicating poor control. Addition of equimolar free initiator resulted in much better M_n and PDI control for both ligands, at the expense of grafting yield.

3.0 Overview

Methacrylates are used extensively in industry and academics, both for commercial applications and as model monomers. There has been much research carried out on grafting methacrylates from substrates, including a number of studies on ATRP grafting-from surfaces, and the following is a brief review of the relevant work.

3.1 Background

The ATRP of MMA will be discussed first, before describing heterogeneous systems. Components of the ATRP system such as initiator, ligand, and solvent will be explored. In order to graft MMA from polymeric microspheres, the appropriate initiator particles need to be prepared. Arenesulfonyl halides, called universal initiators, are well suited to initiate MMA; however, the isobutyrate initiator was chosen as it has been shown to be as efficient as the arenesulfonyl halide,[1] and its functionalisation chemistry is quite simple, and has already been used with the analogous propionate and MA system in Chapter 2.

3.1.1 Solution Polymerisation of Methyl Methacrylate

The ATRP of MMA has been investigated in a variety of conditions (solvent, initiator, catalyst etc.). In general, the greatest success has been obtained using diphenyl

ether[1-3] as solvent and initiator/catalyst systems such as *para*–toluenesulfonyl chloride (*p*-TsCl)/CuCl,[1] *p*-TsCl/CuBr,[2,3] or CuBr/ethyl 2-bromoisobutyrate (Et-2-BriB)[1,4,5].

Wang *et al.*[1] examined different initiators for the polymerisation of MMA, and found that the polymerisation with Et-2-BriB/CuBr was faster than with the *p*-TsCl /CuCl system.[1,3]

In this work the bromoisobutyrate initiator will be used, because it can be easily attached to the polymeric microspheres and because it is a cleavable linker. The CuBr/dNbipy catalyst system will be explored in addition to the CuBr/PMDETA catalyst, since there has been only limited literature concerning the homopolymerisation of MMA using PMDETA. Although solvents have been used without detriment in MMA ATRP, here both model and graft polymerisations will be carried out using neat monomer in order to draw comparisons to the MA case.

3.1.2 Grafting Methacrylates from Silicon and Silica surfaces

The following table summarises some of the previous work done on grafting methacrylates from silica and silicon surfaces (**Table 3.1**).

Table 3.1:

Summary of ATRP grafting of methacrylates from silicon/silica substrates:

Substrate	**Surface-bound Initiator**	**Monomer(s)**	**Catalyst**	**Polymer Cleaved?**	**Notes**
Wafers Particles[6,7]	CTS	MMA	CuBr/ dHbipy	No	Free initiator added
Wafers[8]	BriB	HEMA	CuBr/ bipy	Yes	M_n inconsistent with graft thickness
Wafers[9]	BriB	MMA, DMAEMA, PEGMA	CuBr/ HMTETA	No	Free initiator, $Cu^{II}Br_2$ added Linear increase in brush thickness with polymerisation Linear increase in M_n of free polymer and brush thickness
Au coated[10]	BriB	MMA	CuBr/ bipy	No	ATRP slowed at longer grafting times
Au coated[11]	BriB	HEMA	CuCl/ $CuBr_2$/ bipy	Yes	Halogen exchange HEMA insoluble
Particles[12]	BriB	MMA	CuBr/ dNbipy	No	Sacrificial initiator Cu^{II} no help
Particles[13]	BriB	Meth (acrylates)	CuCl/ dNbipy	No	Linear increase in M_n with conversion
Particles[14]	BriB	Sty, BzA	CuBr/ dNbipy	Yes	Cleavage of PS-*b*-PBzA
Particles[15]	BriB	Sty, BA, MMA	CuBr/ $CuBr_2$/ dNbipy	Yes	Cu^{II} added Cleavage of PSty, PBA, and PMMA with low MWD

Immobilisation of 2-(4-chlorosulfonylphenyl) ethyl trichlorsilane (CTS) on silicon wafers and particles was carried out by Fukuda's group in order to graft MMA from the surfaces using CuBr/dHbipy (**Scheme 3.1**).[6]

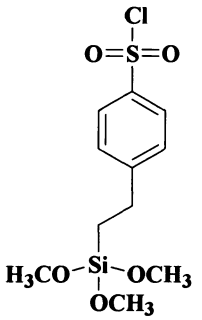

Scheme 3.1:

CTS initiator used by Fukuda's group.

Free "sacrificial" initiator was added to the solution in order to control the polymerisation; otherwise free polymer of PD greater than 3 was formed. The resulting grafted polymer was not cleaved, but the assumption was made that the M_n and MWD (< 1.5) of the free polymer was equal to that on the surface.[6]

Tirelli *et al.*[8] functionalised silicon wafers with bromoisobutyrates (BriB) with a low initiator density in order to carry out aqueous grafting of HEMA; the grafted polymer layer was found to be 100 nm to a few microns thick, implying high molecular weight polymer. The grafted polymer was cleaved using boiling 5M NaOH, and found to have an M_n of 1000–2000 g/mol, significantly less than expected considering the graft thickness.[8]

Hydrogen terminated Si(100) substrates were functionalised with BriB groups and grafted with MMA, DMAEMA, and poly(ethylene glycol)monomethacrylate (PEGMA) using CuBr/1,1,4,7,10,10-hexamethyltriethylenetetramine (HMTETA) in a 1:1 mixture of anisole and MeCN.[9] Free initiator was added so that the free polymer could be analysed by GPC; conversely, $Cu^{II}Br_2$ was added in order to control the polymerisation.[9] A near linear increase in the thickness of the grafted PMMA brush with polymerisation time was found.[9] Cleavage was not attempted, but instead the living nature of the procedure was assumed from the linear relationship between the M_n of the free polymer and the thickness of the PMMA brush.[9]

Jones and Huck [10] showed that ATRP of (meth)acrylates initiated by BriB groups tethered from gold coated silicon wafers slowed at longer reaction times. This was attributed to a decreasing number of growing radicals caused by termination,[10] which is consistent with the findings of Xiao and Wirth[16] who found an unexpected decrease in halide content during the surface initiated polymerisation of acrylamide from silica as observed by X-ray photoelectron spectroscopy and microanalysis. In a more recent study Jones *et al.*[17] similarly found that surface bound initiation is not quantitative, and grafting is well–controlled only after initiation.[17]

Huang and coworkers[11] grafted HEMA under aqueous conditions from gold surfaces using an isobutyrate linker. They noted rapid polymer growth early in the reaction, followed by a decrease in film growth, even in the presence of added $Cu^{II}Br_2$. They increased control by employing halogen exchange using CuCl. Quantitative detachment of the polymer films was successful using either I_2 or potential cycling;

however, the PHEMA was insoluble in all organic solvents examined,[11] which is likely due to transesterification of HEMA leading to a cross–linked swollen gel.

In order to control polymerisations from the surface of silicon wafers, either "sacrificial" initiator or Cu^{II} is added to the grafting procedure. When "sacrificial" initiator is added, the free polymer can be analysed by GPC, and the assumption is often made that the M_n and PDI of the free polymer matches that of the grafted polymer. Cu^{II} is added in order to increase the concentration of deactivating species in solution, and hence reduce active radical concentration and termination.

A linear relationship between the M_n of the soluble polymer and the thickness of the polymer brush has been used to indicate a living system. Conversely, rapid growth at the beginning of the reaction, and then a decrease in growth has been used to indicate excessive termination. Cleavage, when attempted, has not been quantitative, has required harsh conditions, and resulted in insoluble polymer, or material with measured M_n inconsistent with graft thickness.

When MMA was grafted from 75 nm silica nanoparticles, von Werne and Patten[12] found that polymerisation was only controlled when free initiator was added, contrary to when Sty was grafted, which did not require free initiator. Additionally, when larger silica particles (300 nm) were employed, neither the grafting of Sty nor MMA was controlled, which was attributed to the very high $[M]_o/[I]$ ratio of 500 to 800, where it was calculated that only 25 % of the initiator present in the nanoparticles in fact initiate polymerisation. The addition of Cu^{II} species did help control the polymerisation.

Sty, MMA, and *n*-butyl acrylate (BA) were grafted from BriB groups tethered to silica particles under bulk conditions using CuBr/$Cu^{II}Br_2$/dNbipy as catalyst with a high $[M]_o/[I]$ ratio and polymerisations were terminated at low conversions.[15] Cleavage using HF yielded PMMA with a PDI < 1.4, PSty with a PDI between 1.2-1.3, and PBA with a MWD between 1.3 and 1.5.[15] Decreased growth was observed for PMMA grafting which was attributed to steric crowding of the isobutyrate groups,[15] based on the study by Miller *et al.*[18] who used partially deuterated MMA to study initiation from 12-arm dendrimers, for which they observed incomplete initiation for star polymers of low DP and low M_n.

Grafting from silica nanoparticles offers the advantage that the grafted polymer may be cleaved using HF after the reaction has been terminated. Grafting density and the size of the nanoparticles play an important role in grafting from particles. Fukuda has outlined a number of observations which indicate a good grafting process: M_n of the grafted polymer increases linearly with monomer conversion; the M_n and MWD of the graft polymer are nearly equal to those of the free polymer; the amount of graft polymer increases proportionally to monomer conversion, and thus to the M_n of the grafted polymer.[7]

3.1.3 Grafting from Organic Polymer Particles

Grafting has been carried out from hard polymeric microspheres, as well as from swellable polymeric particles, and some select results are shown below (**Table 3.2**).

Table 3.2:

Grafting methacrylates from polymeric microspheres:

Substrate	Surface-bound Initiator	Monomer(s)	Catalyst	Polymer Cleaved?	Notes
Hard cross–linked PSty[19,20]	BriB	MMA, BzMA, DMA	CuBr/ Pyridineimine	Yes	TFA cleavage of PMMA No cleavage of PDMA Mechanical damage Free polymer
PSty latex beads[21]	NCSA	MMA EA	CuBr/ Hexacishexyl triethylene-tetramine	No	High weight gains Free polymer
PSty latex beads[22-24]	Cl P	DMA NIPAM	CuBr, CuCl/ PDMETA, HMTETA, Me_6TREN	Yes	High graft densities Cu^{II} added M_n of 600 000 PDI 1.3-1.8
P(DVB80)[25]	BzCl	Sty	CuBr/bipy	No	Slight Size increase
PS-*co*-PEG1100MA[26,27]	BriB	HEMA	CuBr/bipy	No	Grafting up to tens of μm
P(DVB80-*co*-HEMA)[28]	BrP	MMA	CuBr/ Me_4Cyclam	No	Large weight gains

Wang–type and Merrifeld resins, made of hard cross–linked PSty, have been functionalised with ATRP initiators in order to carry out grafting of MMA, BzMA, and *N*,*N*-dimethylacrylamide (DMA) using CuBr/*N*-(n-propyl)-2-pyridylmethanimine by Haddleton's group.[19,20] The ease of cleavage from the Wang resin with TFA, via the formation of a stabilised carbocation intermediate, is an advantage since they were able to isolate the soluble, catalyst free homo- and block copolymers with well controlled M_n and

narrow PDI (PMMA with an M_n of 7 000 g/mol, where 8 200 g/mol was expected, and PDI of 1.18) with yields between 68 and 77 %.[19] The authors proposed that these resins could be used in the preparation of targeted polymers, as scavenger resins or as solid supports for the synthesis of oligopeptides.[19]

Initiator loading was examined for 0.87 and 3.48 mmol g^{-1} initiators to investigate the effect of initiator density on the control of the grafting procedure.[19] The higher loading gave polydisperse polymers with M_n significantly higher than that expected. The lower loading resulted in narrow M_n grafts with M_n similar to that expected. The authors concluded that at higher initiator loadings, termination is increased due to the proximity of the propagating chains.[19] At the lower loadings, M_n increases linearly with conversion, although some broadening of the M_n and PDI occurs at conversions greater than 80 % where viscosity is high, and stirring may no longer be efficient.[19] Between 5 and 8 % monomer was converted to free polymer.[19] Grafting DMA from derivatised Wang resins resulted in over 1000 % weight gain under similar conditions where grafting was carried out for 55 h.[20] Mechanical damage of the resins due to stirring was observed using SEM.[20]

Filiz and coworkers[21] grafted neat MMA and ethyl acrylate (EA) from PSty latex beads, cross-linked with 10 % DVB and surface functionalised with N-chlorosulfonamide groups (NCSA), and with CuBr/hexakishexyltriethylenetetramine catalyst. They observed weight gains of 380 % after 6 h for MMA, and 160 % after 44 h for EA, in addition to 6 % free polymer.[21]

Kizhakkedathu *et al* grafted DMA[22,23] and *N*-Isopropylacrylamide (NIPAM) [24] from a copolymer shell of 2-(methyl-2'-chloropropionato)ethyl acrylate and PSty attached to negatively charged PSty latex beads using either CuCl or CuBr and PMDETA, HMTETA or Me_6TREN under aqueous conditions. Base catalysed cleavage using NaOH released high M_n (600 000–800 000 g/mol) and polydisperse (1.25–1.8) polymer chains.[22]

Tirelli and coworkers have found that ATRP polymerisation from highly swellable, cross-linked PS-*co*-PEG1100MA beads occurs from the surface as well as from the sub-surface.[27] After grafting, the structures "exploded" such that PSty domains were observed. Correspondingly grafted HEMA was labeled with fluorescent dansyl glycine and the cross-sections showed homogeneous polymerisation.[27] When low swelling cross-linked PS-*g*-PEG600MA beads were used to graft the fluorescently labeled HEMA, surface polymerisation was noted as also observed from TEM,[27] and IR.[26] They have reported the polymerisation of extremely thick layers of polymers from their surfaces, up to several tens of microns in size,[26] starting with latexes that have hydroxyl groups homogeneously throughout.

Zheng and Stover grafted PSty from hydrochlorinated P(DVB80) microspheres with particle size increase of 2.96 μm to 3.07 μm, which resulted from surface grafting. The soluble polymer had an M_n of 26 500 g/mol and a PDI of 1.67.[25] Other work in our group has consisted of using propionate functionalised swellable P(DVB80-*co*-HEMA) microspheres to graft MMA at r.t. using CuBr/Me_4Cyclam, which were then used as macroinitiators for a second grafting of DMAEMA, to yield diblock grafted particles.[28] Aqueous dispersions of these microspheres were viewed by optical microscopy and the

microspheres were perfectly spherical in shape; however, the swellable, block copolymer grafted particles deform substantially upon drying from different solvents. When DMAEMA was grafted from DVB80-*co*-HEMA particles, weight gains of 398 % and amine loadings of 4.6 mmol g^{-1} were found, and thus, these microspheres could potentially be used as highly functional polymer supports.

Grafting from polymeric microspheres results in the formation of soluble polymer, which may be due to transfer to solvent or monomer, residual initiator from initiator functionalisation, or partial cleavage of the polymer chains from the substrate. Mechanical damage by stirring has been observed by Haddleton's group,[20] as well as in the present work, which may lead to this partial cleavage. Again, initiator density is important, since a high initiator density may lead to increased termination. Cleavage from polymeric microspheres has not been fully explored to date.

3.1.5 Chapter Objectives

Monodisperse DVB80-*co*-HEMA microspheres were prepared as previously described and functionalised with 2-bromoisobutyryl bromide. MMA was then grafted from these initiator particles, and the formed PMMA was cleaved from the microspheres to draw conclusions about MMA grafting in a gel environment.

3.2 Experimental Section

Chemicals

Alumina, basic, Brockman activity I (60–325 mesh) was purchased from Fisher Scientific and used as received. Ammonium hydroxide (NH_4OH) (28 %) was purchased from Anachemia and used as received. Dichloromethane (CH_2Cl_2) (distilled in glass), diethyl ether (99 %) and methanol (MeOH) (99.8 %) were purchased from Caledon, and used as received. 2-Bromoisobutyryl bromide (98 %), 4,4'-dinonyl-2,2'-dipyridyl (dNbipy) (97%), ethyl 2-bromoisobutyrate (Et-2-BriB) (98 %,), *N,N,N',N',N''*-pentamethyldiethylenetriamine (PMDETA) (99 %), sodium methoxide (NaOMe) (25 wt. % in MeOH, Aldrich), and triethylamine (Et_3N) (99 %) were purchased from Aldrich, and used as received. 2,2'-Azo-bis-(2-methylpropionitrile) (AIBN) (Eastman Kodak Co.) was recrystallised from methanol. Tetrahydrofuran (THF) (99+ %, Caledon) was refluxed over potassium and distilled under nitrogen. Methyl methacrylate (MMA) (99 %, Aldrich) was passed through an inhibitor removal column prior to use.

The preparation of the precursor DVB80-*co*-HEMA particles (E1) and CuBr was described in **Section 2.2**.

Preparation of Butyrate Initiator Particles (E1BBr)

Precursor particles (4.00 g) were suspended in THF (40 mL) and Et_3N (5.13 g, 51 mmoles) in a 100 mL round-bottomed flask for 2 h under a flow of nitrogen. The round-bottomed flask was placed in an ice-water bath prior to dropwise addition of 2-bromoisobutyryl bromide (11.66 g, 51 mmoles). The suspension was allowed to return to

r.t. and stirred under nitrogen overnight. The initiator particles were washed with THF (3x), a mixture of THF and MeOH (3x), MeOH (3x), and once with diethyl ether. The yield of the clean particles was 6.22 g after drying under vacuum at room temperature for 7 days corresponds to esterification of 80 %.

Solution Homopolymerisation of Methyl Methacrylate (PMMA)

Under a nitrogen environment, a 10 mL round bottom flask equipped with a stir bar, was charged with CuBr (71.64 mg, 0.50 mmol), dNbipy (408.29 mg, 0.999 mmol), or PMDETA (86.55, 0.50 mmol) and MMA (5.00g, 50 mmol). The reaction mixture was allowed to stir until it became homogeneous. Et-2-BriB (97.41 mg, 0.50 mmol) was added via a nitrogen filled syringe, and the flask was placed in an oil bath equilibrated to 90°C. After 2 hours, 95 % conversion was reached with an M_n of 10 100 g/mol (for dNbipy) and 99 % conversion for PMDETA with a M_n of 10 200 g/mol, which was followed by removing 0.2 mL aliquots every 15 minutes, and was found to be complete after 2 hours. Polymeric solutions were diluted with THF prior to passing through a basic alumina column to remove copper and ligand. The polymeric solution was precipitated into pentane and dried for 24 hours under vacuum (4.95 g, 95 %, dNbipy).

Methyl Methacrylate Grafted Particles (E1-PMMA-Br)

The procedure for the bulk polymerisation of MMA was followed with the exception that isobutyrate initiator particles (173.0 mg) were added to a 10 mL round bottom flask equipped with a stir bar with a monomer to initiator ratio of 100:1. Et-2-

BriB (97.41 mg, 0.50 mmol) was only added for select graftings. 0.2 mL aliquots were removed from the reaction flask every 15 minutes, until the reaction was terminated after 2 hours. The particles were washed with THF (3x), a 9:1 mixture of THF:MeOH containing 1 % NH_4OH (3x), followed by a final wash with THF. The clean white particles were allowed to dry for 7 days under vacuum yielding 3.794 g of E1-PMMA-Br.

Cleavage of Grafted Methyl Methacrylate from Methyl Methacrylate Grafted Particles (E1-PMMA-Br$_{cleaved}$)

E1-PMMA-Br particles (1.00g), THF (50 mL), and MeOH (12.5 mL), were placed in a 100 mL round bottom flask fitted with a condenser and allowed to stir under nitrogen for 2 hours. NaOMe (3.0 g, 56 mmol) was added via a nitrogen filled syringe. The reaction mixture was brought to reflux, and allowed to continue refluxing, while under nitrogen for 96 hours. The resultant microspheres were washed with THF (3x), 9:1 THF: MeOH (3x), and water (3x) to remove any sodium salts. Beige coloured particles remained (50 mg). The soluble polymer was isolated from the washings by first reducing the volume of the THF and MeOH mixture, dissolving the residue in CH_2Cl_2 and washing with water to remove any sodium salts. The CH_2Cl_2 was removed and the polymer was dissolved in THF for GPC analysis.

Bulk Polymerisation of Methyl Methacrylate in the presence of precursor DVB80-co-HEMA particles ($PMMA_{E1}$)

DVB80-*co*-HEMA precursor particles (0.173 g) were allowed to swell in MMA (5.00g, 58 mmol) under a nitrogen atmosphere for 0.5 hours. CuBr (71.64 mg, 0.50 mmol) and dNbipy (408.39mg, 0.999 mmol) were then added, and the solution was allowed to stir for an additional 15 minutes prior to the addition of Et-2-BriB (70.09 mg, 0.50 mmol) via a nitrogen filled syringe. The round bottom flask was then immersed in a 90 °C oil bath. The microspheres were washed with THF (3x), and with diethyl ether (1x), yielding a white solid (0.175 g). The washings were combined and reduced in volume to remove diethyl ether, and passed through an alumina column. This polymeric solution was precipitated into pentane, and a fluffy white polymer was dried for 24 hours (3.8 g, 76 %).

Swelling Measurements

As described in **Section 2.2**.

Characterisation

As described in **Section 2.2**.

3.3 Results and Discussion

3.3.1 Preparation of Isobutyrate Initiator Particles

The P(DVB80-*co*-HEMA) E1 microspheres were treated with 2-bromoisobutyryl bromide in the presence of Et_3N in THF to form ATRP initiator microspheres, E1BBr (**Scheme 3.2**).

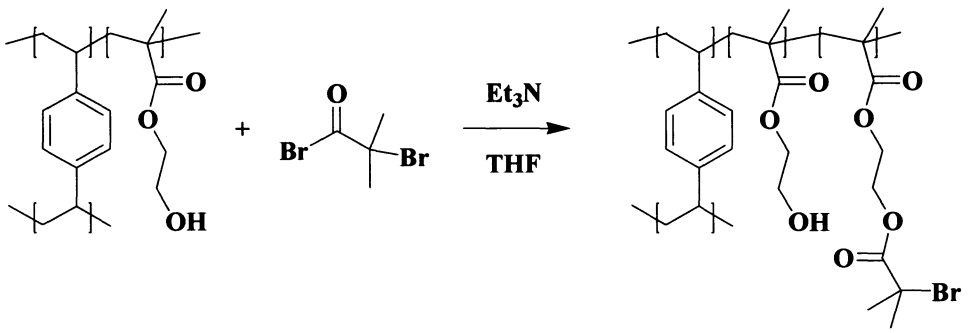

Scheme 3.2:

Preparation of E1BBr from E1.

The functionalisation to form the bromoisobutyrate initiator particles (E1BBr) was 80 % determined gravimetrically. The size of the microspheres increased from an average diameter of 1.6 ± 0.2 μm to 1.7 ± 0.2 μm. The surfaces of the E1BBr particles remained smooth, and the particles pack in a crystalline array, and are quite monodisperse (**Figure 3.1a**) just as was seen with the E1PBr particles. The core shell morphology again appears more distinct after functionalisation, where knife cutting artifacts are apparent in the core (**Figure 3.1b**). Knife cutting artifacts appear when the particle is harder than the resin, which is likely the case for the core, which has a high

DVB80 content; knife cutting artifacts do not appear in the outer 200 nm shell, thus it can be assumed that this area is lightly cross–linked.

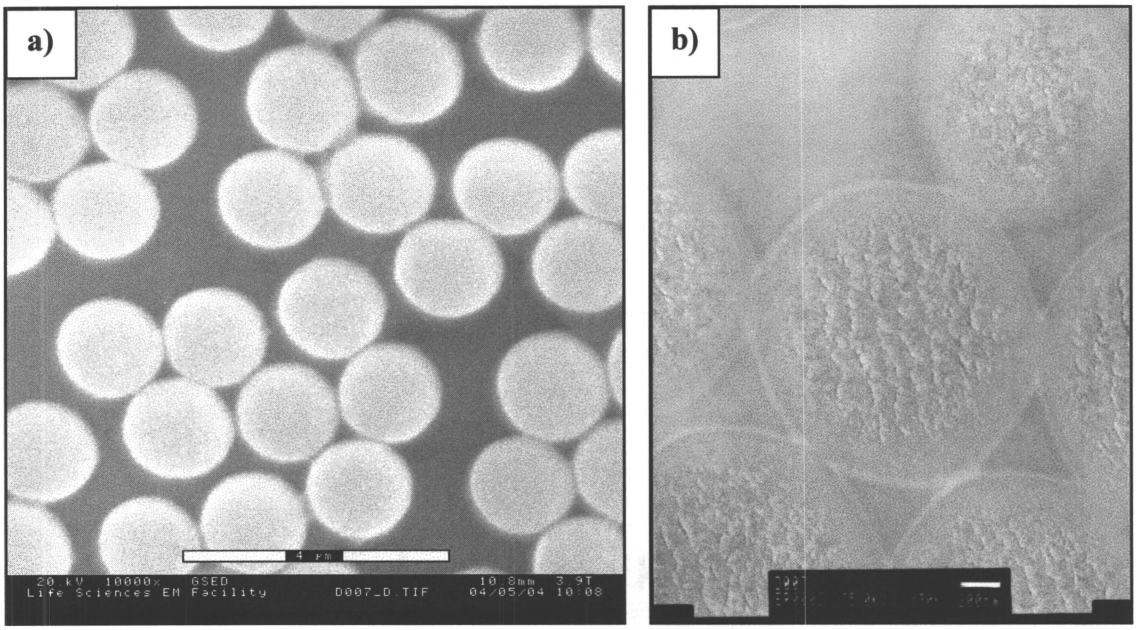

Figure 3.1:

E1BBr: **a)** ESEM (scale bar is 4µm); **b)** TEM (scale bar is 200 nm).

The E1BBr microspheres had similar swelling properties to the E1PBr microspheres, indicating the hydrophobic nature of the E1BBr particles (**Table 3.3**).

Table 3.3:

Swelling ratios of E1 and E1BBr microspheres in select organic solvents and MMA:

Solvent	E1 Swelling ratio (%)[a]	E1BBr Swelling ratio (%)
Ethanol	190	140
H_2O	160	100
MeOH	140	130
MMA	-	160
THF	170	210

a) Swelling ratios were determined according to **Equation 2.1**.

3.3.1.1 Study of Isobutyrate Initiator Particles by FTIR

When the isobutyrate group is added to the E1 microspheres there is a significant decrease in the hydroxyl signal at 3450 cm^{-1} (**Figure 3.2**). The ester carbonyl peak is shifted from 1724 cm^{-1} ($\underline{CO}OCH_2CH_2OH$) to 1735 cm^{-1} ($\underline{CO}C(CH_3)_3Br$).

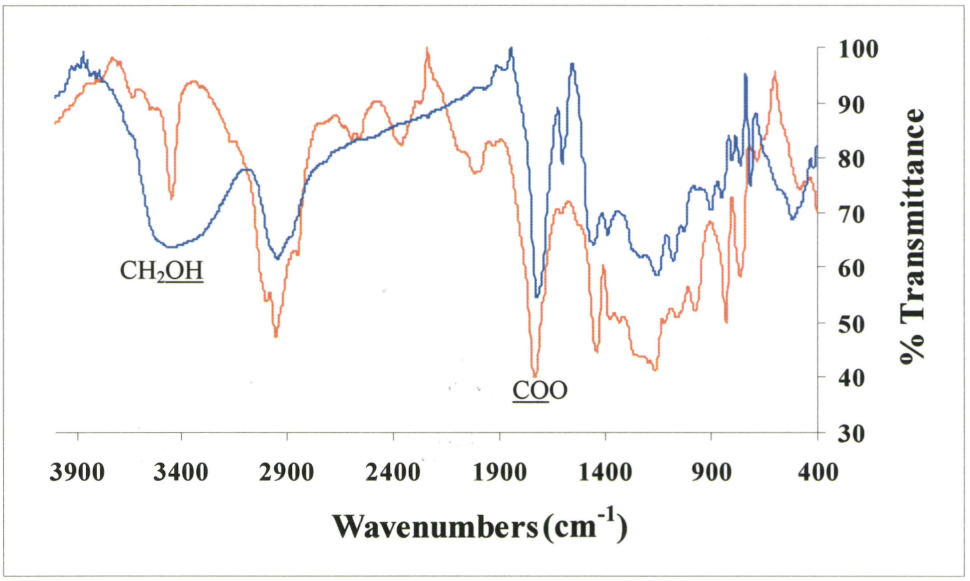

Figure 3.2:

FT-IR spectrum of E1BBr (in orange), and E1 microspheres (in blue).

3.3.1.2 Study of Isobutyrate Initiator Particles by CPMAS-NMR

CPMAS-NMR (**Figure 3.3**) confirms the functionalisation, with the carbonyl for the isobutyrate apparent at 171.1 ppm, and the $COO\underline{C}H_2$ and $\underline{C}H_2OH$ peaks of HEMA (**Figure 2.6**) replaced by a single peak at 63.5 ppm due to the $COO\underline{C}H_2$ groups.

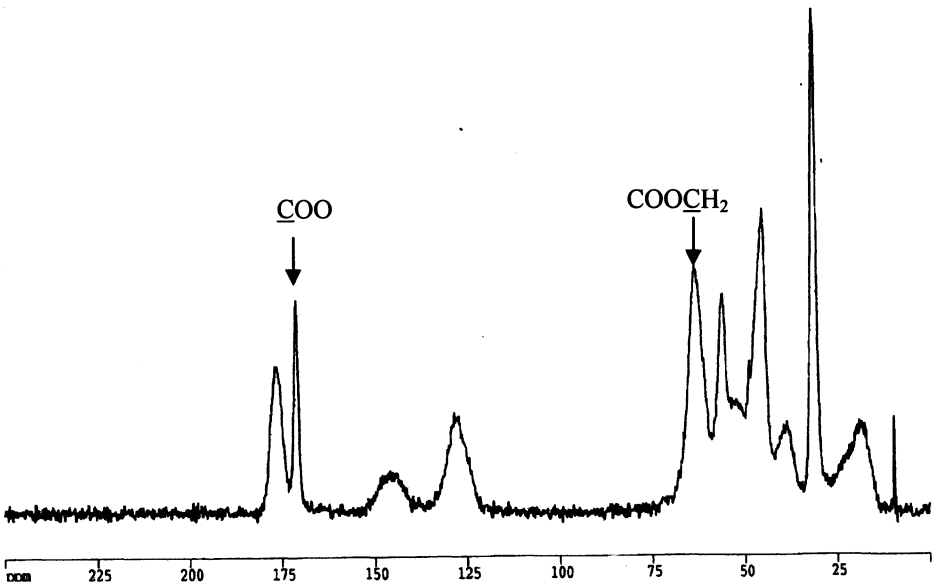

Figure 3.3:

CPMAS-NMR of E1BBr particles.

The disappearance of the $\underline{C}H_2OH$ signal at 59.9 ppm (**Figure 2.6**) is in agreement with the gravimetric assessment of 80 % esterification. Peak areas of the isobutyrate and the HEMA carbonyl signals do not match, and this discrepancy may be a result of the less efficient cross-polarisation to the more mobile isobutyrate. Functionalisation is also seen in the STXM, which is very similar to that of the propionate particles. The butyrate carbonyl is slightly higher energy, and so it is diagnostic in the STXM of the grafted particles.

3.3.2 Polymerisation of MMA

Bulk polymerisation of MMA using either CuBr/dNbipy or CuBr/PMDETA and Et-2-BriB with an MMA:initiator:catalyst ratio of 100:1:1 was carried out at 90 °C. Bulk conditions were used to give continuity between the polymerisations of MA and MMA. The kinetic plots of the bulk polymerisation at 90 °C using CuBr/dNbipy and CuBr/PMDETA are shown (**Figure 3.4**). Conversion increases with time, but radical concentration remains constant, as seen in **Figure 3.4a**. Additionally, M_n increases linearly with conversion, while PDI decreases (**Figure 3.4b**), which is indicative of a well controlled ATRP.

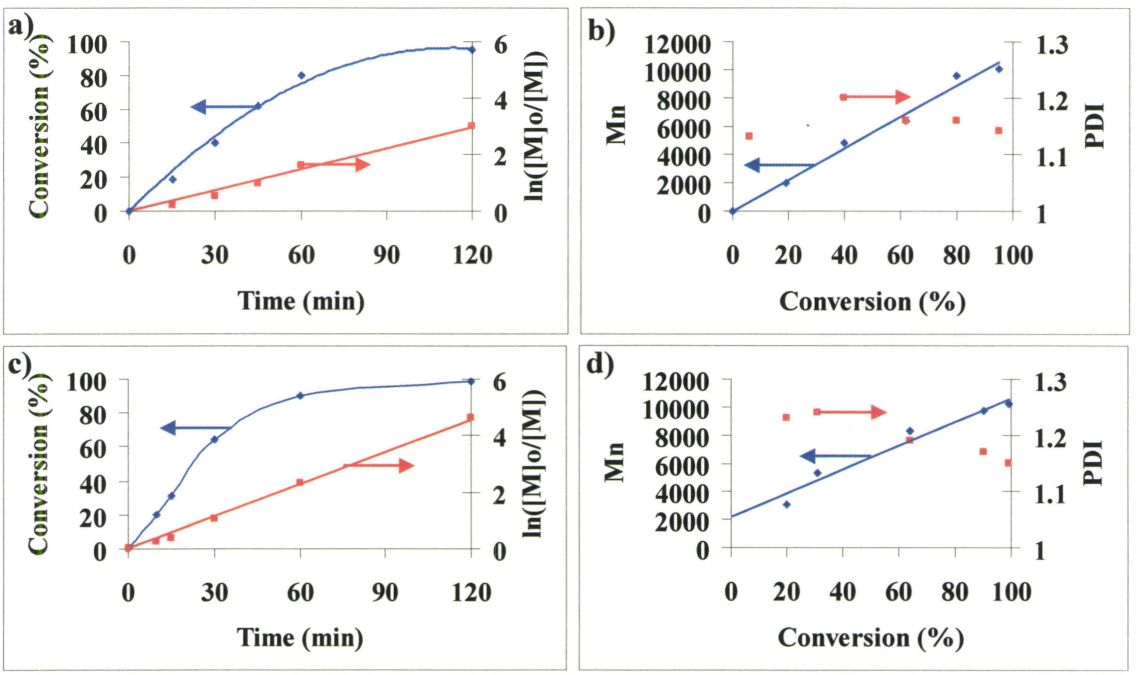

Figure 3.4:

MMA homopolymerisation with CuBr/dNbipy: **a)** plot of monomer conversion (blue) and $\ln([M]_o/[M])$ (red) with time, and; **b)** plot of M_n (blue), and PDI (red) with conversion. With CuBr/PMDETA: **c)** plot of percent conversion (blue) and $\ln([M]_o/[M])$ (red) with time, and; **d)** plot of M_n (blue), and PDI (red) with conversion.

The following table summarises the results of the bulk homopolymerisations of MMA after 2 hours (**Table 3.4**):

Table 3.4:

Homopolymerisation of neat MMA using either CuBr/dNbipy or CuBr/PMDETA and Et-2-BriB at 90 °C:

Catalyst	Conversion (%)	M_n expected (g/mol)	M_n (g/mol)	PDI
CuBr/dNbipy	95	9 700	10 100	1.13
CuBr/PMDETA	99	9 700	10 200	1.15

3.3.3 Grafting MMA from Isobutyrate Initiator Microspheres

Grafting MMA from E1BBr was carried out using CuBr and either dNbipy or PMDETA; additionally; it was carried out in the presence and the absence of "sacrificial"/free initiator, Et-2-BriB. The results of grafting using these conditions on the particles are shown below (**Table 3.5**).

Table 3.5:

Results of grafting MMA from E1BBr particles using CuBr/dNbipy or CuBr/PMDETA in bulk without and with Et-2-BriB:

Experimental Conditions	Weight Gain (%)	Conversion to Grafted Polymer (%)	Particle Size (μm)[a]
E1BBr	-	-	1.7 ± 0.2
E1-PMMA$_{dNbipy}$-Br	2000	72	4.4 ± 0.5
E1-PMMA$_{dNbipy+Et\text{-}2\text{-}BriB}$-Br	260	9	3.5 ± 0.4
E1-PMMA$_{PMDETA}$-Br	2200	83	4.5 ± 0.6
E1-PMMA$_{PMDETA+Et\text{-}2BriB}$-Br	920	33	4.3 ± 0.5

a) measured with Coulter Multisizer

The monomer conversion to grafted polymer is 2–3 times as high as for the E1-PMA-Br particles. This could be due to the stability of the propagating methacrylate monomer, which would lead to decreased termination. The size increase of the microspheres as a function of time (**Figure 3.5**) was found to be very rapid at first in the absence of free initiator, and to level off towards the end of the grafting procedure with dNbipy (**Figure 3.5 a**). In the presence of free initiator, the size increased more slowly, but throughout the polymerisation. When PMDETA was used, there was a rapid initial increase in particle size even in the presence of free initiator (**Figure 3.5 b**).

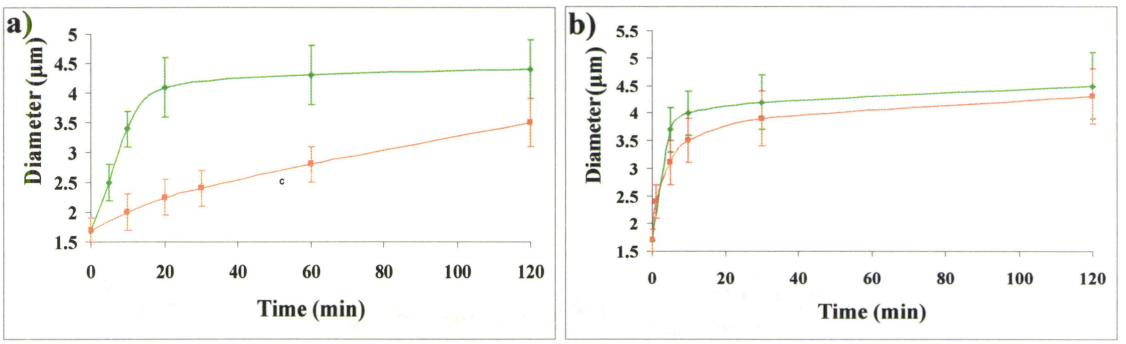

Figure 3.5:

Plot of diameter increase as a function of time for **a)** E1-PMMA$_{dNbipy}$-Br (◆), and; E1-PMMA$_{dNbipy + Et\ 2\text{-}BriB}$-Br (■), and **b)** E1-PMMA$_{PMDETA}$-Br (◆), and; E1-PMMA$_{PMDETA+\ Et\ 2\text{-}BriB}$-Br (■).

These grafted particles have interesting morphology as seen in **Figure 3.6**. Though the initiator microspheres E1BBr are monodisperse, and the grafting reactions were carried out under stirring, ESEM images of the grafted microspheres show a range of diameters and corresponding surface morphologies. For example, the E1-PMMA$_{dNbipy}$-Br microspheres (**Figure 3.6 b**) show mainly large (approximately 4.5 µm) particles with rounded surface convolutions suggestive of grafting through the

scaffolding. Conversely, the corresponding microspheres grafted in the presence of free initiator, E1-PMMA$_{dNbipy+Et\text{-}2\text{-}BriB}$-Br (**Figure 3.6 c**) appear as a mixture of smaller smooth microspheres with about one quarter larger, surface cracked microspheres reminiscent of some of the PMA grafted microspheres. It is currently unclear whether this range in size and surface morphology is due to different functionalisation /grafting or work-up and ESEM sample preparation.

The microspheres grafted using PMDETA show smooth surface undulations and narrower size distributions. The ESEM images of these microspheres show smaller diameters than those measured by Coulter Multisizer.

There is an observable difference in the size of those microspheres grafted without sacrificial initiator and those grafted with sacrificial initiator, indicating decreased grafting efficiency in the presence of free initiator.

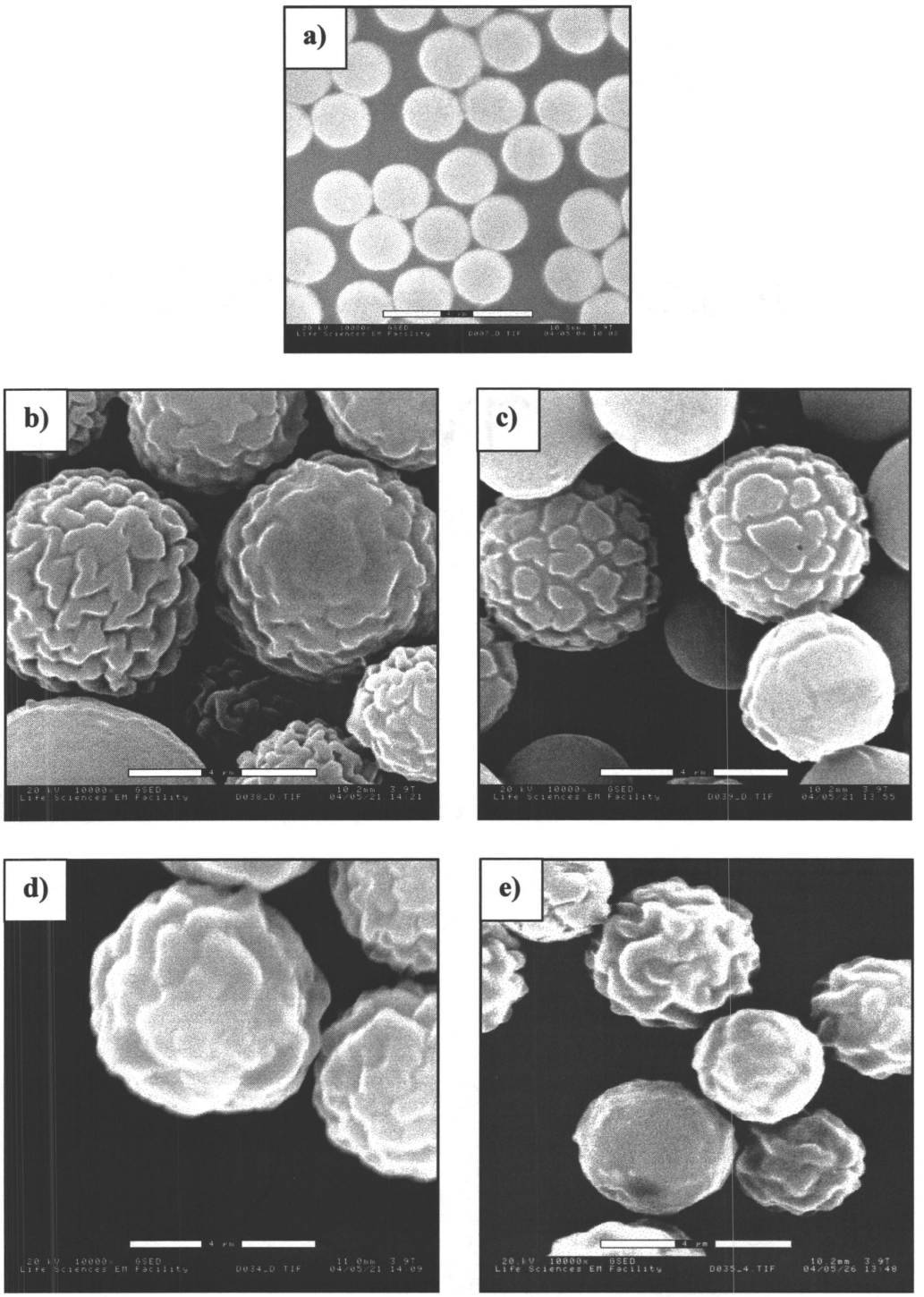

Figure 3.6:

ESEM images of **a)** E1BBr; **b)** E1-PMMA$_{dNbipy}$-Br; **c)** E1-PMMA$_{dNbipy + Et\ 2\text{-}BriB}$-Br; **d)** E1-PMMA$_{PMDETA}$-Br, and; **e)** E1-PMMA$_{PMDETA+Et\ 2\text{-}BriB}$-Br (scale bars are 4 μm).

The internal morphology of these microspheres is also quite different from the interior of the E1-PMA-Br microspheres, where concentric onion–type morphology was observed (**Figure 3.7**). The core is visible, and even demonstrates knife cutting features as was seen with E1BBr. The internal morphology of these microspheres as observed by TEM corresponds to the ESEM images of their surfaces.

The cross-sections of E1-$PMMA_{dNbipy}$-Br (**Figure 3.7a**) reveal lace-like coronas around defined cores. The coronas correspond to the smooth undulations seen for these particles by ESEM, and indicate macroporous layer likely formed by partial collapse of a solvent-swollen shell during drying. The corresponding E1-$PMMA_{dNbipy+Et\text{-}2\text{-}BriB}$-Br particles (**Figure 3.7b**) reveal a dense core surrounded by a homogenous and apparently dense shell containing grafted PMMA. The outer, cracked surface seen by ESEM appears in the TEM image as a thin cracked shell showing good contrast to both the major PMMA graft layer beneath it, and the aliphatic epoxy resin of the matrix. This layer likely constitutes mainly linear PMMA, likely penetrated by liquid resin components. There may well have been a chemical reaction between the active end groups carrying bromoisobutyrate, and the amine component of the resin, leading to covalent linkage between resin and particles (**Scheme 2.5**).

In the TEM images the core appears to be 500–700 nm in diameter. This is smaller than the "core" identified in the initiator particle (**Figure 3.1**), indicating partial grafting-induced swelling of the initiator cores.

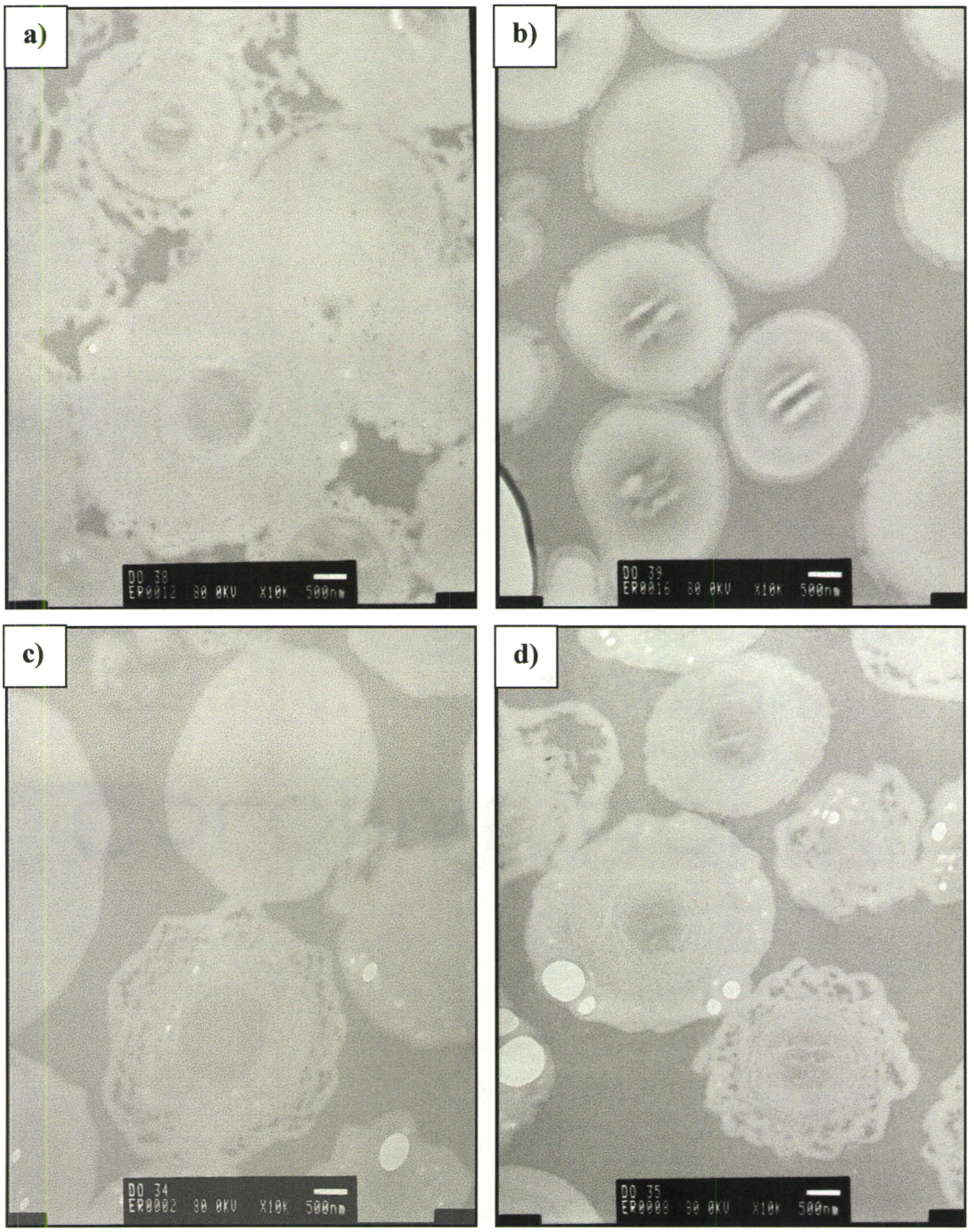

Figure 3.7:

TEM of **a)** E1–$PMMA_{dNbipy}$-Br; **b)** E1-$PMMA_{dNbipy\ +\ Et\text{-}2\text{-}BriB}$-Br; **c)** E1-$PMMA_{PMDETA}$-Br; and; **d)** E1-$PMMA_{PMDETA+Et\text{-}2\text{-}BriB}$-Br (scale bars are 500 nm).

3.3.3.1 Soluble Polymer Prepared During Grafting

MMA was also converted to soluble polymer in the grafting process. This soluble polymer was isolated from the washings of the grafted particles, and the properties of the polymers are shown below in **Table 3.6**

Table 3.6:

Table of soluble PMMA extracted from washings of E1–PMMA-Br prepared with either CuBr/dNbipy or CuBr/PMDETA without, and with free Et-2-BriB:

Experimental Conditions	M_n expected (g/mol)	M_n (g/mol)	PDI	Conversion to Soluble Polymer (%)	Total Conversion to Polymer (%)
$PMMA_{dNbipy}$	9 700	10 100	1.13	95	95
E1-$PMMA_{dNbipy}$-Br	-	68 800	1.75	4	76
E1-$PMMA_{dNbipy+Et\text{-}2\text{-}BriB}$-Br	8 300	7 400	1.20	81	90
$PMMA_{PMDETA}$	10 100	10 200	1.15	99	99
E1-$PMMA_{PMDETA}$-Br	-	17 000	2.41	3	86
E1-$PMMA_{PMDETA+Et\text{-}2\text{-}BriB}$-Br	5 600	11 400	1.39	54	87

In the absence of free initiator, a small amount of high M_n, polydisperse PMMA is formed. There is a significant narrowing of the PDI of this soluble polymer when free initiator is added, in addition to an increase in the conversion and a decrease in the M_n. The M_n is of 7 400 g/mol is quite close to that expected of 8 300 g/mol when grafting was carried out with dNbipy, and approximately twice as high when grafting with PMDETA where 11 400 g/mol was observed, and 5 600 g/mol was expected. The molecular weight evolution of the soluble polymer was followed by GPC, and the results are shown below in **Figure 3.8**.

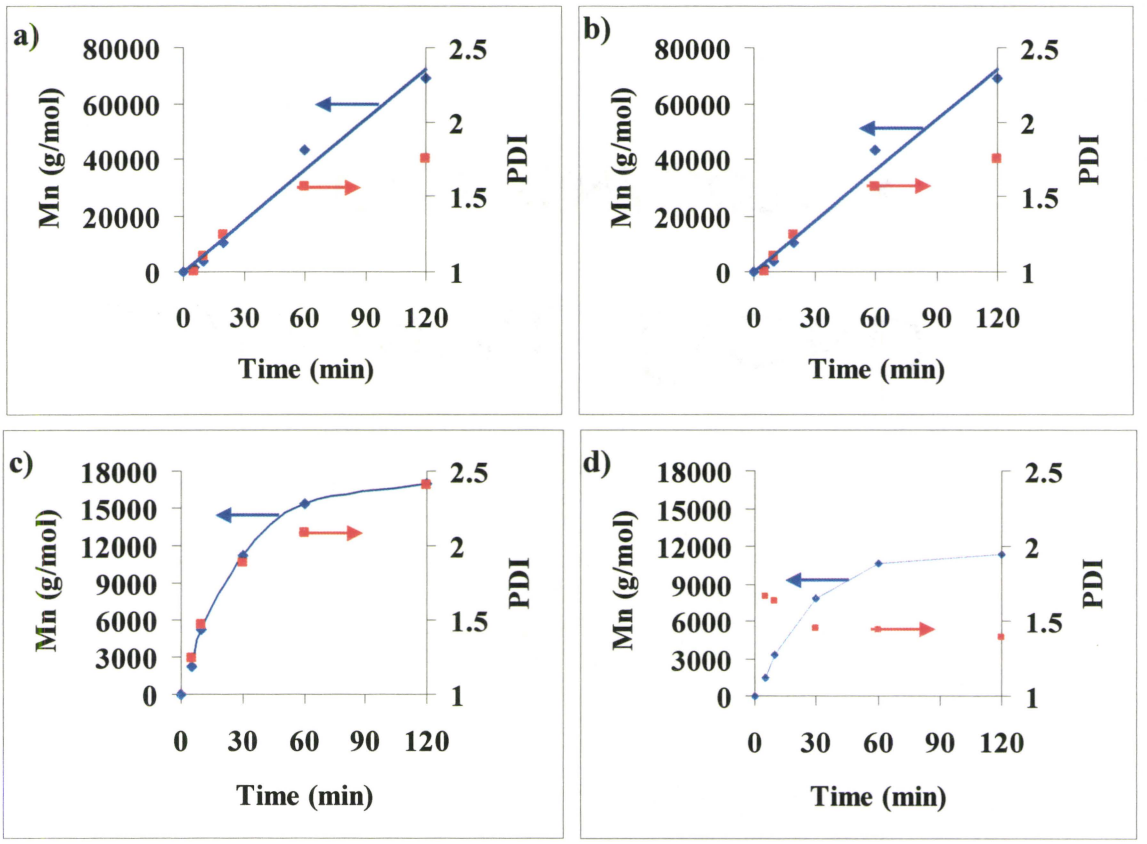

Figure 3.8:

Grafting MMA with CuBr/dNbipy: **a)** monomer conversion to soluble polymer (blue) and PDI (red) with time for E1-PMMA$_{dNbipy}$-Br without Et-2-BriB and; **b)** with Et-2-BriB. Grafting MMA with CuBr/PMDETA: **c)** monomer conversion to soluble polymer (blue) and PDI (red) with time for E1–PMMA$_{PMDETA}$-Br without Et-2-BriB and; **d)** with Et-2-BriB.

M_n is plotted as a function of time since the conversion to soluble polymer is less than 5 % at the end of the polymerisation, which is quite small, in the absence of free initiator. In the presence and in the absence of free initiator the M_n increases with time; whereas PDI increases in the absence of free initiator but decreases in the presence.

3.3.3.2 FT-IR Study of E1-PMMA-Br

In accordance with the 2200 % weight gain of E1-PMMA$_{PMDETA}$-Br, the FT-IR shows significant grafting (**Figure 3.9**). The carbonyl ($\underline{CO}OCH_3$) has shifted to 1731 cm^{-1}, indicating the dilution of the bromoisobutyrate peak. It has also increased in intensity. The hydroxyl peak has also been further reduced, and the aromatic stretches corresponding to the DVB have disappeared into the baseline. The ratio of the hydroxyl stretch to the carbonyl stretch has been reduced compared to either the E1BBr particles.

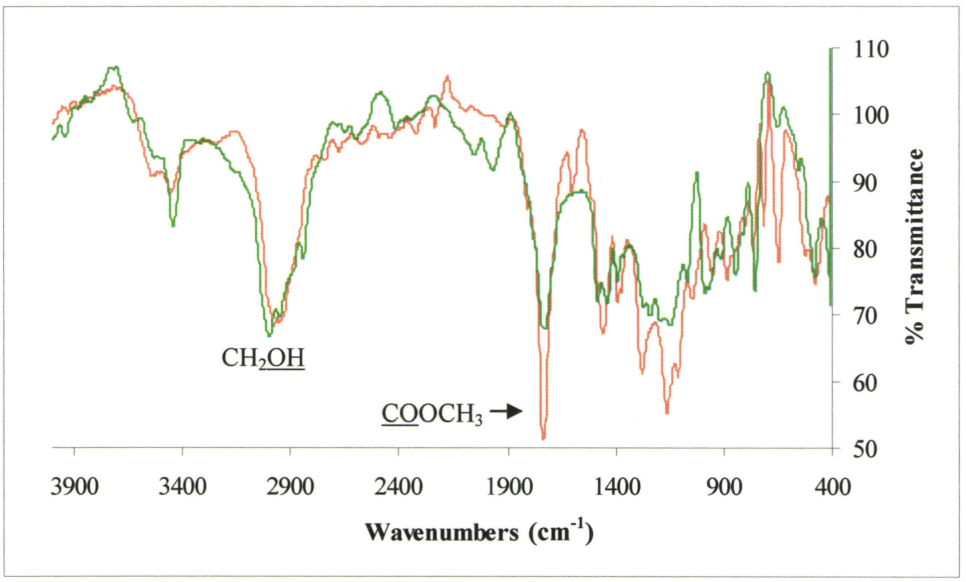

Figure 3.9:

FT-IR of E1-PMMA-Br microspheres (in green), superimposed over E1BBr particles (in orange).

3.3.3.3 CPMAS-NMR Study of PMMA Grafted Microspheres

As was seen with the E1-PMA-Br microspheres, the CPMAS-NMR spectrum of the E1-PMMA$_{PMDETA}$-Br (**Figure 3.10**) is dominated by the grafted PMMA, which

agrees with the weight gain of 2200 %. The following peaks are observed for the PMMA spectrum ($\underline{C}OOCH_3$, $O\underline{C}H_3$, $C(\underline{C}H_3)$, and $\underline{C}H_2C(CH_3)$). The carbonyl stretch for PMMA appears at 177.8 ppm, the methoxy appears at 51.7 ppm, the backbone methylene is found at 44.7 ppm, and the methyl group appears at 16.0 ppm. $CH_2\underline{C}(COO)CH_3$ appears below the peak around 57 ppm. THF is also present in the spectrum.

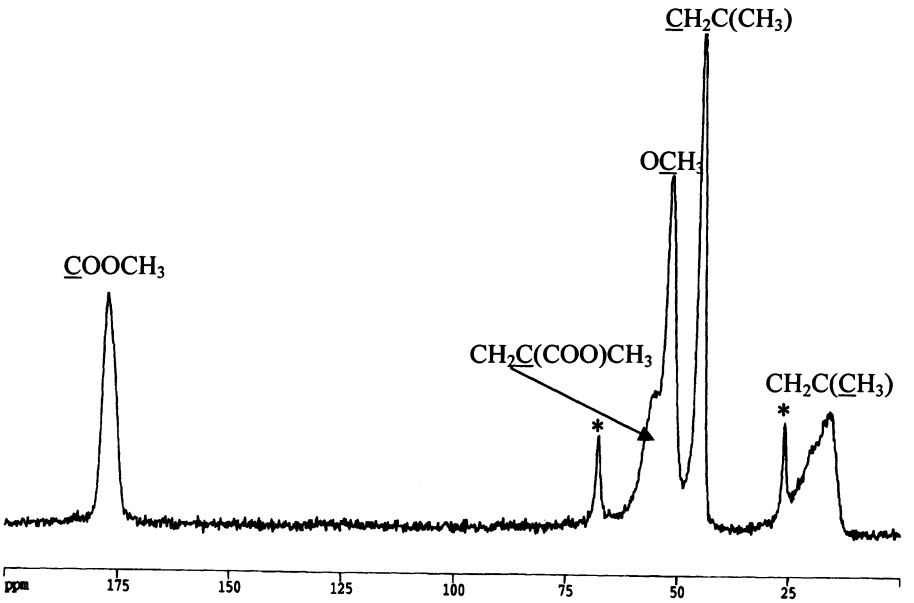

Figure 3.10:

CPMAS-NMR of E1-PMMA-Br microspheres.

STXM confirms the grafting as represented by a large increase in the carbonyl compared to the aromatic signal.

3.3.4 Cleavage of PMMA Grafted Microspheres

Base catalysed cleavage of the grafted PMMA was carried out using NaOMe for the reasons stated in section 2.4, resulting in DVB-*co*-MMA microspheres (**Scheme 3.2**). The cleaved PMMA was recovered nearly quantitatively, as were the particles, where a typical image of the particles is shown below (**Figure 3.11**).

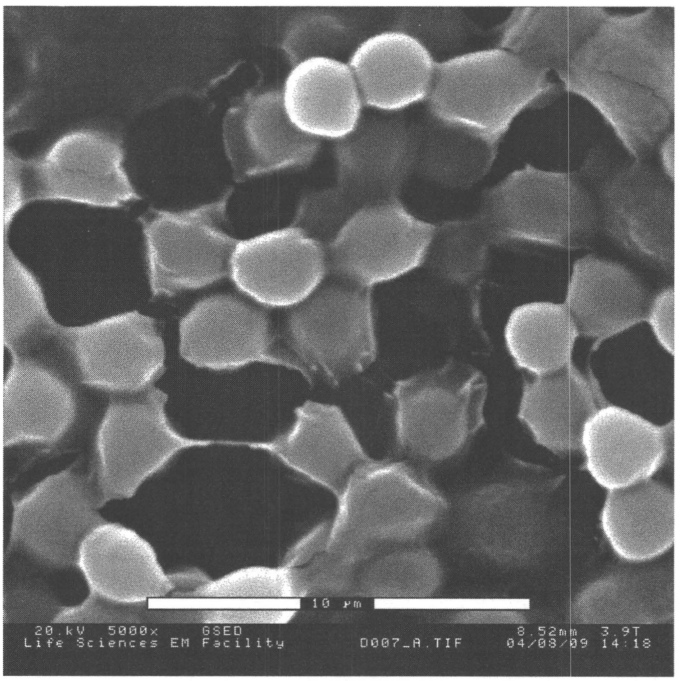

Figure 3.11:

ESEM of E1-PMMA-$Br_{cleaved}$ (scale is 10 µm).

The cleaved microspheres do not completely return to their original spherical shape, and there still appears to be a highly swollen gel layer on the surface despite numerous washings which would remove any soluble polymer. The results of cleaving the grafted PMMA are shown below (**Table 3.7**).

Table 3.7:

Results of graft cleavage:

Experimental Conditions	Grafted Particle Size (μm)	Cleaved Particle Size (μm)	Particles Recovered (%)	PMMA Recovered (%)
E1-$PMMA_{dNbipy}$-Br	4.4 ± 0.5	1.7 ± 0.2	94	91
E1-$PMMA_{dNbipy+Et\text{-}2\text{-}BriB}$-Br	3.5 ± 0.4	1.6 ± 0.2	90	94
E1-$PMMA_{PMDETA}$-Br	4.5 ± 0.6	1.7 ± 0.2	93	95
E1-$PMMA_{PMDETA+Et\text{-}2\text{-}BriB}$-Br	4.3 ± 0.5	1.6 ± 0.2	90	93

The cleaved PMMA cleaved, was analysed by GPC (**Table 3.8**), for M_n and PDI; the results of the soluble polymers isolated from grafting are also shown for comparison.

Table 3.8:

Results of cleaved polymer from E1-$PMMA\text{-}Br_{cleaved}$:

Experimental Conditions	Soluble PMMA			Cleaved PMMA			
	$M_{n\,th}$ (g/mol)	M_n (g/mol)	PDI	$M_{n\,th}$ of graft (g/mol)	M_n (g/mol)	PDI	PMMA Recovered (%)
$PMMA_{dNbipy}$	9 700	10 100	1.13	-	-	-	-
E1-$PMMA_{dNbipy}$-Br	-	68 800	1.75	7 400	60 400	1.90	91
E1-$PMMA_{dNbipy+Et\text{-}2\text{-}BriB}$-Br	8 300	7 400	1.20	1 100	4 600	1.30	94
$PMMA_{PMDETA}$	9 700	10 200	1.15	-	-	-	-
E1-$PMMA_{PMDETA}$-Br	-	17 000	2.41	8 500	22 300	1.98	95
E1-$PMMA_{PMDETA+Et\text{-}2\text{-}BriB}$-Br	5 600	11 400	1.39	3 500	13 800	1.21	93

The cleaved PMMA has an M_n higher than that expected for the grafted polymer, and the cleaved PMMA in the absence of sacrificial initiator is similar in PDI and M_n to

what was found of the soluble polymer. Thus, the assumption that the M_n, and PDI of the soluble polymer is close to that of the grafted polymer can be made for PMMA grafting from the present particles even in the absence of free initiator. The cleaved PMMA hence has higher molecular weight than those found for the E1-PMA-$Br_{cleaved}$.

FT-IR and CPMAS of the cleaved particles confirms that the grafted polymer was indeed almost quantitatively cleaved.

3.3.4 Homopolymerisation of PMMA in the presence of E1 microspheres

The solution homopolymerisation of MMA with Et-2-BriB in the presence of E1 particles was carried out in order to study the effect of a gel environment on the ATRP of MMA. The results are tabulated below along with results for the solution polymerisations in the absence of particles (**Table 3.9**).

Table 3.9:

Results of homopolymerisation of MMA in the presence and absence of E1 microspheres:

Experiment	Monomer Conversion (%)	M_n (g/mol)	PDI
$PMMA_{dNbipy}$	95	10 100	1.13
$PMMA_{PMDETA}$	99	10 200	1.15
$PMMA_{dNbipy+E1}$	76	12 400	1.35
$PMMA_{PMDETA+E1}$	75	16 700	1.69

Monomer conversion of MMA decreases in the presence of E1 particles, but M_n and PDI increase. At low monomer conversion and high M_n indicate loss of control, which is confirmed by the increased PDI. This lack of control may be due to the

hydroxyl groups of the HEMA which may chelate the Cu^{II} species, leading to decreased deactivation. In fact, PDI is much higher when PMDETA was employed, and it is the more active ligand of the two, thus it appears as though the decreased Cu^{II} concentration affects the equilibrium involving PMDETA more so than it does the dNbipy equilibrium.

3.4 Conclusions

Functionalisation of DVB80-*co*-HEMA particles to form ATRP butyrate initiator particles has been carried out successfully. Homopolymerisation of neat MMA using either CuBr/dNbipy or CuBr/PMDETA, as catalyst, initiated by ethyl 2-bromoisobutyrate was shown to be a controlled/living system. The conditions used for the homopolymerisation were applied to grafting MMA from butyrate initiator particles, and the resulting microspheres showed interesting morphologies. Addition of free initiator, ethyl 2-bromoisobutyrate, to the grafting procedures gave improved control, though as in the case of MA grafting shown in Chapter 2, at the expense of decreased grafting and increased soluble polymer. Particle size increase was very rapid at first in the absence of free initiator (dNbipy), and then leveled off towards the end of the grafting procedure; alternatively, when free initiator was added, the size increases at a lower rate but throughout the polymerisation, indicating lower incidence of termination. Added initiator to the grafting process also resulted in narrowing of the PDI of both the soluble and grafted polymer.

Base catalysed transesterification of the grafted microspheres released the grafted PMMA, which was found to be slightly higher in M_n than the soluble polymer, but similar in PDI. Cleavage of the grafted microspheres yielded cleaved DVB-*co*-MMA particles nearly quantitatively according to the weight loss; however. The grafted PMMA had a M_n and PDI very similar to the soluble polymer, which is a similar finding to that found in literature. This confirms that grafting from within lightly cross-linked gels can still be carried out with good control over M_n and PDI.

3.5 References

(1) Wang, J.-L.; Grimaud, T.; Matyjaszewski, K. *Macromolecules* **1997**, *30*, 6507.

(2) Shipp, D. A.; Wang, J.-L.; Matyjaszewski, K. *Macromolecules* **1998**, *31*, 8005.

(3) Matyjaszewski, K.; Wang, J.-L.; Grimaud, T.; Shipp, D. A. *Macromolecules* **1998**, *31*, 1527.

(4) Jewrajka, S. K.; Chatterjee, U.; Mandal, B. M. *Macromolecules* **2004**, *37*, 4325.

(5) Fernández-García, M.; De La Fuente, J. L.; Fernández-Sanz, M.; Madruga, E. L. *J. Appl. Polym. Sci.* **2002**, *84*, 2683.

(6) Ejaz, M.; Yamamoto, S.; Ohno, K.; Tsujii, Y.; Fukuda, T. *Macromolecules* **1998**, *31*, 5934.

(7) Ejaz, M.; Tsujii, Y.; Fukuda, T. *Polymer* **2001**, *42*, 6811.

(8) von Natzmer, P.; Bontempo, D.; Tirelli, N. *Chem. Commun.* **2003**, 1600.

(9) Yu, W. H.; Kang, E. T.; Neoh, K. G.; Zhu, S. *J. Phys. Chem. B* **2003**, *107*, 10198.

(10) Jones, D. M.; Huck, W. T. S. *Adv. Mater.* **2001**, *13*, 1256.

(11) Huang, W.; Kim, J.-B.; Bruening, M. L.; Baker, G. L. *Macromolecules* **2002**, *35*, 1175.

(12) von Werne, T.; Patten, T. E. *J. Am. Chem. Soc.* **2001**, *123*, 7497.

(13) Miller, P. J.; Matyjaszewski, K. *Macromolecules* **1999**, *32*, 8760.

(14) Pyun, J.; Matyjaszewski, K.; Kowalewski, T.; Savin, D.; Patterson, G.; Kickelbick, G.; Huesing, N. *J. Am. Chem. Soc.* **2001**, *123*, 9445.

(15) Pyun, J.; Jia, S.; Kowalewski, T.; Patterson, G. D.; Matyjaszewski, K. *Macromolecules* **2003**, *36*, 5094.

(16) Xiao, D.; Wirth, M. J. *Macromolecules* **2002**, *35*, 2919.

(17) Jones, D. M.; Brown, A. A.; Huck, W. T. S. *Langmuir* **2002**, *18*, 1265.

(18) Heise, A.; Diamanti, S.; Hedrick, J. L.; Frank, C. W.; Miller, R. D. *Macromolecules* **2001**, *34*, 3798.

(19) Angot, S.; Ayres, N.; Bon, S. A. F.; Haddleton, D. M. *Macromolecules* **2001**, *34*, 768.

(20) Ayres, N.; Haddleton, D. M.; Shooter, A. J.; Pears, D. A. *Macromolecules* **2002**, *35*, 3849.

(21) Senkal, B. F.; Bicak, N. *Euorpean Polym. J.* **2003**, *39*, 327.

(22) Kizhakkedathu, J. N.; Takacs-Cox, A.; Brooks, D. E. *Macromolecules* **2002**, *35*, 4247.

(23) Kizhakkedathu, J. N.; Brooks, D. E. *Macromolecules* **2003**, *36*, 591.

(24) Kizhakkedathu, J. N.; Norris-Jones, R.; Brooks, D. E. *Macromolecules* **2004**, *37*, 734.

(25) Zheng, G.; Stöver, H. D. H. *Macromolecules* **2002**, *35*, 6828.

(26) Bontempo, D.; Tirelli, N.; Masci, G.; Crescenzi, V.; Hubbell, J. A. *Macromolecul. Rapid Commun.* **2002**, *23*, 417.

(27) Bontempo, D.; Tirelli, N.; Feldman, K.; Masci, G.; Crescenzi, V.; Hubbell, J. A. *Adv. Mater.* **2002**, *14*, 1239.

(28) Zheng, G.; Stöver, H. D. H. *Macromolecules* **2002**, *35*, 7612.

4.0 Conclusions

4.1 Thesis Summary

Monodisperse precursor swellable DVB80-*co*-HEMA particles were prepared by precipitation polymerisation using 3 % monomer loading in a mixture of MEK and heptane. This system is quite robust between 2–4 % monomer loading, and 40 to 90 % MEK, resulting in an average particle diameter of 1.6 μm. These microspheres exhibit core shell morphology, and a gradient of accessible HEMA.

Functionalisation of HEMA to form two types of ATRP initiator particles, propionate initiator particles, and isobutyrate initiator particles was successful, with 80 % esterification. These microspheres showed core shell morphology, which indicates a gradient of initiator density within the microspheres. Particle size increased to 1.8 μm for the propionate initiator particles, and 1.7 μm for the isobutyrate initiator particles.

Solution homopolymerisations of methyl acrylate and methyl methacrylate using either catalyst system of CuBr/dNbipy or CuBr/PMDETA initiated by either Et-2-BrP at 70 °C or Et-2-BriB at 90 °C, in bulk showed living kinetics.

For MA homopolymerisation using dNbipy conversion reached 79 % after 9 hours with a final M_n of 9 400 g/mol and a PDI of 1.06, where the expected M_n was 7000 g/mol; employing the PMDETA ligand, the final conversion of MA was 84 % after 9 hours, and the M_n was 10 500 g/mol and the PDI 1.07 with an expected M_n of 7 400 g/mol.

These solution conditions were then applied to the grafting procedures. Grafting MA and MMA from their respective initiator particles resulted in large weight gains, as well as particle size increases; the morphology of the grafted microspheres was studied using electron microscopy (ESEM and TEM) and x-ray microspectroscopy.

MA grafted microspheres showed high diameter size increases from 1.8 μm to 4.0 μm with dNbipy and to 3.0 μm for PMDETA. Particle size and soluble polymer formation increased with time. Addition of equimolar sacrificial initiator, Et-2-BrP resulted in particle size increases to 4.3 μm and 3.2 μm, and more controlled soluble polymer (M_n of 3200 g/mol and a PDI of 1.08 with the dNbipy catalyst, and M_n of 5000 g/mol and PDI of 1.11 with the PMDETA) in terms of expected M_n and PDI. Although the PDI of the soluble polymer with free initiator is close to that of the model polymerisations, the M_n and conversion are lower.

90–95 % of the grafted PMA was cleaved and studied using GPC. Grafting carried out with dNbipy yielded cleaved polymer of M_n 7000 g/mol and PDI 1.14, which is roughly one third of the soluble polymer, but it was more narrow disperse, and when free initiator was added, the M_n was found to be 5 800 g/mol with a PDI of 1.03 which is approximately twice the M_n of the soluble polymer prepared. Using the PMDETA catalytic system, the M_n was 7 500 g/mol and the PDI was 1.21 which is slightly lower in M_n than the soluble polymer but similar in PDI, and this became 1 800 g/mol with a PDI of 1.13 with "sacrificial" initiator, which is a lower M_n than the soluble polymer.

It was found that the M_n and PDI of the soluble polymer were higher than what was determined after cleavage, and that the assumption that the M_n of the soluble

polymer is similar to that of the grafted polymer did not apply for grafting MA from swellable DVB80-*co*-HEMA microspheres.

Homopolymerisation of neat MMA using either CuBr/dNbipy or CuBr/PMDETA, as catalyst, initiated by ethyl 2-bromoisobutyrate (Et-2-BriB) was shown to be a controlled/living system. Using dNbipy PMMA conversion was 95 % with M_n of 10 100 g/mol and PDI of 1.13 and with PMDETA conversion was 99 % and the M_n was 10 200 g/mol and the PDI was 1.15.

The conditions used for the homopolymerisation were applied to grafting MMA from isobutyrate initiator particles, and the resulting microspheres showed interesting morphologies. The resulting microspheres had particle sizes of 4.4 μm (dNbipy) and 4.5 μm (PMDETA). Addition of free initiator, Et-2-BriB, to the grafting procedures improved control, though as in the case of MA grafting, at the expense of decreased grafting and increased soluble polymer. The effect of addition of Et-2-BriB on the microsphere formation (diameter of 3.5 μm when the dNbipy ligand was used and 4.3 μm for the PMDETA ligand) resulted in a decrease in the diameter of the microspheres. As expected, the conversion of monomer to soluble polymer increased with the addition of free initiator, and the control also increased: M_n of 7 400 g/mol with a PDI of 1.25 for the dNbipy ligand, and a M_n of 11 400 g/mol and PDI 1.39 for the PMDETA ligand

Particle size increase was rapid at first in the absence of free initiator (dNbipy), and then leveled off towards the end of the grafting procedure; alternatively, when free initiator was added, the size increased at a slower rate but throughout the polymerisation,

indicating a lower incidence of termination. Added initiator to the grafting process also resulted in narrowing of the PDI of both soluble and grafted polymer.

Cleavage of the grafted microspheres yielded cleaved DVB-*co*-MMA particles nearly quantitatively according to particle weight loss, and recovered polymer. The grafted PMMA had a M_n and PDI very similar to the soluble polymer, which is a consistent finding to that found in literature. M_n of 60 400 g/mol and PDI of 1.90 with the dNbipy ligand were improved to M_n of 21 100 g/mol and PDI of 1.20 when free initiator was added. Similarly, the M_n of 22 300 g/mol and PDI of 1.98 obtained from cleavage of the PMA grafted microspheres with PMDETA, improved upon the addition of free Et-2-BriB to an M_n of 22 700 g/mol with a PDI of 1.29. This confirms that grafting from within lightly cross-linked gels can still be carried out with good control over M_n and PDI.

4.2 Future Work

In order to determine whether the gel effect indeed decreases control of the homopolymerisation of MA and MMA, acetate functionalised DVB80-*co*-HEMA particles should be prepared for these control experiments.

Cleavage might be improved by changing the cleavable linker to an easily chemically cleavable site, such as silicon, or using a thermally labile, or photosensitive linker. Incorporation of the arenesulfonyl initiator group attached via silicon might be considered.

A second generation of swellable microspheres could be prepared by suspension polymerisation of HEMA, and (ethylene glycol)dimethacrylate could be prepared in order to graft from. This would eliminate any effects of the HEMA, and derivatised HEMA gradient.

More applicable areas may be explored, such as the grafting DMAEMA (as was previously done) for possible bio-separation. Otherwise, these substrates could be more fully explored as resins for catalysis.